FORAMINIFERAL DISTRIBUTION IN UNCONSOLIDATED SEDIMENT ASSOCIATED WITH A MARGINAL CORAL REEF IN SOUTH AFRICA

by

Stephanie Vivien Hayman

Submitted in fulfilment of the academic requirements for the degree of
Master of Science in the School of Geological Sciences,
University of KwaZulu-Natal, Durban through the Oceanographic Research Institute

Supervisor: Prof. MH Schleyer
Co-supervisor: CF Mackay
August 2015

As the candidate's supervisors we have approved this dissertation for submission.

Signed: _____ Name: _____ Date: _____

Signed: _____ Name: _____ Date: _____

ABSTRACT

South Africa's coral reefs are located at high latitude, but have high biodiversity and recreational value. They potentially provide insight into future scenarios of global change for other sub-tropical and/or tropical reefs affected by human activity and climate change. With this in mind, there is a need to better understand the dynamics of calcifying marine organisms in this region. The aims of this study were to gain insight on foraminiferal distribution in sediments associated with Two-mile Reef (TMR), Sodwana Bay, and to investigate whether they provide a stable record of past climate. Three bioclastic sediment cores were collected at a water depth of 16 m between September and November 2012. This was followed by the collection of extant Large Benthic Foraminifera (LBF) using a spatial crossed design of different substrata and habitats, ranging from sand to reef rubble, in the austral summer of 2013.

Living LBF assemblages occurred in zones across the reef and reef-associated habitats, with discrete assemblages found in sediment habitats and coral rubble. Living LBF were found predominately on reef rubble. The distribution of these organisms appeared to be influenced by sediment characteristics (skewness, fine sand, medium sand and gravel) as well as water chemistry (pH, salinity, temperature and total alkalinity). The marginal nature of these reefs was also corroborated through carbonate analysis of water parameters (mean Ω_{Ar} <3.5 and Ω_{Ca} <5.0). Radiocarbon dating of one core provided a Late Holocene starting calendar age of AD 680-920 (BP 1270-1030) and patterns in down-core foraminiferal assemblages allowed for palaeoenvironmental interpretation. Flooding events, surmised to be linked with tropical cyclones and/or cut-off lows, were revealed in the cores. These events possibly result from south-ward pulses in the Intertropical Convergence Zone (ITCZ). Based on the extant and past foraminiferal assemblages, it was deduced that turbulence was a major factor governing foraminiferal distribution across the study site, with sediment cores only providing a record of major climatic events. Overall, the sediment foraminiferal assemblages were a good reflection of all taxa found within this reef-associated environment but yielded little information on the past climate of TMR.

PREFACE

The work described in this thesis was carried out the Oceanographic Research Institute, an affiliate of the University of Kwa-Zulu Natal, Durban, in the School of Geological Sciences, from June 2012 to April 2015, under the supervision of Professor Michael Schleyer and Ms. Fiona Mackay.

These studies represent original work by the author and have not otherwise been submitted in any form for any degree or diploma to any tertiary institution. Where use has been made of the work of others it is duly acknowledged in the text.

FACULTY OF SCIENCE AND AGRICULTURE
DECLARATION
PLAGIARISM

I, Stephanie Vivien Hayman, declare that:

1. The research reported in this thesis, except where otherwise indicated, is my original research.

2. This thesis has not been submitted for any degree or examination at any other University.

3. This thesis does not contain other persons' data, pictures, graphs or other information, unless specifically acknowledged as being sourced from other persons.

4. This thesis does not contain other persons' writing, unless specifically acknowledged as being sourced from other researchers. Where other written sources have been quoted, then:

    a. Their words have been re-written but the general information attributed to them has been referenced

    b. Where their exact words have been used, then their writing has been placed in italics and inside quotation marks, and referenced.

5. This thesis does not contain text, graphics or tables copied and pasted from the Internet, unless specifically acknowledged, and the source being detailed in the thesis and in the References sections.

Signed:

Stephanie Vivien Hayman

Date: 26 August 2015

TABLE OF CONTENTS

ACKNOWLEDGEMENTS

- Firstly I would like to thank my supervisors; Prof. Michael Schleyer and Ms Fiona Mackay. Thank you for introducing me to the amazing world of Foraminifera and for the guidance, patience and support you have given me. I really appreciate all the help and knowledge you have shared with me.

- I would like to thank the Applied Centre for Climate and Earth System Science (ACCESS) for funding this study. The South African Association for Marine Biological Research (SAAMBR) and the Oceanographic Research Institute (ORI) also need to be thanked for financial assistance and the Mazda Wildlife Fund for the 4 x 4 used during fieldwork.

- The University of KwaZulu-Natal (UKZN) and Western Indian Ocean Marine Science Association (WIOMSA) need to be thanked for financial support with conference attendance.

- I would also like to extend thanks to Dr Stephan Woodborne and iThemba Labs for conducting the stable isotope analysis and for help in the interpretation of the data. Stephan provided valuable discussions and advice. An extremely huge thank you as well to Prof. Andrew Dickson for his help in setting up our Gran titrations. I also need to thank Dr Andrew Green for his help with the core logging and core sampling methods.

- I also need to thank the "coral team" for their help with fieldwork and the core collections as well as all the guys down in technical for their help. Des and Neels need extra special thanks for all their help with manufacturing and setting up equipment.

- And lastly, I would like to thank my amazing family and friends, especially Warren. Thank you for being there for me through all the good, bad and hard times. Your love and support means the world to me and without it, I definitely wouldn't have made it this far.

CHAPTER 1
INTRODUCTION

1.1. Context of study

In the last decade, concern for and awareness of climate change has increased, with tropical reefs experiencing detrimental effects from severe bleaching events (e.g. Hoegh-Guldberg 1994; Bruckner 2012), increased storm damage (e.g. Birkeland 1997; Gardner et al. 2005) and disease outbreaks (e.g. Jones et al. 2004; Boyett et al. 2007; Bruckner 2012). South Africa's reefs are located at high latitude and have a high biodiversity and recreational value (Jordan & Samways 2001; Celliers & Schleyer 2003). As more areas are turning marginal for coral reef growth, South Africa's reefs can potentially provide insight into future scenarios of global change for other sub-tropical and/or tropical reefs stimulated by human and climate change pressures. This study focused on using Foraminifera as an indicator organism to determine changes in the environment associated with Two-mile Reef (TMR) at Sodwana Bay, South Africa. The emphasis of this study is, therefore, to highlight the use of Foraminifera to elucidate environmental events/changes in reef and reef-associated studies.

Foraminifera have been used in numerous studies worldwide, as coral alternatives, to monitor reef health, reef resilience and as early warning signs of stress (Hallock et al. 2003; Hallock 2012; Uthicke et al. 2013). Extensive biophysical studies have been conducted on the coral reefs at Sodwana Bay. Abiotic studies include the geology (e.g. Ramsay 1991; Ramsay 1994; Green & Uken 2008; Green 2009; Green 2011) and physical oceanography (e.g. Morris 2009). Studies have also addressed the fish and benthic communities including species diversity, community structure, coral distribution, genetic diversity and larval recruitment (e.g. Celliers & Schleyer 2003; Floros et al. 2004; Morris 2009; Hart 2011; Floros et al. 2012). Few studies, however, have been conducted on the foraminiferal assemblages associated with South Africa, with none to the author's knowledge, being conducted at Sodwana Bay. As the most abundant shelled microorganism in benthic marine environments (Koukousioura et al. 2011), Foraminifera represent the palaeoenvironmental record and aid in predicting future climate trends (Jansen et al. 2007; Katz et al. 2010).

1.2. Global climate change

Ocean acidification (OA) and warming are two major environmental threats affecting coral reef ecosystems worldwide. While climate change is a natural phenomenon, anthropogenically-produced carbon dioxide (CO_2) has accelerated this process since the beginning of the industrial revolution, by increasing the amount of CO_2 present in the atmosphere. Increased absorption, of CO_2 into the oceans,

causes a shift in the marine carbonate equilibrium, resulting in a decrease in pH. This is termed OA (Doney et al. 2009) and results in a concomitant decrease in carbonate ion concentration, a crucial component of the shells and tests of marine calcifiers (Hoegh-Guldberg et al. 2007). This decrease can negatively affect a wide variety of calcifying marine organisms besides Foraminifera, such as pteropods, corals, coccolithophores and shellfish (e.g. oysters, mussels) (Gazeau et al, 2007; Hofmann et al. 2010; Talmage & Gobler 2010). Increasing concentrations of greenhouse gases produced by human activities, of which CO_2 is the most important contributor, is also resulting in increased temperatures. Radiated heat from the sun is reflected off the earth's surface and is trapped in a greenhouse effect by the atmosphere. Global, surface seawater temperatures (SSTs) have thus increased since the late 19th century by an average of 0.6°C (Solomon et al. 2007).

Besides direct changes to seawater chemistry, additional effects of climate change include an increase in the frequency and severity of extreme weather, e.g. heat waves, droughts, torrential rains (Rosenzweig et al. 2001; Allen et al. 2010; Cai et al. 2014). Easterling et al. (2000) acknowledged the lack of high-quality, long-term data as one of the main problems in detecting extreme events in climate records. In southern Africa, Shongwe et al. (2009) found drought-related disasters to have risen from ±1.5 per year in the 1980s to ±2 per year since 2000, whereas flood related disasters have risen from 1.2 per year to 7 per year since 2000. With this in mind, it is imperative to understand the natural climatic cycles in a region (e.g. floods, cyclones) in order to better recognise an increase in the frequency, duration or severity of these events.

1.3. Morphology and classification of Foraminifera

Foraminifera are currently recognised as a distinct Phylum within the Kingdom Protista (Armstrong & Brasier 2005). There is, however, inconsistency regarding their division into Class, Subclass and Order. Previously classified as the order Foraminiferida (Eichwald 1830) within the Phylum Protozoa (Loeblich & Tappan 1987), Cavalier-Smith (2003) reclassified Foraminifera as an order in the class Reticulosa, and Prothero (2004) classified them as an order in the subclass Rhizopoda, within the class Granuloreticulosa (Toefy 2010). Irrespective of these upper level differences, there is some degree of agreement of the divisions at the suborder level.

These unicellular protists can be planktonic or benthic. Planktonic refers to forms living within the water column whereas benthic denotes individuals living attached to or on a surface (Murray 2006). They are characterised by the presence of a test (internal shell) which surrounds the protoplasm (Loeblich & Tappan 1987). Tests can be secreted mineralogically as silica, calcite or aragonite,

organically as pure tectin, or be agglutinated with detrital material. Calcareous tests can be either perforated (hyaline) or smooth and imperforate (porcelaneous) (Fujita et al. 2011). Hyaline shells are composed of interlocking microcrystals of $CaCO_3$, have a glassy appearance and pores which penetrate the wall, whereas porcelaneous shell walls are composed of rod-shaped crystals of $CaCO_3$ (Hansen 1999). They have a milky, translucent to opaque look and generally lack pores after the first initial chambers. Two types of protoplasm are recognised: the ectoplasm, which lies outside the test in the form of granuloreticulopodia (thread-like pseudopodia with a granular texture) and the endoplasm inside the test which contains the nucleus and algal symbionts, in the case of symbiont-bearing Foraminifera (Hallock 1982) (Figure 1.1). Reticulating pseudopodia are used for shell construction, attachment, motility, protection and for capturing food.

Severin (1983), classified Foraminifera into six morphological groups based on external test morphologies (straight-cylindrical, plano-convex, elongate-flattened, biconvex-keeled, tapered, and rounded-planispiral). It was reported that, with increasing water depth, Foraminifera test morphologies become more angular and asymmetric due to a decrease in sediment turbulence. The angular asymmetrical forms therefore are indicators of less energetic environments, whereas rounded symmetrical forms indicate turbulent environments (Nigam & Chaturvedi 2000; Lakhmapurkar & Bhatt 2010).

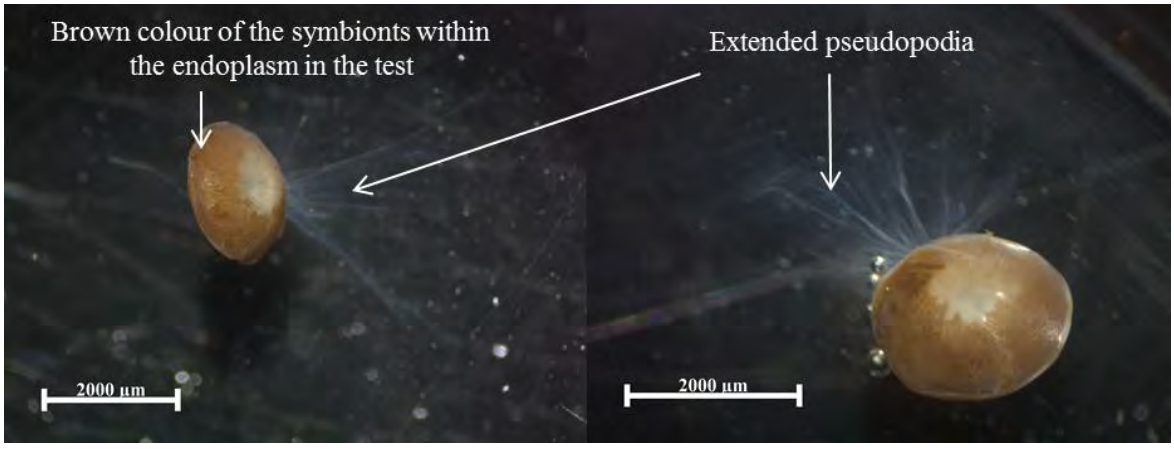

Figure 1.1. *Amphistegina lobifera* specimens with extended pseudopodia. Note brown endoplasm due to presence of symbiotic diatoms.

Foraminifera are found primarily in marine environments, but live in all aquatic environments ranging from fresh to hypersaline waters. These organisms produce ca. 50% of biogenic calcium carbonate in the open oceans (Keul et al. 2013). Planktonic forms are identified according to their shell properties

and wall texture (Kučera 2007), whereas benthic forms are identified primarily according to test composition. However, morphological characteristics such as chamber number and chamber arrangement are also used (Sen Gupta 1999). Foraminifera can be unilocular (one-chambered) or multilocular (having several chambers) (Sen Gupta 1999) depending on age and species.

Their growth mechanism differs from other testate protists. The generation of tests is achieved through the incremental addition of chambers, whereby a new chamber forms over the old external aperture, thereby ensuring continuous contact with the external environment (Loeblich & Tappan 1987). Planktonic Foraminifera reproduce by sexual reproduction and there are ±44 recent species (Hemleben et al. 1989), whereas benthic Foraminifera generally have alternating sexual and asexual generations (Murray 2006) (Figure 1.2). Approximately 30 out of ±10 000 extant benthic species have been studied in terms of their life cycles. According to Boltovskoy and Wright (1976), the asexual reproductive mode is typically prevalent to the sexual reproductive mode. A distinct morphological difference is noted in the different generations, with offspring produced sexually having a small first chamber and a large test (agamont, microspheric form) and the asexually produced offspring having a large first chamber and a small test (gamont, megalospheric form) (Goldstein 1999). Harsher environmental conditions are thought to cause the dominance of microspheric forms (Boltovskoy & Wright 1976). The two generations, agamont and gamont, reproduce asexually and sexually, respectively, and this cycle usually takes a year. Some larger benthic Foraminifera display a variation in this life cycle whereby a schizont generation occurs after the gamont phase and this can delay the life cycle by several years (Figure 1.3). During asexual reproduction, if all the cytoplasm of the parent test is utilized by the offspring, the parent dies (Figure 1.2).

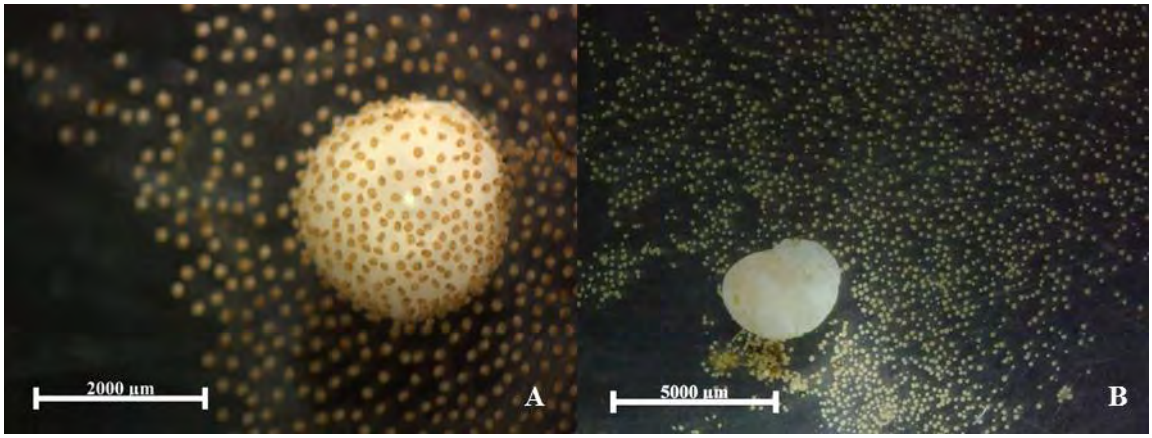

Figure 1.2. **A** *Amphistegina lobifera* and **B** *Heterostegina depressa* adults with asexually reproduced offspring. Note the "dead" adult test.

Foraminiferal diets vary between species and can include bacteria, diatoms, other smaller protists, crustaceans, molluscs, nematodes and invertebrate larvae (Armstrong & Brasier 2005). Symbiont-bearing Foraminifera make up <10% of the 150 families of the Foraminifera and symbionts can include diatoms, chlorophytes, rhodophytes, cyanobacteria, haptophytes and dinoflagellates (Lee 2006). The habitat of benthic Foraminifera is either epifaunal or infaunal (Murray 2006). The former denotes individuals living on soft sediment or attached to hard substrata such as shells, rocks or other animals. They can be sessile, clinging or free-living and attachment is achieved through the secretion of organic glue (Murray 2006). According to Murray (2006) Foraminifera use a "grip and tug" mechanism to move over hard, flat surfaces. This process involves an individual holding itself in an upright position and contracting a set of pseudopodia which pull the test forward. These pseudopodia then reposition themselves, anchor on the surface and repeat the process. The movement is very slow (1-50 μm/min) (Murray 2006) and is partly regulated by the surrounding temperature and the need for food. The infaunal habitat is typified by individuals living within the sediment, with living individuals being recorded down to 60 cm in marshes; however, in most environments Foraminifera only live in the top few centimetres (Murray 2006).

1.3.1 Large Benthic Foraminifera

Large Benthic Foraminifera (LBF) are found within each of the three major living suborders of Foraminifera, the Textulariina, Miliolina and Rotaliina. This study follows the classification of Buchan (2006) who classified juvenile LBF as being >500 μm in size, and adults >1000 μm. Renema et al. (2013), similarly classified LBF as larger than 500 μm but the accepted size of LBF differs according to various authors (e.g. Ross 1974; Haynes 1980; Murray 1991; Fujita et al. 2009). LBFs can host algal endosymbionts and have a complex internal structure (Troelstra et al. 1996). Symbionts are hosted within the cytoplasm chamber and Hallock (1985) attributes the larger size of these Foraminifera to turbulence, salinity, depth, pH and food availability, all of which affect their chance of survival. The size of a Foraminifera is also important for its survival as smaller juveniles (<500 μm) are more susceptible to predation by polychaetes, nematodes, crustaceans and gastropods (Lipps 1983). A survival mechanism employed by a large proportion of Foraminifera is to delay maturation and instead, use their energy to grow to a larger size (Buchan 2006). The parent organism is directly proportional to the number of offspring it produces asexually. Therefore, the larger the parent the greater number of offspring it produces, thereby increasing the chances of survival (Buchan 2006). Additional energy provided by endosymbionts also allows LBF to reach a larger adult size in oligotrophic environments. Their reliance on symbionts for carbohydrates and lipids can, however, be detrimental when there is an increase in dissolved nutrients in the host's environment. This can lead to symbionts being released from nutrient limitation as occurs in symbiont-bearing corals (Uthicke & Altenrath 2010). These protists are, therefore, characteristic of oligotrophic waters, as a result of

hosting symbionts, and are also among the main primary and carbonate producers in coral reef systems (Lee & Hallock 1987; Langer et al. 1997; Hohenegger 2006; Fujita & Fujimura 2008).

1.3.2 Importance of Foraminifera in coral reef and reef-associated research

Coral reefs support 32 out of the 34 recognised animal phyla and are the most diverse habitats in the world (Wilkinson 2002). They are of great ecological importance and economic value, globally supporting more than 500 million people (Wilkinson 2002). The LBF share similar traits and habitat requirements to scleractinian corals (Weinmann et al. 2013), making them particularly valuable in interpreting responses of the coral reef benthic community to environmental stressors (Hallock et al. 2003). Corals and LBF both host endosymbionts and require shallow, clear, nutrient-poor waters for survival. As a whole, benthic foraminiferal assemblages respond quicker than corals to environmental changes, this being attributable to their short life cycles as well as their sensitivity to environmental conditions (Hallock et al. 2003). According to Fujita et al. (2011), the high Mg calcite tests of these large, algal symbiont-bearing Foraminifera make them the "first responders" to OA on coral reefs, as their test solubility exceeds that of corals.

1.3.3 The influence of abiotic parameters

According to Renema et al. (2013), the modern-day distribution of LBF, associated with reef environments, is dependent on the depth-related parameters of light intensity, temperature, nutrients, substratum type and hydrodynamic energy. There is still a debate, however, regarding the effects sediment grain size has on foraminiferal diversity and density (Armynot du Châtelet et al. 2009).

Grain size is the most essential physical property of sediment due to grain size preferences by various organisms within benthic communities (Blott & Pye 2001). The purpose of a grain size analysis is therefore to accurately measure individual particle sizes, to determine their frequency distribution and also to calculate a statistical description that sufficiently describes the sample using a single measure (Poppe et al. 2000). It also allows trends in surface processes linked to the dynamic conditions of deposition and transportation to be analysed in marine environments. Sorting is a method employed to show the grain size variation of a sample through the incorporation of the largest parts of the size distribution, using measurements from a cumulative curve (Rapp et al. 2006). Skewness, calculated from the grain size statistics, is another sediment characteristic which defines the extent to which a cumulative-distribution curve approaches symmetry (Rapp et al. 2006). Two samples can have identical sorting and average grain size; however, differ in their degrees of symmetry.

According to Diz et al. (2004), very coarse substrata are a favourable settlement for living benthic Foraminifera, yet Debenay et al. (2001) reported that benthic Foraminifera favour a high proportion of fine particles. According to Murray (2006), grain size has no effect on test size for living individuals; however, dead tests undergo sorting with the sediment grains. Studies of live LBF assemblages, in reef-associated environments, have identified only a few living taxa in the reef sediments (e.g. Martin 1986; Cockey et al. 1996; Stephenson 2011). This fact has led to research on reef rubble and phytal substrata (e.g. Hallock et al. 1986; Hallock et al. 2006) in conjunction with reef sediments when investigating their living and total populations.

Calcium carbonate ($CaCO_3$) is produced by marine organisms in the form of two main polymorphs, calcite and aragonite (Hauck et al. 2011). Both are water soluble at pH<7 and are known cementing agents (ASTM D4373 - 14) with the majority of the $CaCO_3$ in marine deposits found in the form of calcite. Aragonite and calcite saturation sate (Ω) horizons denote the depth levels in the water column below which these polymorphs are under saturated. This component of the sediment is important, as the water is regarded saturated when Ω is >1 and under saturated when Ω <1, with respect to the either aragonite or calcite (Hauck et al. 2011).

1.3.4 Foraminifera as geochemical proxies

The chemostratigraphy and reconstruction of past ocean and climate conditions are based on geochemical analyses of fossil Foraminifera tests (Kasemann et al. 2009; Katz et al. 2010). Geochemical analysis is used to reconstruct ocean palaeocirculation patterns, the carbon cycle, marine carbonate chemistry, chemostratigraphy, palaeoproductivity and climate history (including ice volume in the polar regions, temperature and salinity) (Katz et al. 2010). Proxies developed for Foraminifera include $\delta^{18}O$, $\delta^{13}C$, trace elements (Mg, Cd, Ba, Zn, and B), $^{87}Sr/^{86}Sr$, $\delta^{11}B$, and ε_{Nd} (Table 1.1). Benthic Foraminifera provide information in this regard on the seawater near the seafloor and of porewaters within the sediment, whereas planktonic Foraminifera yield information regarding the upper few hundred meters of the surface ocean (Katz et al. 2010).

In some samples, an isotopic offset is evident between different species, both in benthic (e.g. Shackleton 1974; Belanger et al. 1981; Katz et al. 2003) and planktonic Foraminifera (e.g. Bè et al. 1966; Ravelo & Fairbanks 1992); this may constitute a confounding factor related to Foraminifera species. Differences in microhabitat (e.g. Belanger et al. 1981; Corliss 1985), vital effects (e.g. Duplessy et al. 1970; Rollion-Bard & Erez 2010) and the presence of symbionts (e.g. Spero & Lea 1993; Saraswati et al. 2004) have all accounted for interspecies isotopic offsets in benthic

Foraminifera (Katz et al. 2010). A vital effect constitutes a biological process which distorts environmental signals recorded within the carbonate during biomineralisation (Weiner & Dove 2003). Katz et al. (2010) suggested using monospecific or monogeneric specimens for palaeoclimatological studies in order to avoid bias from isotopic signals. This avoids introducing species isotopic offsets.

Table 1.1. Geochemical proxies in calcareous Foraminifera (Katz et al. 2010).

Parameter	$\delta^{18}O$	$\delta^{13}C$	$\delta^{11}B$	$^{87}Sr/^{86}Sr$	Mg/Ca	Cd/Ca	Ba/Ca	Zn/Ca	B/Ca	$\delta^{11}Nd$
Ice volume	x									
Temperature	x				x					
Circulation		x				x	x	x		x
Productivity		x								
Carbonate saturation								x	x	
pH			x							
Chemostratigraphy	x	x		x						

In aquatic environments, the oxygen isotope composition of calcite is related to temperature and salinity as the relative proportions of oxygen isotopes, of the carbonate and water, is a temperature dependent process (Sharp 2007). Foraminiferal $\delta^{13}C$ ratios are related to carbon cycling. The deviations in isotopic composition are so minor, that they are expressed in the conventional δ notation (‰) (Allégre 2005). In marine carbonates, high $\delta^{18}O$ values reflect colder conditions, whereas low $\delta^{18}O$ values reflect warmer conditions. The relationship between $\delta^{18}O$ and temperature is dependent on both the fractionation factor and ice volume present at the poles. Stable isotope data are always reported relative to a known standard rather than an absolute ratio. Two widely used standards are the Vienna Standard Mean Ocean Water (VSMOW) and Vienna Pee Dee Belemnite (VPDB) (Pearson 2012).

The inference of past ocean conditions from geological records utilises traditional proxies (e.g. $\delta^{18}O$ and $\delta^{13}C$) as well as new emerging proxies (e.g. $\delta^{11}B$ and ε_{Nd}) which still require some development in their application in Foraminifera. Size variation in LBF tests is a factor to consider in isotope studies (Saraswati et al. 2004), as well as the analytical technique (Kasemann et al. 2009; Katz et al. 2010). Sediment core dating is performed using foraminiferal ^{14}C or ^{210}Pb and ^{137}Cs signals. The development of accelerator mass spectrometry (AMS) has made it possible to radiocarbon-date marine sediment cores using single- or mixed-species foraminiferal samples (Broecker et a1. 1984). The ^{14}C dating provides dates from 64–50 000 years ago (Brown et al. 2001), whereas ^{210}Pb is restricted to dating in the last 75-100 years (Arnaud et al. 2006). ^{137}Cs signals are even more limited,

detecting signals from nuclear weapon testing in the 1950s and 1960s and are generally used to confirm ^{210}Pb dates (Arnaud et al. 2006).

1.3.5 Foraminiferal studies in South Africa

Foraminifera studies along the South African coast have been limited, with the majority concentrating on off-shore and deep sea environments (Toefy 2010). Initial foraminiferal research was conducted during mineralogical exploration and geological surveys and, subsequently, lacked environmental parameters and conclusions (Toefy 2010). The first studies by Chapman (1904, 1907, 1916, 1923, 1924, 1930) were followed by work undertaken in the 1950s, 1960s and 1970s (Biesiot 1957; Parr 1958; Albani 1965; Lambert & Scheibnerová 1974). Geological surveys were conducted in the 1970s and 1980s by the Joint Geological Survey and the University of Cape Town, providing species lists for the west coast of South Africa (Martin 1974; Salmon 1979a, 1979b, 1980). The most recent work on extant populations was in two bays along the south west coast of South Africa, resulting in a better understanding of present-day Foraminifera assemblages, how they cope with ambient environmental conditions and their use as pollution indicators (Toefy et al. 2003; Toefy 2010). These studies revealed 38 morpho-species in live assemblages collected around Robben Island and St Helena Bay. On the east coast, a study on the range expansion of *Amphistegina* spp. predicted its rapid south-westwards expansion along South Africa due to climate change (Langer et al. 2013b). *Amphistegina*, considered an invasive genus in the Mediterranean, displays the widest latitudinal ranges across the oceans (Langer et al. 2013b) and, subsequently, could pose a threat to the native biodiversity on South African reefs.

1.4. Aims and Objectives of the study

Calcifying marine organisms have survived past climate changes and thus provide valuable insight into these events. Palaeo-environmental records can be extracted from their skeletal deposits and the nature of these changes monitored and compared with present-day climate change. The aims of this study were to gain insight into foraminiferal distributions in sediments associated with a marginal coral reef in South Africa, and whether they provide a record of past climate.

To do this, two questions were addressed:

1. What is the present-day LBF distribution across subtropical, reef-associated sediments at Sodwana Bay?
2. Can a palaeo-environmental record of South Africa's coral reef environment be reconstructed using Foraminifera?

1.5. Structure of thesis

This thesis is presented in five Chapters. An introduction (Chapter 1) and materials and methods (Chapter 2). A habitat comparison with associated water chemistry (Chapter 3), analysis of sediment cores (Chapter 4) and a general discussion and synthesis (Chapter 5).

The subject is introduced and the literature reviewed in Chapter 1. An overview of Foraminifera is given with an explanation of their importance in coral reef climate change research. A brief synthesis is also provided on Foraminifera studies conducted in South Africa and Foraminifera geochemical proxies. The project aims and objectives are also outlined in this Chapter. Chapter 2 defines the materials and methods employed. This includes a description of the study site, laboratory procedures and statistical analysis. The specific methodology and results of the first project component, a Foraminifera distribution, ecology and habitat comparison on reef-associated bottom types, is given in Chapter 3. The phyisco-chemical parameters of the study site is provided and discussed. Sediment characteristics and foraminiferal assemblages at three locations and two substrata are also given. The subject of live versus dead versus total assemblages is explored and an overview of key taxa is provided. Chapter 4 presents data on the bioclastic sediment cores that were collected and explores their down-core geochemical proxies, as well as the foraminiferal assemblages in relation to grain size and carbonate content. Notable environmental events recorded in the cores are discussed. Chapter 5 synthesises all the findings and discusses the outcomes in the context of present day climate change and the suitability of Foraminifera in future reef studies in South Africa.

CHAPTER 2
MATERIALS AND METHODS

2.1. Study area

Sodwana Bay, KwaZulu-Natal, has a humid, sub-tropical climate. Characteristically, this stretch of coastline experiences summer rainfall and is affected by southward shifts of the Inter-Tropical Convergence Zone (ITCZ). At times, the effects of storms and coastal flooding from cyclonic activity (Kovacs et al. 1985; Reason & Keibel 2004) and cut-off lows (Rouault et al. 2002) are experienced. Sodwana Bay lies in the iSimangaliso Wetland Park, a United Nations Educational, Scientific and Cultural Organisation (UNESCO) World Heritage Site (McIntosh 2010). It is home to the southernmost distribution of coral reefs along the east African coastline (Ramsay 1994), with its coral reefs being divided into three complexes; a northern, southern and central reef complex (Figure 2.1). Two-mile Reef (TMR) (Figure 2.2) is located within the central reef complex. It is a patch reef, lies at depths of -6 to -27 m below mean sea level and is coast parallel (Celliers & Schleyer 2002). It is located 1 km offshore, is 2.1 km in length and has a maximum width of 0.9 km (Ramsay & Mason 1990). Indo-Pacific type corals on TMR have colonised a submerged and eroded Pleistocene, dune and beach rock sequence (Ramsay & Mason 1990; Ramsay 1991).

The sandy shoreline of northern KwaZulu-Natal is composed of barrier beaches forming Holocene-aged zeta bays, shaped through littoral erosion (Ramsay 1994). Offshore of northern KwaZulu-Natal is the Natal Valley, which exceeds depths of 2000 m with the Mozambique Basin exceeding 5000 m further east (Martin 1978). The Delagoa Bight is situated north of the South African border in Mozambique. Sodwana Bay is located between the Natal Bight to the south and the Delagoa Bight to the north. The north east coast of KwaZulu-Natal is characterised by a very narrow, steep shelf with a gradient of 1.0–2.5º in comparison with the global average of 0.116º (Ramsay 1994; Ramsay 1997; Lutjeharms et al. 2000). The Natal Bight, however, is an uncharacteristically wide area of the shelf, which extends for 160 km and is 50 km at its widest point at the Thukela River (Lutjeharms and Roberts 1988, Lutjeharms 2006). It is a productive shelf habitat due to influence from local oceanographic features and fluvial input from the Thukela River (Begg 1978).

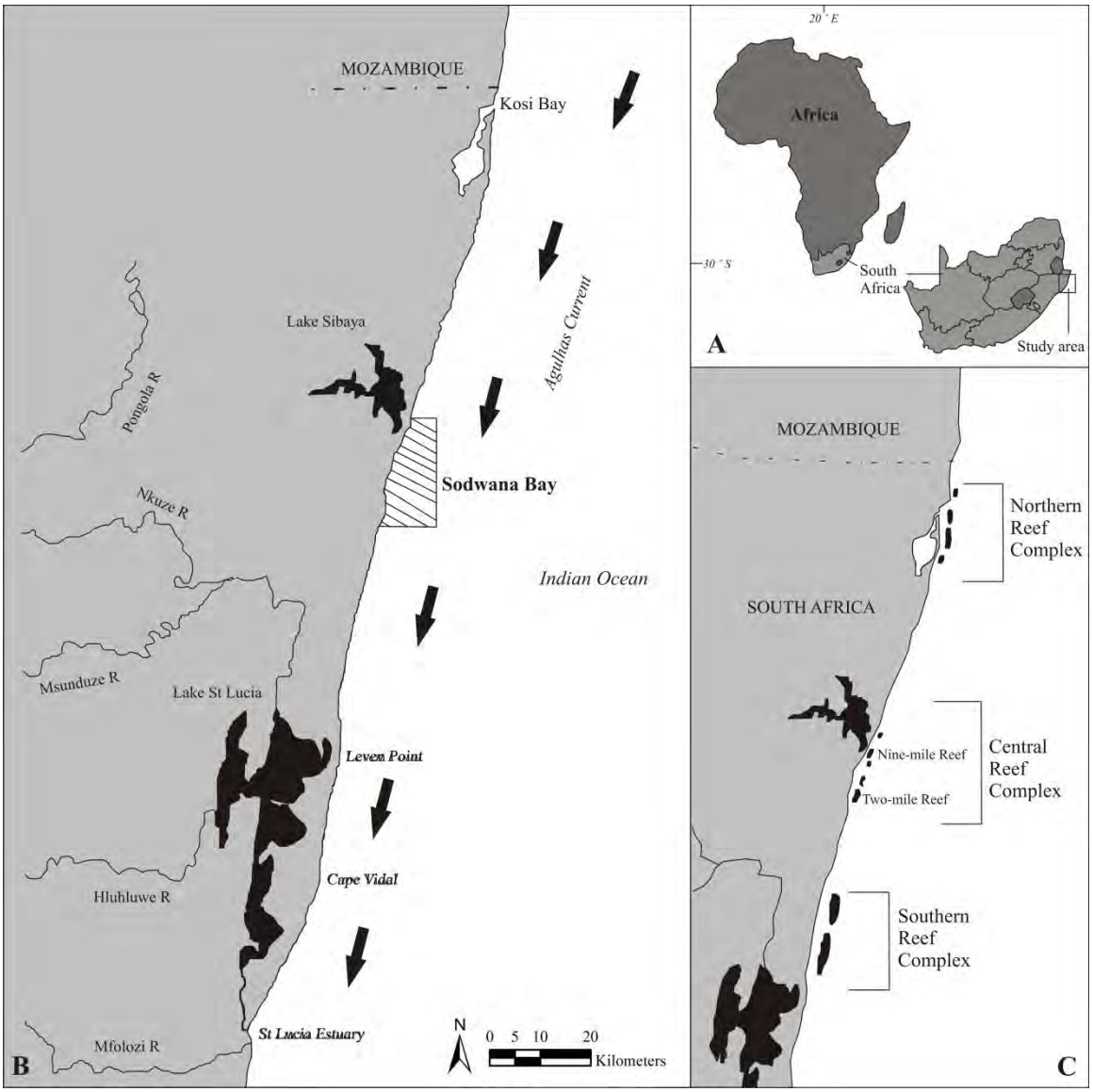

Figure 2.1. **A, B** Location of the study area, Sodwana Bay on the north-east coast of South Africa with **C** location of Two-mile Reef within the central reef complex (after: Ramsay & Cohen 1997; Celliers & Schleyer 2003; Roberts et al. 2006).

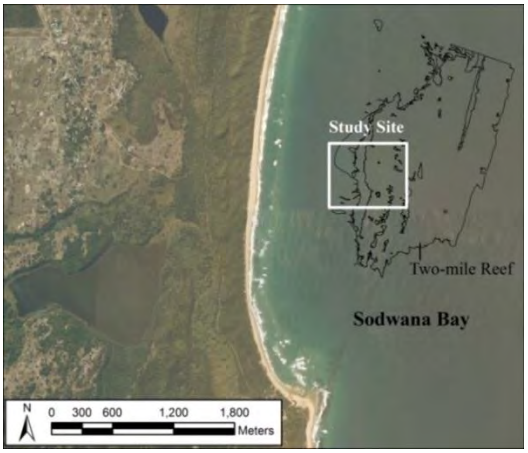

Figure 2.2. Location of study site on Two-mile Reef, Sodwana Bay.

The Agulhas Current is the main oceanographic feature affecting the east coast of South Africa (Figure 2.3). It is a major western boundary current in the south-west Indian Ocean and includes a partially wind-driven return circulation, transporting warm tropical and subtropical water southwards (Lutjeharms 2006). This current is present year round and can reach velocities of 2 m/s (Lutjeharms, 2006). Roberts et al. (2006), however, measured velocities of between 0.5–0.75 m/s, at 12m water depth on the shelf, at Nine-mile Reef (Figure 2.1).

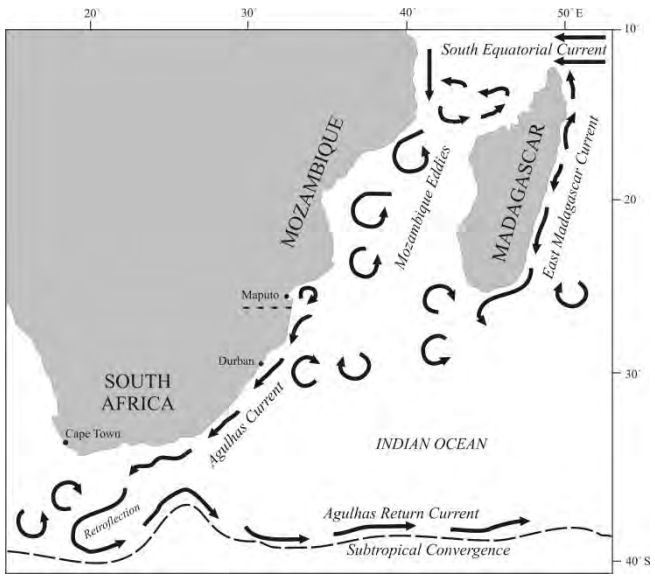

Figure 2.3. The south-west Indian Ocean circulation (after: Lutjeharms 2004).

Both Tropical Surface Water (TSW) and Subtropical Surface Water (STSW) contribute to the Agulhas Current. The TSW, provided by the South Equatorial Current, consists of low salinity (<35.3), warmer (>24°C) water (Duncan 1970). This enters the Mozambique Channel above northern

Madagascar. The STSW, of high salinity (>35.5) enters the Agulhas Current from the east, via the East Madagascar Current (Duncan 1970). According to Duncan (1970), mixed surface water with relatively low salinities (<35.3) are found in both seasons along the coastal edge of the Agulhas Current. Lutjeharms (2006) also reported the dominance of TSW along the east African coastline including South Africa.

2.1.1 Physico-chemical parameters on Two-mile Reef

The waters along the Sodwana Bay coastline, where the Agulhas Current forms, are oligotrophic and lack terrigenious sediment input due to the absence of large rivers in the area (Ramsay 1994). Thus, the local water conditions are clear, but nutrient poor which have allowed colonisation of Sodwana Bay by corals and Large Benthic Foraminifera (LBF). The nutrients, nitrates (NO_3^-), phosphates (PO_4^{3-}) and silicate (SiO_2) are important components of the carbonate system cycle and their relative concentrations affect the benthic communities present in this oligotrophic environment.

According to Dickson et al. (2007), total alkalinity (T_A) of a seawater sample is defined as "the number of moles of hydrogen ion equivalent to the excess of proton acceptors (bases from weak acids with a dissociation constant $K \leq 10^{-4.5}$ at 25°C and zero ionic strength) over proton donors (acids with $K > 10\text{-}^{4.5}$) in one kilogram of sample". In the oceans, the majority of the negatively charged ions are present as bicarbonate (HCO_3^-) and carbonate (CO_3^-) (Chester & Jickells 2012), however, due to increased levels of atmospheric CO_2; the balance of these ionic species is changing. The T_A is therefore important to monitor. Based on modelling by Takahashi et al. (2014), seawater at Sodwana Bay should range between 2300 to 2350 µmol/kg (Figure 2.4).

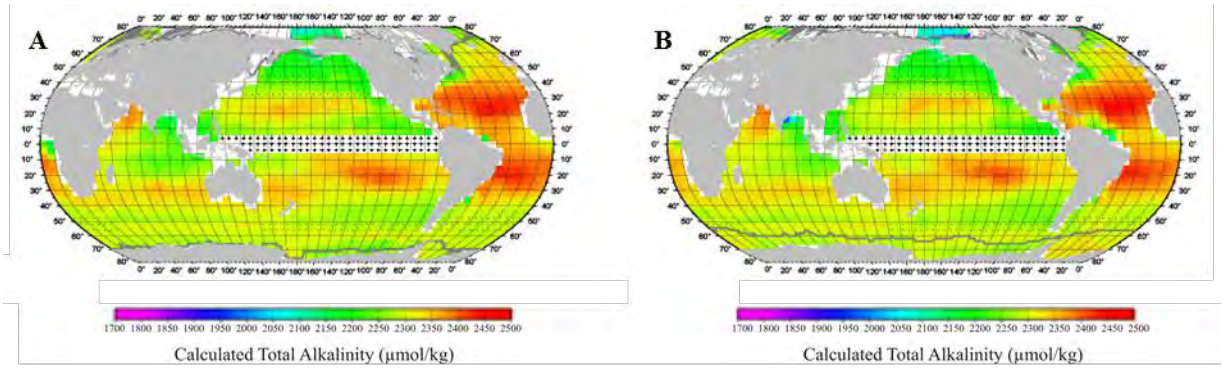

Figure 2.4. Mean distribution of the total alkalinity (T_A), for **A** February and **B** August, across the oceans. These values were calculated using the potential alkalinity-salinity relationships, measured during 1990-2008, and mean values for surface water salinity and nutrients. The black dots represent areas with large-scale variations (from: Takahashi et al. 2014).

The most recent work on the physico-chemistry parameters at TMR was conducted in a study between October 2009 and February 2011 (Grimmer 2011). In-situ measurements of pH and salinity are presented in Table 2.1. Salinity is an important physicochemical property of seawater, which forms part of the carbonate system parameters. It is a measure of the dissolved salts and numerous studies have shown it to be an important factor governing the structure of benthic communities (e.g. Lirman et al. 2003; Uwadia 2009; Naser 2011). Temperature measurements from an underwater temperature recorder (UTR) located at Nine-mile Reef, Sodwana Bay yielded mean sea temperatures of 24.45±1.74˚C with summer and winter peaks of 28.6 ˚C and 21.0 ˚C, respectively. Mean summer and winter pH values were 8.25±.06 and 8.22±0.04 and mean summer and winter salinity values were 32.73 and 32.19, respectively.

Table 2.1. Mean summer and winter pH and salinity of Two-mile Reef (Grimmer 2011).

Parameter	Summer average	Winter average
pH	8.25±0.06	8.22±0.04
Salinity	32.73	32.19

In a food web and trophic connectivity study conducted by Parkinson (2012), seaweeds (excluding certain red seaweeds) together with phytoplankton were the main sources of primary production at Sodwana Bay. Chlorophyll a (Chl-*a*) is a measure of the primary productivity within an ecosystem and is, therefore, important to consider when conducting ecological studies (Jamshidi & Bin Abu Baka 2011). Low chlorophyll *a* levels are usually observed at Sodwana Bay. This is attributed to the Agulhas Current diverging from the coast, south of Cape St Lucia, subsequently supporting upwelling in the Natal Bight (Roberts et al. 2006).

2.2. Field collection

Present day and palaeo-foraminiferal assemblages were studied as two distinct components, 1) a habitat comparison of reef-associated unconsolidated sediments and coral rubble adjacent to TMR as well as the analysis of ambient physico-chemistry parameters and 2) a Late Holocene study of TMR associated unconsolidated sediments through bioclastic sediment core analysis. The study of these particular components were selected as the results supplement each other, with the various techniques employed including water chemistry analysis, grain size distribution, sediment characterisation, foraminiferal assemblage analysis, and stable isotope analysis. The habitat comparison study was designed across and adjacent to the reef at three locations between coral rubble and unconsolidated sediment and involved the collection of 45 samples. A palaeoclimatic study of TMR was achieved

through the analysis of three bioclastic sediment cores (X, Y and Z) collected on the inshore side of TMR. Overall 32, 16 and 18 samples were analysed from cores X, Y and Z. All samples, for both components, were collected by scuba divers.

2.2.1 Water chemistry

One winter (September 2013) and summer (January 2014) measurement was taken for nutrients (PO_4^{3-}, NO_3^- and SiO_2) and chlorophyll *a* (Chl-*a*) values. Additional water sampling was conducted on TMR on six occasions spanning summer (December 2013, January 2014 and February 2014) and winter (June 2014, July 2014 and September 2013) to characterise the spatio-temporal variability of the study area water. Nine water samples were collected on each occasion, for measurement of temperature, pH, total alkalinity (T_A) and salinity.

A 3.6 L horizontal Van Dorn water bottle was manufactured in-house for collection of seawater samples. Prior to use, the sampler was acid washed with 1M HCL and thoroughly rinsed with distilled water at least 4 times. The sampler was taken down vertically by a SCUBA diver and triggered, horizontally, 1 m above the reef (Figure 2.5). On the surface, the full sampler was shielded from the sunlight. Temperature and pH were measured immediately and water samples were collected for analyses in the following order T_A, Chl-*a*, nutrients (PO_4^{3-}, NO_3^- and SiO_2) and salinity (Karl et al. 1990; Karl & Church 2014).

Figure 2.5. Van Dorn bottle being triggered by a diver to collect a water sample.

Prior to use, sample bottles, filtration units and apparatus were acid-washed with 1M HCL, and thoroughly rinsed four times with distilled water to ensure no residual acid remained.

Temperature and pH

A water sample was collected in a clean 50 ml, sterile Falcon tube. The temperature (°C) and temperature compensated pH of each sample was recorded using a Eutech pH610 pH meter with a single junction Eutech pH probe. The pH meter was calibrated using Metrohm certified pH buffers 4 and 7 and all data was reported on the US National Bureau of Standards (NBS) pH scale.

Total Alkalinity

A brown 250 ml borosilicate sample bottle was rinsed three times with water from the sampler. Silicon tubing attached to the van Dorn tap was inserted to the bottom of the bottle and twice the volume allowed to overflow before the sample was collected. A 3 ml plastic bulb dropper was then used to remove 2 ml of sample from the neck to prevent the bottle from overflowing when the stopper was inserted. The inside of the neck was dried with a Kimwipe and 50 µL of saturated mercuric chloride added to poison the sample. The stopper, lightly greased with Apiezon L high vacuum grease, was inserted into the bottle and the bottle inverted several times. The stopper was secured to the bottle with a rubber band and covered in foil and placed on ice for transportation and then refrigerated until analysis.

A Metrohm Titrando 888 potentiometric titrator with LL Aquatrode+ Pt1000 F/4mm and Tiamo light software was used for T_A analysis using a two-stage open cell titration as outlined in Dickson et al. (2007). This method uses the Gran titration method, which involves the titration of a sample beyond the bicarbonate end point (de Andrade et al. 2005). A series of back calculations were then used to determine the equivalence points for hydroxide, carbonate, and bicarbonate. The titrator was operated in a temperature-controlled room and the sampling vessel fitted with a water jacket connected to a water bath at 25ºC. Samples were allowed to equilibrate to this temperature prior to analysis and ± 80 ml sample was titrated with 0.1M (0.1N) HCL. Certified reference materials (CRM) obtained from the Marine Physical Laboratory, Scripps Institution of Oceanography were used to calibrate the titrator. The total alkalinity results were calculated using, the raw data from the titrations, in a spreadsheet provided by the Marine Physical Laboratory, Scripps Institution of Oceanography. Readings were further corrected for mercuric chloride using the following equation (Dickson et al. 2007):

$$T_A = 1.0002\ x\ T_A{}' \qquad 2.1$$

Where, T_A = corrected total alkalinity; $T_A{}'$ = calculated total alkalinity value from the spreadsheet

Chlorophyll a

Care was taken to ensure all filtration occurred out of direct sunlight to prevent photodegradation of the Chl-*a*. A Sartorious filtration unit was rinsed three times with water from the sampler. A hand vacuum pump was used to filter 1L of sample through a 47 mm GF/F Whatman filter, ensuring the pressure did not exceed 5 psi. Using filter forceps; the filter paper was then carefully folded over, taking care not to touch and contaminate the filter. The folded filter was placed in a 20 ml, screw-top, glass vial with 10 ml of 90% reagent grade acetone, ensuring the filter was completely submerged. The lids were sealed with parafilm to prevent evaporation and vials were wrapped in aluminium foil and placed immediately on ice and frozen on return to the laboratory. Samples were analysed within two days for Chl-*a* (µg/L) content using a Turner 10AU fluorometer at the Coastal Systems Research Group at the Council for Scientific and Industrial Research (CSIR) in Durban.

Nutrients

A single sample for each of NO_3^-, PO_4^{3-} and SiO_2 analysis was collected. At collection, a Sartorius filtration unit was rinsed three times with sample water. Water was passed through a sterile MCE membrane (0.45 µm, 47 mm) using a hand vacuum pump ensuring the pressure did not exceed 5psi. A 500 ml, opaque high-density polyethylene (HDPE) sample bottle was rinsed three times with filtrate and the sample bottle filled with 375 ml of filtrate, wrapped in aluminium foil and placed upright on ice. Samples were frozen until analysis by the Consulting and Analytical Services (CAS) Laboratory, Durban T0064 at the CSIR in Durban within one week. All samples were analysed using a SEAL BRAN+LUEBBE Auto Analyser 3. The NO_3^- and PO_4^{3-} samples were assessed using automated colourimetry and SiO_2 using the colorimetric method.

Salinity

A 30 ml plastic falcon tube was filled, placed on ice and refrigerated in the laboratory until analysis. The conductivity of each sample was measured using an 856 Metrohm conductivity module with a five ring conductivity measuring cell at 25ºC. A 12.87 mS/cm Metrohm conductivity standard was used to calibrate the probe prior to use. The conductivity and temperature of each sample were then used to calculate the salinity value.

2.3. Unconsolidated sediment and rubble laboratory procedures

2.3.1 Grain size analysis

Grain size distributions of the spatial representation of habitats on TMR and down core were analysed, by Environmental Mapping and Surveying (EMS), using ±5 g of sediment. The percentages

of gravel (gravel), very coarse sand (vcs), coarse sand (cs), medium sand (ms), fine sand (fs) and very fine sand (vfs) were determined for all sites using the Wentworth design of graded, nested sieves (Wentworth 1922) (Table 2.2). These values together with mean and median grain size were presented on the Wentworth scale and phi notation.

The samples were initially oven-dried overnight at 70ºC, the dry mass recorded and then wet-sieved using a 63 µm sieve. The sieved samples were collected and re-dried. Mass percent of mud (i.e. <63 um) was calculated. The sand and gravel fraction (i.e. >63 um) were then dry-sieved in a nested sieve array from 4000 µm to 90 µm with the 63 µm to 90 µm fractions being retained in a tray at the base. Using the mass of the sediment retained in each sieve, the grain size statistics were then calculated.

Table 2.2. Wentworth grain size classification of sediments and corresponding phi notation (after: Wentworth 1922).

Sediment type	Grain size (mm)	phi (φ) scale
Gravel (gravel)	>2	<-1.0
Very coarse sand (vcs)	1-2	-1.0 - 0.0
Coarse sand (cs)	0.5-1	0.0 - 1.0
Medium sand (ms)	0.25-0.5	1.0 - 2.0
Fine sand (fs)	0.125-0.25	2.0 - 3.0
Very fine sand (vfs)	0.0625-0.125	3.0 - 4.0
Mud (mud)	<0.0625	>4.0

2.3.2 Sorting and skewness

Grain size variation was represented per sample using a sorting and skewness co-efficient. Classes are presented in Table 2.3. Sorting and skewness determinations for sediment samples were conducted by EMS, using the grain size statistics previously calculated.

Table 2.3. Sorting sediment classes, identified by Folk (1968), used in classification.

Sorting class	Phi (φ) scale
Very well sorted	<0.35
Well sorted	0.35 – 0.50
Moderately well sorted	0.50 -0.71
Moderately sorted	0.71 – 1.00
Poorly sorted	> 1.00

2.3.3 Sediment carbonate content analysis

The carbonate 'bomb' method was employed at EMS to determine the carbonate content (calcite equivalent) of sediment samples (±2 g). Hydrochloric acid (HCL) was added to 1 g dried sediment within an enclosed reaction cylinder (reactor). During this reaction, CO_2 is released and the resulting pressure within the reactor is proportional to the calcite of the sample.

2.3.4 Foraminiferal assemblages

Habitat comparison samples (Chapter 3) were wet-sieved into the >500 µm fraction only. Core samples (Chapter 4) were wet-sieved using a nested sieve design ranging from 500 µm, 250 µm and 125 µm. The surface of sieved samples was blot-dried with paper towel and the wet weight obtained for each individual size fraction. In turn, each sample, excluding the 125 µm fraction, was placed in a perspex bogorov counting tray and all the Foraminifera were picked out under a stereomicroscope (Zeiss Stemi DV4, 20 – 32x magnification coupled with a 2.0x lens). Wet picking was achieved using the bristles of a fine (000) paintbrush and at least 300 Foraminifera were picked from each sample. Forams from the 125 µm sediment samples were not picked, but rather photographs of each Foraminifera were taken using the Carl Zeiss Axiovision 4.8 software. The 125 µm samples were placed in a perspex bogorov counting tray and viewed under a Zeiss fully automated SterREO Discovery V12 stereomicroscope with a Zeiss PlanApo S 0.63x FWD 81 mm objective, connected to an Axiocam MRc 5 camera.

Foraminifera were identified to the lowest possible taxonomic level using available literature (e.g. Loeblich & Tappan 1987, 1994; Yassini & Jones 1995; Langer et al. 2013a). Live Foraminifera counts of genera and species were also recorded. Live Foraminifera were identified on the basis of visual identification of cytoplasmic colouration due to the presence of endosymbionts. The vital dye, Rose Bengal, was initially used to identify live Foraminifera specimens. However, based on a pilot study on samples collected from TMR, it was decided not to continue with this method as numbers of live specimens were overestimated after staining. This has also been noted by other authors (e.g. Bernhard 2000; Murray & Bowser 2000). Following identification, Foraminifera were either stored dry or were transferred to 70% ethanol for long term storage. Physical and/or photographic reference collections were compiled of all taxa.

2.3.5 Stable isotope analysis

The foraminiferal stable oxygen and carbon isotopes were analysed at iThemba LABS in November 2014. Samples were run on a Thermo Gasbench II coupled to a Thermo Delta V Advantage mass

spectrometer. As the tests were picked from bioclastic sediment, with very little organic matter, pre-treatment merely involved mechanical cleaning of the tests through repeated rinsing with distilled water. Tests, of a single species, *Amphistegina lobifera,* and from the size range 500-800 μm were used. The phosphoric acid (H_3PO_4) method was used to liberate carbon dioxide (CO_2) from the carbonates. A sample weight of ± 0.5 mg, treated with H_3PO_4, was used in this study to extract the $\delta^{18}O$ and $\delta^{13}C$ values of the carbonate samples. Samples were run against internal carbonate standards (CSS and MHS1) with all results reported in the standard δ notation (‰) relative to Vienna Pee Dee Belemnite (VPDB).

2.3.6 Radiocarbon analysis

Adult tests of *A.lobifera* from the >500 μm fraction, with comparable sizes, were picked out using bristles of a moistened fine (000) paintbrush. Tests were rinsed with distilled water, placed on a piece of foil, allowed to air dry before packaged in the foil, placed in a sealable plastic bag and sent off for analysis. No further pre-treatment was applied to the tests prior to analysis. The ^{14}C dating was performed at the Beta Analytic Radiocarbon Dating Lab in Florida in April 2013 and January 2015. This is an ISO/IEC 17025:2005 accredited Radiocarbon Dating Laboratory and uses the Accelerator Mass Spectrometry (AMS) method (Broecker et al. 1990) to date Foraminifera tests. AMS carbon dating involved the initial reduction of the sample carbon to graphite. The graphite is then analysed together with standards for its ^{14}C content in an accelerator mass spectrometer. The result is then corrected for isotopic fractionation and then converted into a calendar-calibrated date. A local reservoir correction of DeltaR = 213 and DeltaRErr = 57 from Natal (Southon 2002) was used in the interpretation of the results and the Marine09 calibration curve was used to convert the conventional radiocarbon age to its representative calendar-calibrated age.

2.4. Statistical techniques used

An overview of statistical techniques used in this study is given in this Section. However, the specific formula followed for each project component is given in the respective chapters. Software used for data analysis included Excel 2010, Brodgar v2.7.2, Sigma Plot v11.0, Primer v6 and Past v3.

2.4.1 Abiotic variables

The abiotic variables were tested for collinearity using a nonparametric Spearman rank correlation (*p*). This correlation requires transforming both measurements to ranks with no assumptions of distribution normality (Pollard 1979; Clarke & Ainsworth 1993). In general, environmental variables that were highly correlated (p= ±0.90) were reduced to a single representative (Clarke & Ainsworth

1993). Each correlation was assessed individually, and the variable not deemed vital for the analysis was omitted from the model. Draftsman and pairwise scatter plots were used to determine if variable distributions were skewed. A draftsman plot plots the values of each variable against each other. Skewed variables were appropriately transformed. If the data were right skewed a square-root or log transformation was applied with an inverse transformation (1/x) used for left skewed data (Clarke & Gorley 2006). Following transformation, the Euclidian distance similarity coefficient was calculated from the abiotic data.

2.4.2 Univariate analyses

Univariate community measures, abundance (*N*: ind/m^2) and richness (*S*: no. of taxa) and diversity measures, Shannon-Wiener diversity index (*H'*), Pielou's Evenness index (*J'*) and Margalef's Richness (*d*) were calculated from raw taxon data, for all *a priori* selected factors, using the DIVERSE procedure within PRIMER v6 (Clarke & Warwick 1994; Clarke & Warwick 2001).

Shannon-Wiener diversity index (*H'*) relies on both on the number of taxa and their relative abundances (Shannon & Weaver 1963). In this way rare species provide little contribution. The maximum value of *H'* is obtained when there is an equal abundance of all species in a sample (Shannon & Weaver 1963). It was used to identify changes in the structure of foraminiferal assemblages.

$$H' = -\sum_{i=1}^{S} p_i \ln p_i \qquad 2.2$$

Where p_i is the proportion of specimens of the *i*th taxon.

Pielou's Evenness index (*J'*) defines the spread of individuals between species (Pielou 1966). The evenness is low when there is a dominance of one species with *J'*=1 when all species are equally abundant (Pielou 1966).

$$J' = \frac{H'}{\ln S} \qquad 2.3$$

Where *H'* is the Shannon-Wiener diversity index.

Margalef's Richness (*d*) defines the taxon richness of the sample (Margalef 1958).

$$d = \frac{S - 1}{InN} \qquad 2.4$$

Where: *S* = Number of taxa, *N* = total number of individuals in the sample.

One and two-way analysis of variance (ANOVA) were used to test for significant differences ($p<0.05$) in the abiotic parameters between seasons and locations across the reef. ANOVA is a parametric technique; therefore, normality and homogeneity of variance were determined prior to analysis. Tukey's test was used as a post-hoc test when significant differences were found. When conditions of normality and equality of variance could not be satisfied, alternative non-parametric tests (e.g. Kruskall-Wallis, Mann-Whitney, U-test, Holm-Sidak) were used. These tests were performed on ranked data.

2.4.3 Multivariate analysis

Prior to analysis, foraminiferal data was transformed. It is not necessary for data to be normally distributed, however, for some types of multivariate analyses, transformations are still applied to down-weight more abundant taxa. Following transformation, the Bray-Curtis (B-C) similarity coefficient was calculated from the biotic data. This is a widely used method as it gives equal weight to all taxa and is not affected by absences (Yoshioka 2008). It provides a single measure displaying the similarity in community structure between samples. Following transformation and similarity coefficient calculation, various multivariate analyses were carried out. Multivariate statistics used in this study included Q-type cluster analysis, non-metric multidimensional scaling (nMDS), similarity profile analysis (SIMPROF), similarity percentage (SIMPER) analysis, permutational multivariate analysis of variance (PERMANOVA), RELATE function, BVSTEP method, global BEST test and canonical analysis of principal coordinates (CAP).

Hierarchical clustering (cluster analysis) and nMDS ordinations are used to show similarities between samples, depicted in their distances apart. Clustering segregates samples according to groupings and denotes the similarity between these groups/clusters (Parker & Arnold 1999). An nMDS attempts to display the samples in a two or three dimensional space whereby the proximity of samples reflects their similarity (Parker & Arnold 1999). The Kruskall stress value expresses how well the ordination map reflects the actual data (Rees et al. 2004). A stress value >0.2 indicates the ordination does not

adequately depict the data in 2D space whereas a stress <0.2 indicates a satisfactory result and <0.1 is an ideal ordination (Rees et al. 2004). SIMPROF analysis is used to objectively define groups within datasets (Clarke et al. 2008). It has the advantage over the classical hierarchical clustering method which is more subjective. It determines if observed similarities within the data are smaller/larger than what would be expected by chance (Clarke et al. 2008). The structure is determined through plotting the similarity profile with the resultant mean permuted profile (Clarke et al. 2008).

A SIMPER test uses a pairwise comparison and finds the average contribution (δ_i) of each taxon (Rees et al. 2004). These together with the associated standard deviation SD (δ_i) are computed. The resultant ratio ($\delta_i/SD\delta_i$) defines how consistently taxa contribute to the average similarity within groups as well as to the average dissimilarity between groups. A good discriminating taxon contributes consistently to the similarity/dissimilarity and therefore has a low SD and subsequently high SIM/SD ratio (Clark & Gorley 2006). A PERMANOVA is a permutation test, testing the null hypothesis of no differences between the factors under consideration (Clark & Gorley 2006). According to Anderson and Walsh (2013), PERMANOVA is a more robust test in comparison to an Analysis of Similarity (ANOSIM), testing the H_0: "the centroids of the groups, as defined in the space of chosen resemblance measure, are equivalent for all groups" whereas the ANOSIM null hypothesis is more general with a significant result potentially caused by a variety of factors (e.g. difference in group location, dispersion, skewness). A *p* statistic < 0.05 in PERMANOVA indicates a significant result. The RELATE function calculates a rank correlation coefficient (e.g. Spearman's (ρ)) between samples from two datasets. When ρ=1 the datasets match perfectly (Clark & Gorley 2006).

The BVSTEP method is used to determine which single variable or combination of abiotic variables best describe the biotic dataset. The Spearman Rank Correlations (ρ) between the biotic and abiotic similarity matrices are computed (Clark & Gorley 2006). This method uses a stepwise search of variables. It uses both forward and backwards steps successively to determine the best combination of variables best describing the biotic dataset (Clark & Gorley 2006). A "global BEST test" is then used to determine the significance of the subset of environmental variables. It tests the null hypothesis of no relationship between the biotic and abiotic data collected for the selected samples (Clark & Gorley 2006). A CAP analysis is used to find axes through the biotic dataset which have the highest correlation with the variables identified in the BVSTEP analysis. Eigenvalues (e.g. δ_1^2, δ_2^2) define how much of the variance is explained by each axis (Clark & Gorley 2006). The Euclidian distance and Bray-Curtis similarity measure are used for abiotic and biotic data, respectively.

CHAPTER 3
FORAMINIFERAL DISTRIBUTION, ECOLOGY AND HABITAT AT TWO-MILE REEF

3.1. Introduction

Like corals, Large Benthic Foraminifera (LBF) are organisms which are calcareous, can host symbionts and are sensitive to ocean property changes predicted over the next century (Fujita et al. 2009). These changes, involving primarily increasing sea temperatures and decreasing pH, will potentially have negative impacts on calcareous organisms due to the associated change in the carbonate system. Monitoring of the carbonate system parameters (temperature, pH, salinity, total alkalinity and/or dissolved inorganic carbon) is, therefore, imperative. Nutrients are also important, as measurements of silicate and phosphate are required to calculate the remaining carbonate system parameters, aragonite (Ω_{Ar}) and calcite (Ω_{Ca}) saturation state. Major nutrient elements such as nitrogen, phosphorus and silicon, together with certain trace metals (e.g. iron) also control primary production within oceanic environments (Martin & Fitzwater 1988; Falkowski et al. 1998).

Functionally, LBF play important ecological and geological roles through the fixation of inorganic carbon (Lee 2006); they aid in buffering daily pH in shallow water environments (Santos et al. 2011) and their calcareous tests accumulate and contribute to sedimentary landforms (Hohenegger 2006).These protists are also among the main primary and carbonate producers in a variety of reef environments (Lee & Hallock 1987; Langer et al. 1997; Hohenegger 2006; Fujita & Fujimura 2008). They make up the majority of sand-sized sediments of Pacific reef islands (Fujita et al. 2009). They contributed up to 80% of the carbonate in tropical Cenozoic settings and are dominant in Holocene carbonate (Renema et al. 2013). Tudhope and Scoffin (1988) also estimated Foraminifera to have contributed a third of the carbonate on the Great Barrier Reef (GBR) shelf.

Numerous, in situ and ex situ, studies have demonstrated the usefulness of these protists in assessing environmental changes on coral reefs and in reef-associated environments, through assessment of environmental parameters relative to occurrence patterns (e.g. Troelstra et al. 1996; Fujita et al. 2009; Mazumder et al. 2012) and laboratory experiments (e.g. Fujita et al. 2011; McIntyre-Wressnig et al. 2011). The distribution of modern day LBF associated with reef environments is dependent on the depth-related parameters of light intensity, temperature, nutrients, substratum type and hydrodynamic energy (Renema et al. 2013). This emphasises the need to include water chemistry (carbonate system

parameters, nutrients and chlorophyll *a*) analysis in conjunction with present-day foraminiferal sampling initiatives.

Considering the complexity of coral reefs and reef-associated environments, a habitat comparison study was undertaken to establish a baseline of the present-day LBF population associated with Two-mile Reef (TMR). Two-mile Reef is comprised of four distinct habitats, namely reef, scattered reef, bioclastic sediment and quartzose sediment. The live (coloured protoplasm) population together with the total Foraminifera assemblage (entire assemblage: live and dead) was investigated. Three different locations, experiencing varying degrees of turbulence, were sampled. Two different substrata, sediment and rubble, were also sampled. Only the Large Benthic Foraminifera (LBF) assemblage (>500 µm) was addressed and this was not considered to impact negatively on the study, given the significance LBF play in reef habitats (Doo et al. 2012). Various water chemistry parameters were also measured across the sampling locations to elucidate the primary environmental factors affecting these foraminiferal assemblages.

3.2. Objectives and hypotheses

3.2.1 Objectives

1. Determine if there is a difference in the living and total LBF assemblages within reef-associated sediment and coral rubble.
2. Establish whether certain abiotic variables influence the distribution of Foraminifera on TMR.

3.2.2 Hypotheses

H_{a1}: Living LBF and total foraminiferal assemblages differ with substratum type and location across the reef-associated environment.

H_{a2}: There is a relationship between the foraminiferal assemblages and the measured environmental parameters.

3.3. Unconsolidated sediment, rubble and water sampling across Two-mile Reef

During January and February 2013, 45 samples were collected using SCUBA along three transects, each including a bioclastic sediment (BS) location, a near-reef (NR) location adjacent to the reef (representing scattered reef) and a reef gully location (G) with unconsolidated substratum (Figures 3.1 and 3.4). The BS locations were situated 200 m off the reef, adjacent to the quartzose sediment boundary. The NR location represented the transition from reef zone to sediment. Three replicates

were collected of both coral rubble and sediment at each of three sites at locations, G and NR. Only sediment samples were collected at the three BS sites, as no rubble was present. Due to difficult field sampling conditions, sediment and rubble samples were collected during different field trips (January and February 2013) and from different gullies at location G. However, the samples were collected in the same season, eliminating seasonality as a confounding factor. The water chemistry parameters (temperature, pH, total alkalinity (T_A) and salinity) were measured at all nine sites over six sampling months, over summer and winter. However, only one summer and one winter chlorophyll *a* (Chl-*a*) and nutrient (phosphate - PO_4^{3-}, nitrate - NO_3^- and silicate - SiO_2) measurement was taken across the nine sites (Chapter 2).

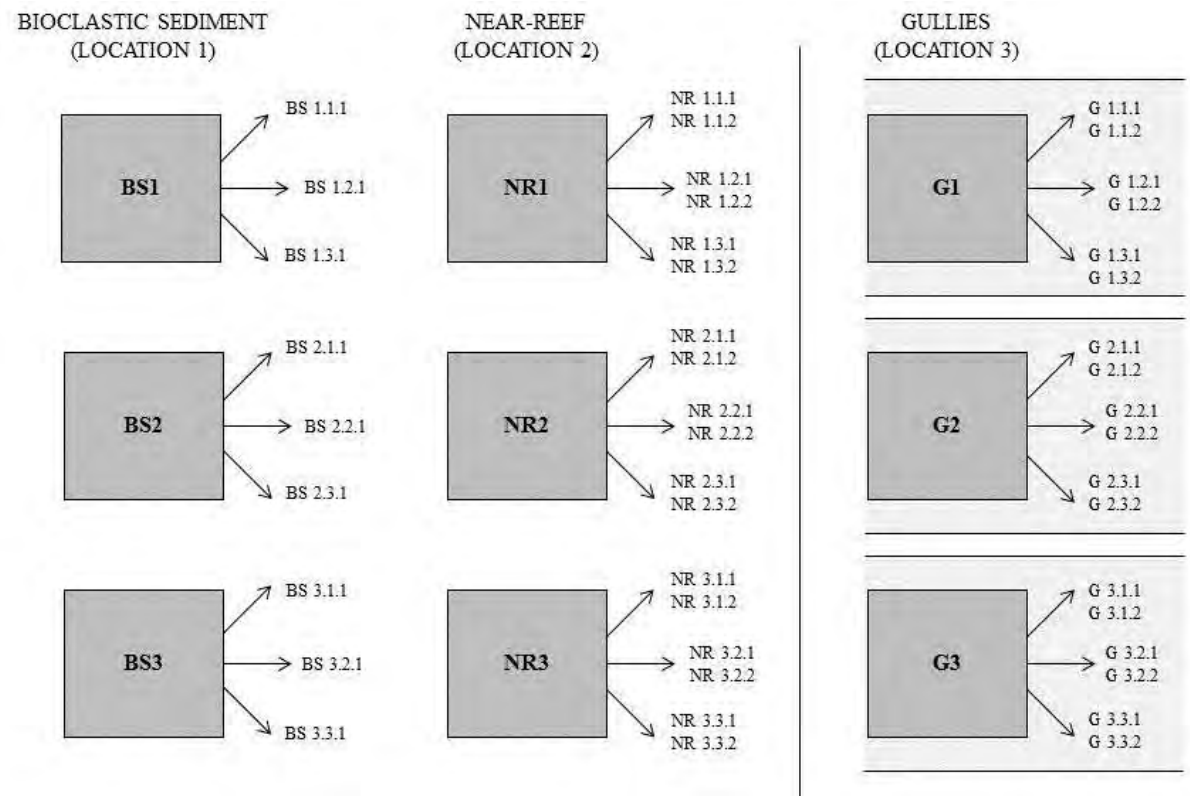

Figure 3.1. Diagram of the sampling strategy employed. Sites with #.1 as a third subcategory number (e.g.: NR 1.1.1) denote sediment samples, whereas sites with #.2 as their third subcategory (e.g. NR 1.1.2) denote coral rubble samples (BS= bioclastic sediment, NR= near-reef and G= gully).

The size of the rubble differed across sampling sites resulting in variable sample sizes. Coral rubble collection involved selecting two to four fist-sized rubble fragments (Figure 3.2A), which were placed directly into Zip-lock plastic bags and brought to the surface. On the surface, each fragment of rubble was gently scrubbed with a soft toothbrush and placed in a sonicator for 20 minutes to dislodge remaining Foraminifera. The resulting slurry was fixed in 4% formal-saline buffered with borax.

A 10 x 10 cm stainless steel frame was used to demarcate the area for sediment collection (Figure 3.2B). Once the frame was placed on the selected sampling site, a small spade was used to collect the surface 1-2 cm sediments and stored in a sealable plastic bag for transportation to the water surface. The sediment was fixed in 4% formal-saline buffered with borax.

In total, 27 sediment samples and 18 rubble samples were collected. One replicate from each sediment site was selected for grain size and carbonate content analysis (Chapter 2).

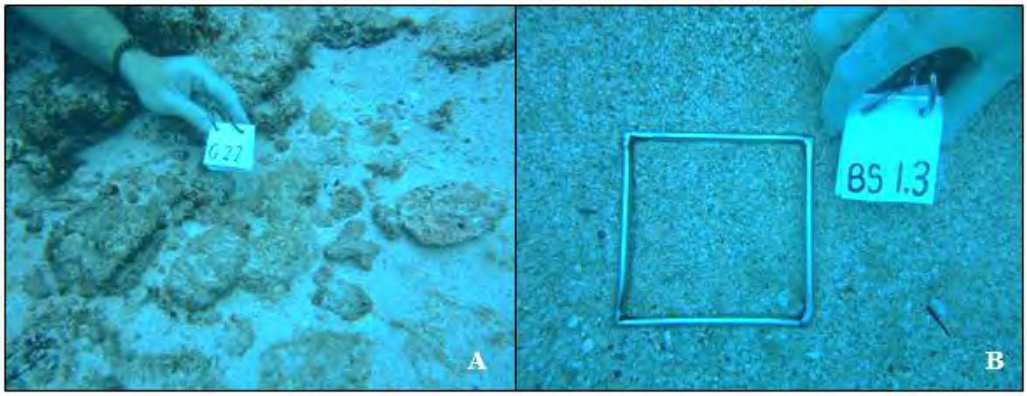

Figure 3.2. **A** Coral rubble and **B** sediment sampling.

The surface area of the rubble fragment collected at each site, was calculated using Carl Zeiss Axio Vision 4.8 software. The cleaned and air-dried rubble fragments were placed on gridded paper and photographed from a standard height (Figure 3.3). The outline of each fragment was determined using the outline tool in Axio Vision. Only the 2D surface area (m^2) was considered, in order to eliminate the confounding influence of the third dimension (volume - m^3).

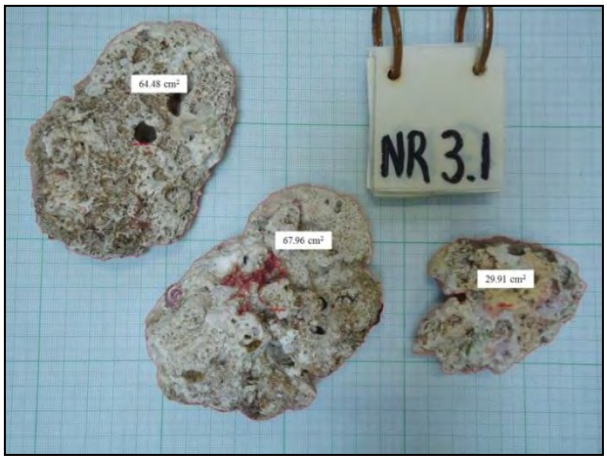

Figure 3.3. Photograph of coral rubble on gridded paper after tracing on Carl Zeiss Axio Vision 4.8 software.

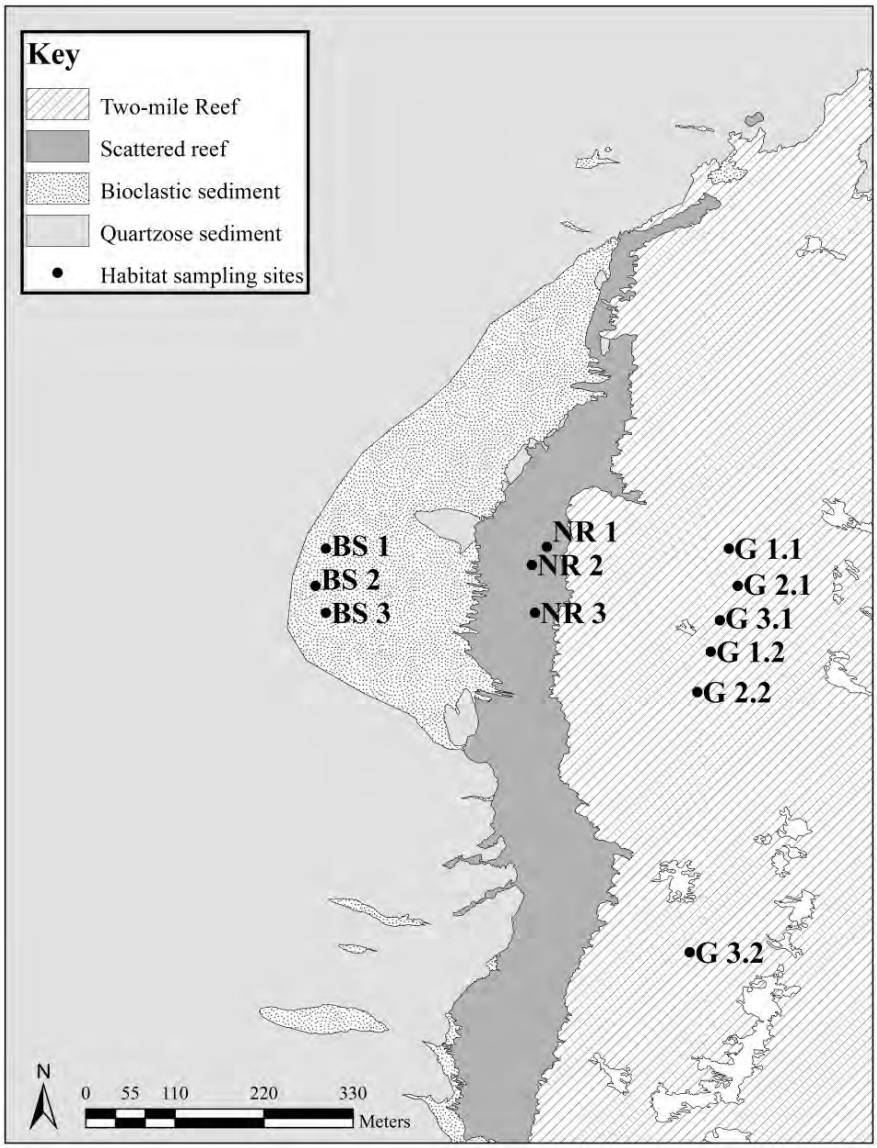

Figure 3.4. Habitat comparison sites at Two-mile Reef. G locations with #.1 as the second subcategory denote gullies where sediment samples were collected. Locations with #.2 as the second subcategory denote gullies where rubble samples were collected (BS= bioclastic sediment, NR= near-reef and G= gully).

3.3.1 Foraminiferal analysis

The >500 µm Foraminifera fraction (pre-adults and adults) was picked from the 45 samples collected. The abundance of Foraminifera (ind/m^2) was calculated at each site, utilising the cumulative seafloor area of the rubble pieces and frame size for the sediment samples. All sediment counts were additionally standardised to ind/g. The wet weight of each sediment sample, previously recorded during the wet sieving process, was used to calculate the density of Foraminifera per gram of sediment. In this way a comparison of the two metrics, ind/m^2 and ind/g, could be compared. Comparisons of foraminiferal assemblages, across substrata and locations, were assessed using percentage contributions at the genus and species level.

3.3.2 Statistical analysis

An explanation of statistical tests used in this Chapter is given in Chapter 2. The measured water chemistry parameters were first tested for any significant relationships between sites, months and seasons. Descriptive statistics are given for each parameter and sediment characteristics defined for all locations. The full set of 15 sediment characteristic variables together with the water chemistry parameters (Table 3.1) were tested for collinearity using draftsman plots and a Spearman correlation matrix. The redundant variables, not deemed important for the analysis, with very strong correlations ($\rho>0.9$) were subsequently omitted from the model.

Table 3.1. Measured physico-chemical and sediment characteristics.

Environmental variable	
Physico-chemical	Temperature (°C)
	pH
	Salinity
	Total alkalinity (µmol/kg)
	Ω_{Ar}
	Ω_{Ca}
	Chlorophyll *a* (µg/L)
	Nitrate (mg/L)
	Phosphate (mg/L)
	Silicate (mg/L)
Sediment characteristics	Depth (m)
	Gravel (%gravel)
	Very coarse sand (%vcs)
	Coarse sand (%cs)
	Medium sand (%ms)
	Fine sand (%fs)
	Very fine sand (%vfs)
	Mud (%mud)
	Carbonate content (%)
	Mean (phi)
	Mean (mm)
	Median (phi)
	Median (mm)
	Sorting
	Skewness

For the Foraminifera analyses, three factors were tested namely assemblage type, substratum type and location. Foraminifera assemblages were classified as living, 'other' or as being part of the total assemblage. The 'live' assemblage represented those Foraminifera which displayed coloured protoplasm, a characteristic of a living specimen. Specimens classified as 'other' included all Foraminifera which either had no coloured protoplasm or the protoplasm was not visible due to the

nature of the test. As staining was not used, it was not easy to distinguish the majority of the living, non-symbiont bearing individuals (e.g. *Textularia* and *Quinqueloculina*), thus, as a precaution, the assemblage was categorised as 'other', rather than dead. The remaining category (total assemblage) comprised pooled Foraminifera, the sum of 'live' and 'other'. Only the live and total assemblages were assessed further.

All taxonomic counts were first standardised to ind/m^2 and fourth-root transformed to down-weight the dominance of highly abundant taxa, in particular *Amphistegina* spp. Analysis of the distribution and community structure of living LBF assemblages were made first. Abundance was compared between the substrata. The main living taxa at each location are also given for each substratum. A SIMPER analysis was used to determine the distinguishing taxa for each substratum as well as to determine which accounted most for the dissimilarity. A PERMANOVA was then used to test if significant differences existed between the rubble and sediment Foraminifera assemblages. A pairwise PERMANOVA was utilised as a *post hoc* test.

Subsequent to determining the dispersion of the live LBF, the total foraminiferal assemblage was then assessed. Univariate statistics, abundance, number of taxa, diversity and evenness were explored for each substratum at each sampling location. Significant differences were tested for, both between the substratum types and across locations for all the univariate measures. A Q-mode cluster analysis, based on similarity, was used to determine how the samples were clustering and to visually assess if any groupings were evident. Following the Cluster analysis a SIMPER test was performed to establish which taxa accounted the most for the dissimilarity between the two substratum assemblages, irrespective of location. The nMDS ordinations were performed separately on the rubble and sediment samples to determine if any samples were grouping together. Following the nMDS, a PERMANOVA was used to determine the significance of the groupings.

The main taxa contributing to the sediment as a whole were explored at the level of suborder and genus. A PERMANOVA was then used to test for any significant differences in the assemblages across the three locations. A pairwise PERMANOVA was performed as a *post-hoc* test to establish which location accounted for the difference detected. The main taxonomic contributions to the sediment samples, across each location, were then explored. SIMPER analyses was run for each location to determine which taxa contributed most and were the most distinguishing for each location. A PERMANOVA was then utilised, to establish if there were any significant differences across the three sites at each location. This was used to test how homogenous the sample locations were. The

same analysis was performed for the rubble samples; firstly an assessment of the contribution of the main suborder and genera to the rubble samples was determined. A PERMANOVA was used to test for differences in assemblages between the two rubble locations. This was followed by an overview of the rubble assemblages at each location. A PERMANOVA was again used to test for homogeneity across the three sites at each rubble location.

Following the method outlined by Stephenson et al. (2015), an abundance index (S/R_R) was then calculated by dividing the mean total relative abundances (%) of the 20 most common genera in the sediment (S) and rubble (R) samples. An index (S/R_{Tot}) was also calculated using the absolute abundances (ind/m^2). These were used to determine, were the taxa originated and were concentrated in this reef-associated environment. Two measures were also compared here, namely abundance (ind/m^2) and density (ind/g) for the total sediment assemblages, as the latter is used in the following Chapter. The nMDS ordinations were performed to depict the similarities within the data. The RELATE procedure was then performed to compare the Bray-Curtis matrices between the sediment abundance (ind/m^2) and density (ind/g) data and establish how well they compared. On obtaining an overview of the biotic and abiotic data, the BVSTEP method was then used to establish if there were any correlations between the measured abiotic variables and the foraminiferal assemblages. The live and total assemblages were assessed separately for each substratum. A CAP analysis was performed, using the identified variables from the BVSTEP, to establish the best axes through the multivariate Foraminifera data and their relation to the abiotic variables. Vectors of the most distinguishing taxa were also plotted to ascertain the relationships.

3.4. Results

3.4.1 Water chemistry parameters

In winter, NO_3^-, PO_4^{3-} and SiO_2 values were below detection limits and Chl-*a* ranged from 0.17 – 0.64 (µg/L) with a mean of 0.39 ± 0.14 SD (µg/L) across all locations. In summer, NO_3^- values were below the detection limit (0.005mg/L) except at two sites, BS3 and NR4 (0.005 mg/L). All PO_4^{3-} values were below the detection limit (0.004mg/L). Summer SiO_2 values ranged from 0.10 – 0.30 mg/L with a mean of 0.20 ± 0.09 SD mg/L. In summer, Chl-*a* values ranged from 0.18 – 0.38 (µg/L) with a mean (0.29 ±0.07 SD µg/L) lower than in winter (0.39 ± 0.14 SD µg/L). No significant difference was found between summer and winter Chl-*a* values (t= 1.907, df= 16, p= 0.075) and no nested location effect was evident in winter (p> 0.05). A location effect was evident in summer Chl-*a* values (Kruskall-Wallis: H= 6.006, df= 2, p= 0.025), with the NR and G concentrations being significantly different (Tukey: q = 3.373, p < 0.05). A significant difference between summer and winter silica

concentrations (Mann-Whitney: U= 18, p= 0.013, n= 9) was found, however, no location effect (p< 0.05) was evident in either season.

The in-situ temperature ranged from 24.97 - 27.23°C in summer and 22.17 - 23.33°C in winter, and pH ranged from 8.14 - 8.31 and 8.04 - 8.23 in the summer and winter months, respectively. Salinity ranged from 34.84 - 35.92 in the summer months and 34.33 - 35.59 in the winter months. The T_A ranged from 2310.64 - 2332.09 µmol/kg and 2224.46 - 2320.81 µmol/kg in the summer and winter respectively with a standard deviation of replicate samples for all analyses averaging ± 0.17% (n= 106). The measured T_A, pH, temperature, salinity and nutrient concentrations were used to calculate the Ω_{Ar} and Ω_{Ca} values across the nine sites for all six sampling months (Table 3.2). The Ω_{Ar} ranged from 3.32 - 4.21 in summer and 2.43 - 3.51 in winter with Ω_{Ca} ranging from 5.00 - 6.39 in summer and 3.71 - 5.35 in winter. The Figures A1 and A2 (Appendix A) reveal no spatial separation, however, temporal variation, showing a strong seasonal effect was evident. These differences can also be seen in Figures 3.5. The box plots depict the variation in pH, salinity and temperature across the months, particularly the large seasonal difference between winter and summer temperatures. Variability is also evident in the December pH values.

Two-way ANOVAs (Table 3.3) revealed a significant difference between the seasons for the variables, temperature and salinity (p<0.05) with no significant seasonal effect in pH (p>0.05). No location effect was evident in the temperature, salinity and pH values with a significant difference between months (p<0.001) for all three environmental variables. Figures A3 and A4 (Appendix A) reveal an insignificant site effect with the exception of sites BS2, BS3 and NR5 in December Ω_{Ar}. A difference between months is evident in Figure 3.6. The box plots depict the variation in T_A, Ω_{Ar} and Ω_{Ca} across the months, particularly the variability evident in the T_A in June and the Ω_{Ar} and Ω_{Ca} in December. A Two-way ANOVA (Table 3.3) revealed a significant difference between the seasons (p= 0.002) but not between locations for T_A values. Similarly a seasonal effect was evident in the Ω_{Ar} and Ω_{Ca} values (p<0.001), however, again no location effect was evident across the reef (Table 3.3). No interactive effects were found (Table 3.3).

Table 3.2. Mean (± SD) water chemistry at bioclastic sediment (BS), near-reef (NR) and reef gully (G) locations on Two-mile Reef.

Date	Location	Temperature (°C)	pH	Salinity	Total alkalinity (T_A) (µmol/kg)	Ω_{Ar}	Ω_{Ca}
18/09/2013	BS	23.07 ± 0.17	8.17 ± 0.03	35.45 ± 0.02	2320.14 ± 8.03	3.20 ± 0.19	4.89 ± 0.29
	NR	22.93 ± 0.05	8.22 ± 0.01	35.56 ± 0.04	2320.81 ± 1.94	3.45 ± 0.03	5.26 ± 0.05
	G	22.87 ± 0.05	8.23 ± 0.01	35.59 ± 0.03	2315.14 ± 5.63	3.51 ± 0.05	5.35 ± 0.08
15/12/2013	BS	24.97 ± 0.12	8.31 ± 0.06	34.86 ± 0.08	2310.64 ± 5.71	4.21 ± 0.42	6.39 ± 0.64
	NR	25.43 ± 0.34	8.20 ± 0.09	34.84 ± 0.04	2315.76 ± 3.79	3.57 ± 0.54	5.41 ± 0.82
	G	24.97 ± 0.05	8.17 ± 0.02	34.90 ± 0.02	2313.85 ± 0.69	3.32 ± 0.09	5.04 ± 0.13
15/01/2014	BS	26.63 ± 0.05	8.17 ± 0.01	36.14 ± 0.21	2328.71 ± 5.57	3.58 ± 0.04	5.40 ± 0.05
	NR	26.40 ± 0.08	8.17 ± 0.00	35.92 ± 0.08	2329.79 ± 7.29	3.55 ± 0.04	5.36 ± 0.05
	G	26.50 ± 0.14	8.14 ± 0.03	35.82 ± 0.06	2321.24 ± 1.40	3.32 ± 0.17	5.00 ± 0.25
11/02/2014	BS	27.23 ± 0.29	8.15 ± 0.01	35.72 ± 0.08	2332.09 ± 3.72	3.51 ± 0.01	5.28 ± 0.02
	NR	26.57 ± 0.25	8.14 ± 0.01	35.78 ± 0.05	2312.47 ± 4.87	3.34 ± 0.06	5.04 ± 0.09
	G	26.83 ± 0.05	8.15 ± 0.03	35.78 ± 0.08	2320.78 ± 2.60	3.42 ± 0.19	5.15 ± 0.28
07/06/2014	BS	22.97 ± 0.05	8.19 ± 0.01	34.62 ± 0.07	2257.33 ± 36.27	3.13 ± 0.07	4.79 ± 0.11
	NR	23.10 ± 0.29	8.18 ± 0.01	34.71 ± 0.20	2240.38 ± 51.06	3.07 ± 0.10	4.68 ± 0.15
	G	23.33 ± 0.57	8.16 ± 0.00	34.55 ± 0.05	2224.46 ± 36.70	2.95 ± 0.10	4.50 ± 0.14
29/07/2014	BS	22.17 ± 0.05	8.10 ± 0.00	34.42 ± 0.10	2316.60 ± 4.02	2.68 ± 0.02	4.10 ± 0.03
	NR	22.27 ± 0.31	8.09 ± 0.01	34.33 ± 0.12	2314.31 ± 4.19	2.61 ± 0.01	3.99 ± 0.02
	G	22.43 ± 0.29	8.04 ± 0.03	34.36 ± 0.05	2312.83 ± 3.05	2.43 ± 0.16	3.71 ± 0.25

Table 3.3. Two-way ANOVA results for water chemistry on Two-mile Reef.

Parameter	Source of variation	DF	SS	MS	F	P
Temperature	Season	1	154.027	154.027	319.625	**<0.001**
	Location	2	0.029	0.015	0.030	0.970
	Season x Location	2	0.234	0.117	0.243	0.785
	Residual	48	23.131	0.482		
	Total	53	177.421	3.348		
pH	Season	1	0.009	0.009	2.344	0.132
	Location	2	0.011	0.006	1.398	0.257
	Season x Location	2	0.007	0.004	0.886	0.419
	Residual	48	0.191	0.004		
	Total	53	0.219	0.004		
Salinity	Season	1	6.369	6.369	22.595	**<0.001**
	Location	2	0.012	0.006	0.022	0.978
	Season x Location	2	0.022	0.011	0.039	0.962
	Residual	48	13.530	0.282		
	Total	53	19.934	0.376		
Total alkalinity	Season	1	11557.120	11557.120	10.337	**0.002**
	Location	2	821.855	410.927	0.368	0.694
	Season x Location	2	190.464	95.232	0.085	0.918
	Residual	48	53665.160	1118.024		
	Total	53	66234.600	1249.709		
Ω_{Ar}	Season	1	3.846	3.846	29.521	**<0.001**
	Location	2	0.468	0.234	1.796	0.177
	Season x Location	2	0.361	0.180	1.384	0.260
	Residual	48	6.254	0.130		
	Total	53	10.928	0.206		
Ω_{ca}	Season	1	7.726	7.726	25.570	**<0.001**
	Location	2	1.071	0.536	1.772	0.181
	Season x Location	2	0.811	0.406	1.342	0.271
	Residual	48	14.503	0.302		
	Total	53	24.112	0.455		

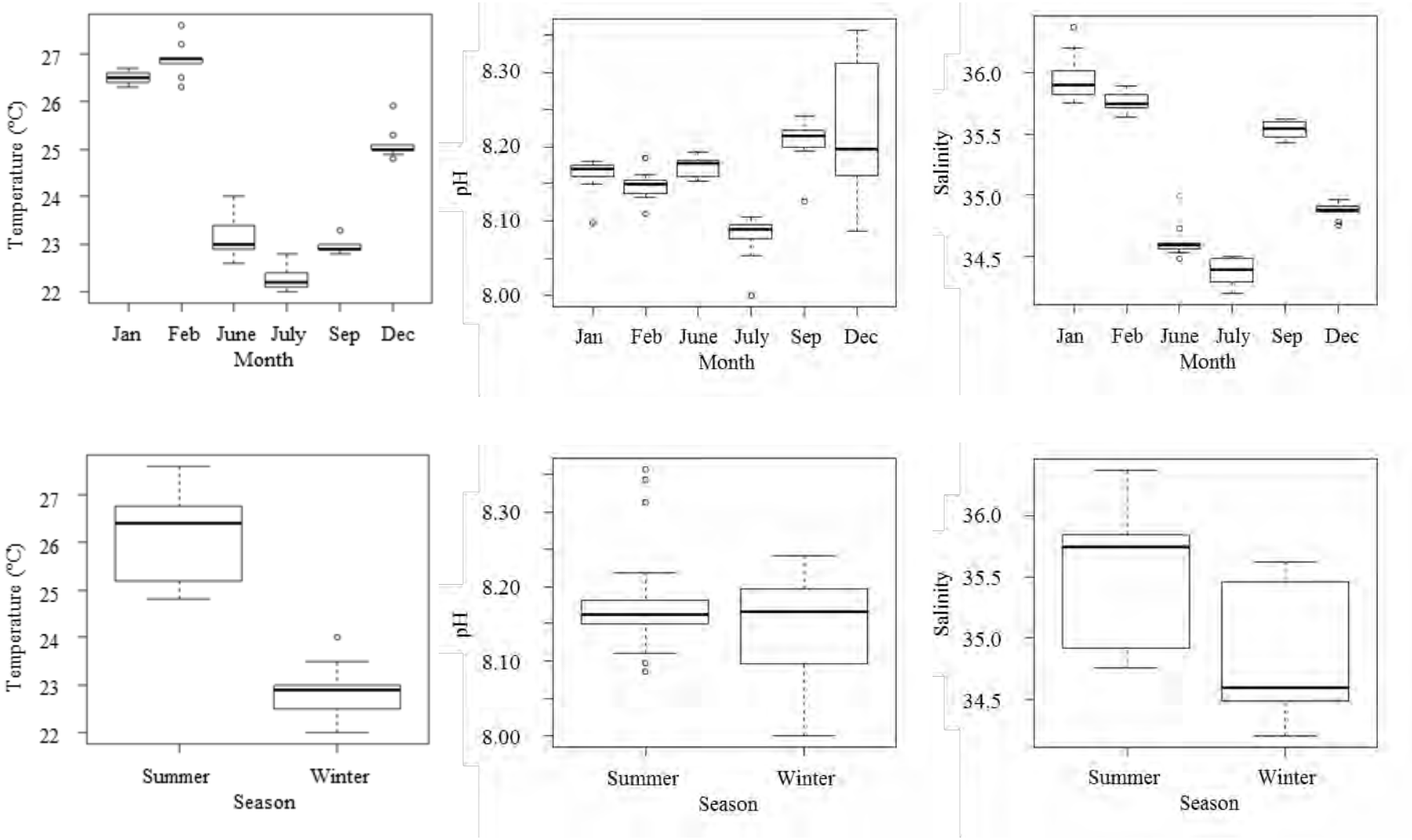

Figure 3.5. Box plots of temperature, pH and salinity on Two-mile Reef.

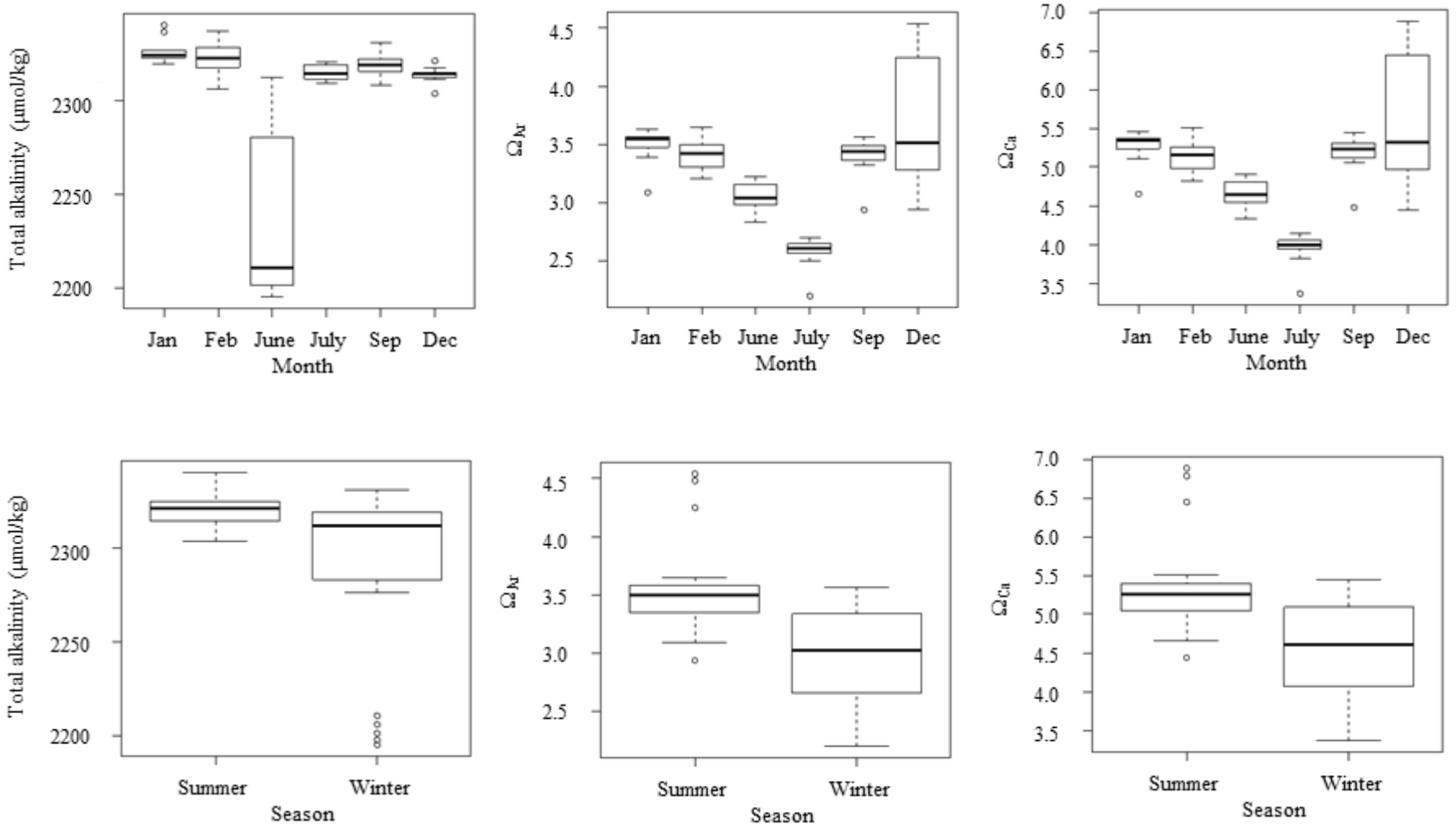

Figure 3.6. Box plots of total alkalinity, Ω_{Ar} and Ω_{Ca} on Two-mile Reef.

3.4.2 Sediment characteristics

The BS and G sites were dominated by coarse- and medium-grained sand, the G sites having higher percentages of coarse sand (Table 3.4; Figure 3.7A). The median grain size for the BS sites ranged from 0.53 – 0.65 mm and for the G sites 0.54 – 0.61 mm. The NR sites were dominated by very coarse and coarse sand and the median grain size ranged between 0.77 – 0.98 mm. NR sites also had a higher percentage of gravel present than the other sites (9.91 ± 4.97 SD %). The median grain sizes at the BS, G and NR sites were 0.58 ± 0.05 SD, 0.58 ± 0.03 SD and 0.91 ± 0.10 SD respectively. No mud was present at any site. The carbonate content varied across all habitats with, the average percentage carbonate at the BS, NR and G sites being 52.22 ± 7.31 SD, 69.17 ± 9.42 SD and 63.49 ± 10.04 SD respectively (Figure 3.7B). The BS (0.97 ± 0.04 SD) and NR (0.91 ±0.14 SD) sites were moderately-sorted, the G sites (0.55 ± 0.01 SD) moderately- to well-sorted. A grain size contour map (Figure 3.7A) revealed the variation in the grain size across all the sites and locations. Some variability was seen across the NR sites and it was immediately evident that the G sites had a higher percentage of cs in comparison to the other locations.

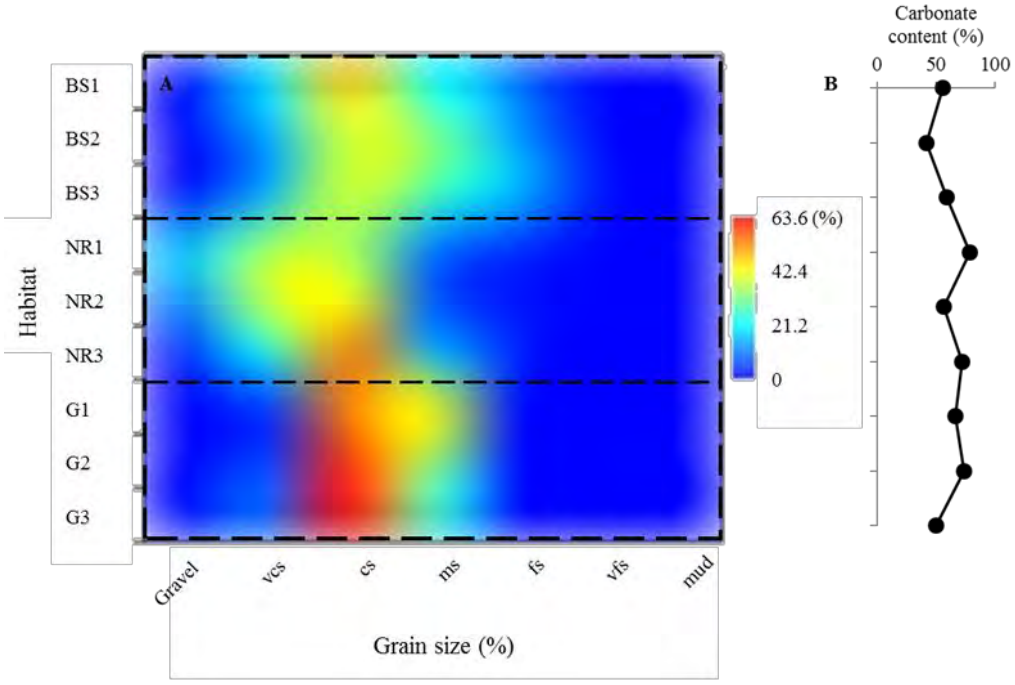

Figure 3.7. **A** Grain size contour map and **B** carbonate content of sediment at sites on Two- mile Reef (BS= bioclastic sediment, NR= near-reef and G= gully sites).

Table 3.4. Sediment characteristics at each site on Two-mile Reef (BS= bioclastic sediment, NR= near-reef and G= gully sites).

Location	Site	Depth (m)	%							Mean (mm)	Median (mm)	Mean (phi)	Median (phi)	Sorting	Skewness	Carbonate (%)
			Gravel	vcs	cs	ms	fs	vfs	mud							
BS	1	16	1.47	18.79	48.19	21.03	9.74	0.78	0.00	0.62	0.65	0.70	0.62	0.93	0.88	55.56
	2		1.08	13.91	38.91	31.79	13.10	1.21	0.00	0.52	0.53	0.96	0.91	0.95	0.45	42.07
	3		1.23	14.63	39.18	26.79	15.86	2.31	0.00	0.50	0.55	1.00	0.87	1.02	1.35	59.02
	Mean		1.26	15.78	42.09	26.54	12.90	1.43	0.00	0.55	0.58	0.89	0.80	0.97	0.89	52.22
NR	1	19	15.14	33.52	35.00	10.99	4.89	0.46	0.00	0.98	0.98	0.03	0.03	1.09	0.31	78.76
	2		11.37	37.41	41.54	7.33	2.07	0.28	0.00	1.00	0.98	-0.01	0.02	0.90	-0.89	56.37
	3		3.23	23.44	54.47	15.85	2.78	0.23	0.00	0.76	0.77	0.40	0.38	0.74	0.17	72.39
	Mean		9.91	31.46	43.67	11.39	3.25	0.32	0.00	0.91	0.91	0.14	0.14	0.91	-0.14	69.17
G	1	13	0.28	5.39	52.97	40.15	1.02	0.19	0.00	0.55	0.54	0.86	0.88	0.54	-0.15	66.41
	2		0.25	6.18	59.97	32.62	0.74	0.25	0.00	0.59	0.58	0.77	0.78	0.54	-0.10	74.07
	3		0.97	9.31	63.56	25.64	0.53	0.00	0.00	0.62	0.61	0.69	0.71	0.56	-0.30	50.00
	Mean		0.50	6.96	58.83	32.80	0.76	0.15	0.00	0.59	0.58	0.77	0.79	0.55	-0.18	63.49

3.4.3 Statistical analysis of abiotic variables

The sediment characteristics, together with the mean summer water chemistry data were used in a BVSTEP analysis (Section 3.4.8). A mean of the water chemistry data, from January and February, was used as the biotic samples were collected in these months. The full set of 15 sediment variables were tested for collinearity with the water chemistry parameters using draftsman plots and Spearman correlation testing. Redundant variables with very strong correlations (ρ>0.9) were omitted from the model. The variables gravel, ms, fs, sorting, skewness, carbonate (%), salinity, pH, temperature, total alkalinity and Chl-*a* were kept in the model. All other variables were omitted as they showed strong correlations and were not deemed important for the analysis. Mud was omitted from the model as none was present at any of the sites. The gravel data was log-transformed as it was right-skewed. The resulting data were then normalised and used for subsequent analysis in Section 3.4.8.

3.4.4 Analysis of foraminiferal assemblages

In total, 186 662 Foraminifera identified to 63 taxa were picked from the > 500 μm size fraction of 45 samples. The live (coloured protoplasm) assemblage was first assessed followed by the total assemblage in a separate comparison. These included comparisons of foraminiferal abundances and main contributing genera for each substrata and location.

3.4.5 Living Large Benthic Foraminiferal assemblage

The majority of the Foraminifera picked were part of the "other" assemblage, with the "live" assemblage only representing 1.7%, of which 95.6% was found among rubble. The live assemblage consisted of 13 taxa from ten genera. *Amphistegina* spp. was dominant, making up 86.3% of the live assemblage, followed by *Asterigerina* sp.1 and *Heterostegina depressa*, each contributing 5.9% and 3.1% to the community, respectively. Symbiont-bearing genera in the samples were *Amphistegina, Sorites, Asterigerina, Heterostegina, Elphidium* and *Borelis.*

The sediment, live assemblages were more variable, with ten of the 13 taxa found in the samples. *Ammonia* sp.1*, Elphidium* sp.2*, Ammonia* sp.3*, Borelis melo* and *Lenticulina* sp.1 were only found alive, albeit in very low abundances, in the sediment samples. The genus *Elphidium* was dominant at the BS location followed by *Ammonia* and *Heterostegina* (Figure 3.8A). *Asterigerina* was the dominant genus in both the NR and G locations, followed by *Amphistegina* and *Heterostegina* (Figure 3.8A). Bar graphs in Figure 3.8B reveal that *Amphistegina* was dominant in the rubble, live assemblages in both the NR and G samples. Minor contributions from *Heterostegina, Sorites, Asterigerina* and *Borelis* were evident.

A large portion (30.6%) of the Foraminifera found in the rubble were alive, with 35.6% and 25.6% attributable to the NR and G samples respectively. *Amphistegina* spp., *Heterostegina depressa, Sorites* sp.1*, Asterigerina* sp.1*, Borelis schlumbergeri* and *Elphidium macellum* contributed the most to the NR samples. *Amphistegina* spp.*, Heterostegina depressa, Sorites* sp.1*, Asterigerina* sp.1*, Sorites* sp.3 and *Elphidium macellum* were the highest contributing taxa in the G samples. The Number of taxa (*S*) in the rubble samples was lower than in the sediment samples (*S* = 8), and *Sorites* sp.1 and sp.3 and *Cibicides refulgens* were only found alive in the rubble samples.

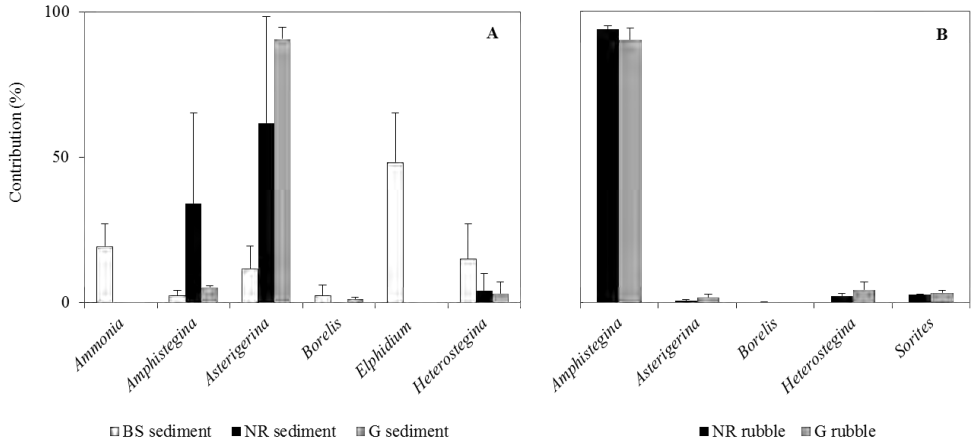

Figure 3.8. Mean Percentage contribution of the main live genera in the **A** sediment and **B** rubble samples (BS = bioclastic sediment, NR= near-reef and G= gully location).

A significant difference was evident in abundance counts between substratum types (Kruskall-Wallis: H= 29.672, df= 1, $p < 0.001$) (Figure 3.9A). The Mean abundance (N: ind/m^2) in all sediment samples was 962 ± 789 SD and rubble samples was 1.54 x 10^4 ± 8.99 x 10^3 SD. A high degree of variation, attested by the large standard deviation values, was found in both substrata. A significant difference was found within the sediment samples only between the NR and G locations (Tukey Test: q= 4.095, $p < 0.05$). Average abundances in the BS, NR and G sediment samples were 911 ± 495 SD, 456 ± 347 SD and 1.52 x 10^3 ± 966 SD ind.m^2 respectively (Figure 3.9B). A significant difference in abundance was evident between locations from the rubble samples (Mann-Whitney: U= 15, n= 9, p= 0.027). Average abundance in NR and G rubble samples was 1.99 x 10^4 ± 7.65 x 10^3 SD and 1.09 x 10^4 ± 7.90 x 10^3 SD ind.m^2 respectively (Figure 3.9C).

SIMPER analysis using the Bray-Curtis similarity matrix of fourth-root transformed abundance data was used to determine which taxa contributed the most to the overall similarities within the sediment

and rubble live assemblages. Species level data were used to determine more specific differences between the substrata. Two taxa, *Asterigerina* sp.1 and *Amphistegina* spp., contributed to a 38.6% similarity between live sediment assemblages, with *Asterigerina* sp.1 being the most distinguishing species (Table 3.5). A 79.7% similarity was found within the rubble sample live assemblages, with *Amphistegina* spp. being the highest contributor as well as the most distinguishing taxon (Table 3.5). *Amphistegina* spp. was found to contribute the most to the dissimilarity (73.5%) and was the most distinguishing taxon between the sediment and rubble live assemblages (Table 3.6).

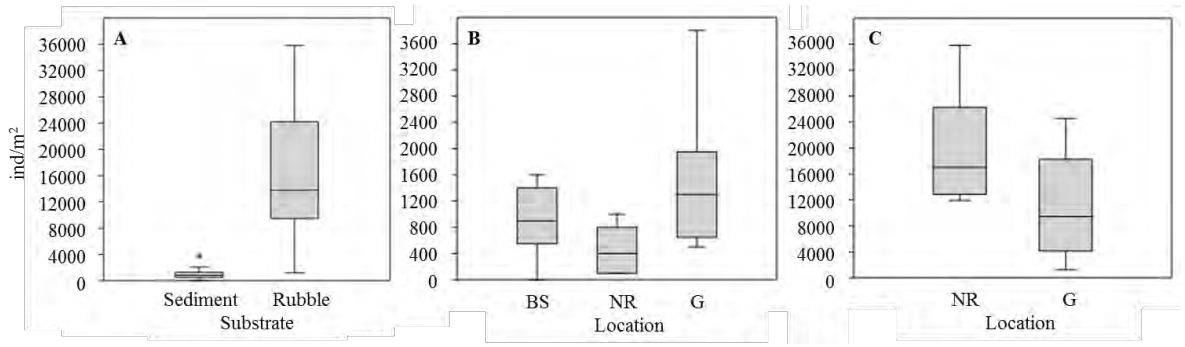

Figure 3.9. Box plot of abundance (*N*: ind.m2) for live Foraminifera between **A** sediment and rubble, **B** sediment locations and **C** rubble locations (BS= bioclastic sediment, NR= near-reef and G= gully).

A PERMANOVA using 9995 permutations revealed a significant difference between the sediment and rubble live foraminiferal assemblages. A pairwise PERMANOVA comparison revealed that location had a significant effect in the rubble assemblages (Pseudo-F= 3.4546, p= 0.02) with a location effect also noted in the sediment foraminiferal assemblages. A difference was noted between the assemblages at the BS and NR location (t = 2.4845, p = 0.0008) and BS and G location (t= 3.2409, p = 0.0002). No significant difference was found between the assemblages at the NR and G locations (t= 1.5868, p= 0.1151).

Table 3.5. SIMPER analysis using the Bray-Curtis similarity matrix on fourth-root transformed abundance data showing the main taxa contributing to the similarity within the live assemblages from the sediment and rubble samples. Only the taxa contributing >2% to the within-group average similarity are shown. Shading denotes taxa with the highest Diss/SD ratio.

Sample	Taxa	Average abundance	Average similarity	Sim/SD
Sediment	*Asterigerina* sp.1	3.65	28.85	1.02
	Amphistegina spp.	1.63	6.07	0.47
Rubble	*Amphistegina* spp.	10.49	37.25	10.11
	Heterostegina depressa	4.33	15.67	8.83
	Sorites sp.1	3.56	10.69	1.82
	Sorites sp.3	3.14	8.71	1.45

Table 3.6. SIMPER analysis using the Bray-Curtis similarity matrix on fourth-root transformed abundance data showing the main taxa contributing to the dissimilarity between the sediment and rubble live assemblages. Only the taxa contributing >2% to the between-group average dissimilarity are shown. Shading denotes the taxon with the highest Diss/SD ratio.

Taxa	Sediment average abundance	Rubble average abundance	Average dissimilarity	Diss/SD
Amphistegina spp.	1.63	10.49	26.75	2.95
Sorites sp.1	0.00	3.56	10.15	2.44
Heterostegina depressa	0.90	4.33	11.15	2.09
Sorites sp.3	0.00	3.14	8.79	2.06
Asterigerina sp.1	3.65	2.73	7.35	1.07

3.4.6 Total foraminiferal assemblage, univariate analysis

The averaged total foraminiferal assemblage data and indices for sediment samples are presented in Table 3.7 and Figure 3.10 across all three sites within each location. The BS sediment samples had the highest abundance counts (*N*) (mean: $N = 7.18 \times 10^5 \pm 16.29 \times 10^5$ SD ind/m^2) and number of taxa (Mean: $S = 21 \pm 1$ SD) whereas the NR sediment samples had the lowest abundance (mean: $N = 5.41 \times 10^5 \pm 1.02 \times 10^5$ SD ind/m^2) and number of taxa (*S*) (Mean: $S = 13 \pm 3$ SD). Within the rubble samples, the NR samples had the highest abundance counts and number of taxa (mean: $N = 5.61 \times 10^4 \pm 1.83 \times 10^4$ SD ind/m^2; $S = 18 \pm 2$ SD) whereas the G samples had the lowest abundances and number of taxa (mean: $N = 4.26 \times 10^4 \pm 1.30 \times 10^4$ SD ind/m^2; $S = 17 \pm 5$ SD).

A significant difference was found for abundance counts between substratum types (Kruskall-Wallis: $H = 31.696$, df = 1, $p < 0.001$), however, no significant location effect was evident in sediment ($F = 0.969$, df = 2, $p = 0.394$) or rubble ($t = 1.351$; df = 16; $p = 0.195$) samples. No significant difference in number of taxa (*S*) was found between substrata ($F = 0.0264$, df = 1, $p = 0.872$). Within the sediment samples, the NR location had a significantly different number of taxa in comparison with the BS (Holm-Sidak: $t = 4.290$, $p < 0.001$) and G (Holm-Sidak: $t = 3.048$, $p = 0.006$) locations. No significant location effect (Mann-Whitney: $U = 37$, n = 9, $p = 0.790$) was found within the rubble samples for number of taxa.

Considering the community structure of the samples, the rubble samples had the highest Shannon diversity index (*H'*) (mean: $H' = 1.49 \pm 0.32$) and Pielou's evenness values (*J'*) (mean: $J' = 0.27 \pm 0.02$). The sediment samples had the lowest diversity (mean: $H' = 1.23 \pm 0.28$) and evenness values (mean: $J' = 0.13 \pm 0.03$). A significant difference (Kruskall-Wallis: $H = 28.891$, df = 1, $p < 0.001$) in

diversity was noted between the substratum types. Within the sediment samples, the diversity in the G samples was significantly different to both the BS (Holm-Sidak: $t = 3.310$, $p = 0.003$) and NR (Holm-Sidak: $t = 3.267$, $p = 0.003$) samples. A significant difference (Kruskall-Wallis: $H = 29.393$, df = 1, $p < 0.001$) between substrata was also noted for evenness with a significant difference (Tukey Test: $q = 4.095$, $p < 0.05$) found between the BS and G sediment location evenness values. No location effect was found for the rubble evenness values ($t = -1.248$, df = 16, $p = 0.230$). A significant difference in Margalef's Richness (d) was found between the substratum types (Kruskall-Wallis: $H = 29.672$, df = 1, $p = < 0.001$). The NR sediment samples had significantly different richness values to both the BS (Holm-Sidak: $t = 4.120$, $p<0.001$) and G sediment samples (Holm-Sidak: $t = 2.949$, $p = 0.007$). No difference in the richness values from the two rubble locations was found (F = 0.107, df = 1, p = 0.748).

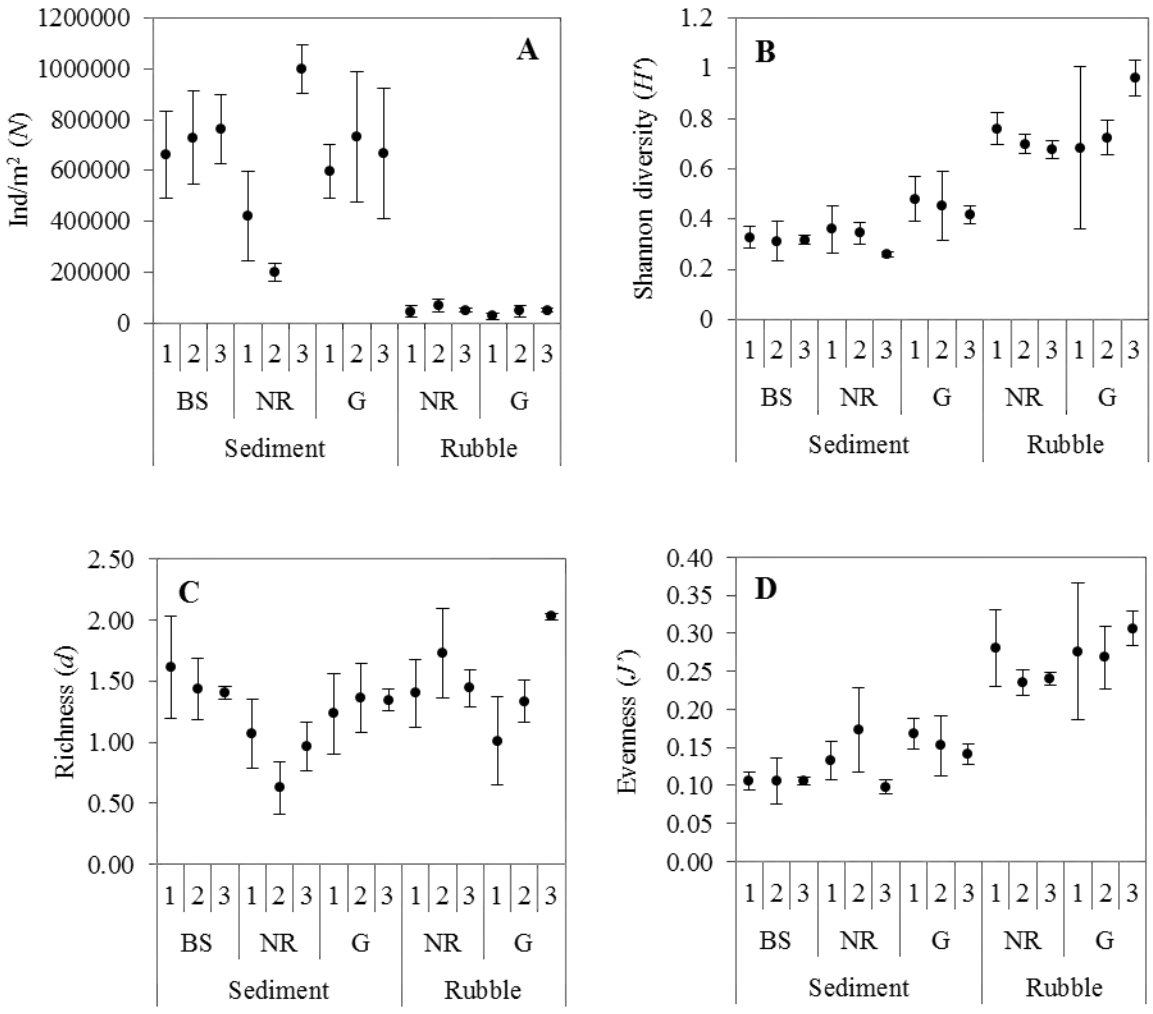

Figure 3.10. Significant univariate statistics: **A** Ind.m^2 (N); **B** Shannon diversity index (H'); **C** Margalef's Richness (d) and **D** Evenness (J') of the various substrata at each site. Standard deviations are shown for all variables. (S = sediment sample, R = rubble sample, BS = bioclastic sediment, NR = near-reef and G = gully).

Table 3.7. Summary of mean (± SD) foraminiferal assemblage data and indices for all sediment and rubble sites (BS= bioclastic sediment, NR= near-reef and G= gully location, S= sediment samples and R= rubble samples).

Location	Site	Total Foraminifera picked	Ind/m^2 (*N*)	Total genera	Total taxa (*S*)	Shannon-diversity (*H'*)	Margalef's Richness (*d*)	Evenness (*J'*)
BS (S)	1	6626 ± 1701	$6.62 \times 10^5 \pm 1.70 \times 10^5$	14 ± 4	23 ± 6	0.33 ± 0.04	1.61 ± 0.42	0.11 ± 0.01
	2	7303 ± 1815	$7.30 \times 10^5 \pm 1.81 \times 10^5$	13 ± 1	20 ± 4	0.31 ± 0.08	1.43 ± 0.25	0.11 ± 0.03
	3	7638 ± 1373	$7.63 \times 10^5 \pm 1.37 \times 10^5$	13 ± 0	20 ± 1	0.32 ± 0.02	1.40 ± 0.05	0.11 ± 0.01
NR (S)	1	4213 ± 1768	$4.21 \times 10^5 \pm 1.76 \times 10^5$	12 ± 3	15 ± 3	0.36 ± 0.10	1.07 ± 0.28	0.13 ± 0.03
	2	2026 ± 354	$2.02 \times 10^5 \pm 3.53 \times 10^4$	8 ± 2	9 ± 3	0.34 ± 0.04	0.63 ± 0.21	0.17 ± 0.02
	3	9997 ± 945	$9.99 \times 10^5 \pm 9.44 \times 10^4$	11 ± 1	14 ± 3	0.26 ± 0.01	0.97 ± 0.20	0.10 ± 0.01
G (S)	1	5985 ± 1054	$5.98 \times 10^5 \pm 1.05 \times 10^5$	12 ± 2	17 ± 4	0.48 ± 0.09	1.23 ± 0.33	0.17 ± 0.02
	2	7337 ± 2578	$7.33 \times 10^5 \pm 2.57 \times 10^5$	14 ± 3	19 ± 4	0.45 ± 0.14	1.36 ± 0.29	0.15 ± 0.04
	3	6662 ± 2560	$6.66 \times 10^5 \pm 2.55 \times 10^5$	13 ± 1	19 ± 2	0.42 ± 0.03	1.35 ± 0.09	0.14 ± 0.01
NR (R)	1	543 ± 260	$4.61 \times 10^4 \pm 2.15 \times 10^4$	12 ± 2	16 ± 4	0.76 ± 0.06	1.40 ± 0.28	0.28 ± 0.05
	2	1217 ± 424	$7.00 \times 10^4 \pm 2.34 \times 10^4$	15 ± 3	20 ± 5	0.70 ± 0.04	1.73 ± 0.37	0.24 ± 0.02
	3	760 ± 121	$5.20 \times 10^4 \pm 9.81 \times 10^3$	13 ± 1	17 ± 2	0.68 ± 0.04	1.45 ± 0.15	0.24 ± 0.01
G (R)	1	360 ± 107	$2.76 \times 10^4 \pm 1.16 \times 10^4$	10 ± 3	11 ± 4	0.68 ± 0.32	1.01 ± 0.36	0.28 ± 0.09
	2	678 ± 200	$4.84 \times 10^4 \pm 2.14 \times 10^4$	12 ± 2	15 ± 2	0.72 ± 0.07	1.34 ± 0.17	0.27 ± 0.04
	3	878 ± 96	$5.17 \times 10^4 \pm 5.99 \times 10^3$	15 ± 0	23 ± 0	0.96 ± 0.07	2.03 ± 0.02	0.31 ± 0.02

3.4.7 Comparison of total foraminiferal assemblages across substrata and locations

In total, 63 taxa were identified from 45 samples which included 18 rubble and 27 sediment samples (Appendix B, Table B1). A Q mode cluster analysis was used to assess if there was a difference between the total foraminiferal assemblages on substrata at the three locations on TMR. A cluster analysis on the Bray-Curtis similarities of fourth-root transformed abundance data of all samples revealed a distinct divide between the sediment and rubble samples at ± 55.0% similarity (Figure 3.11).

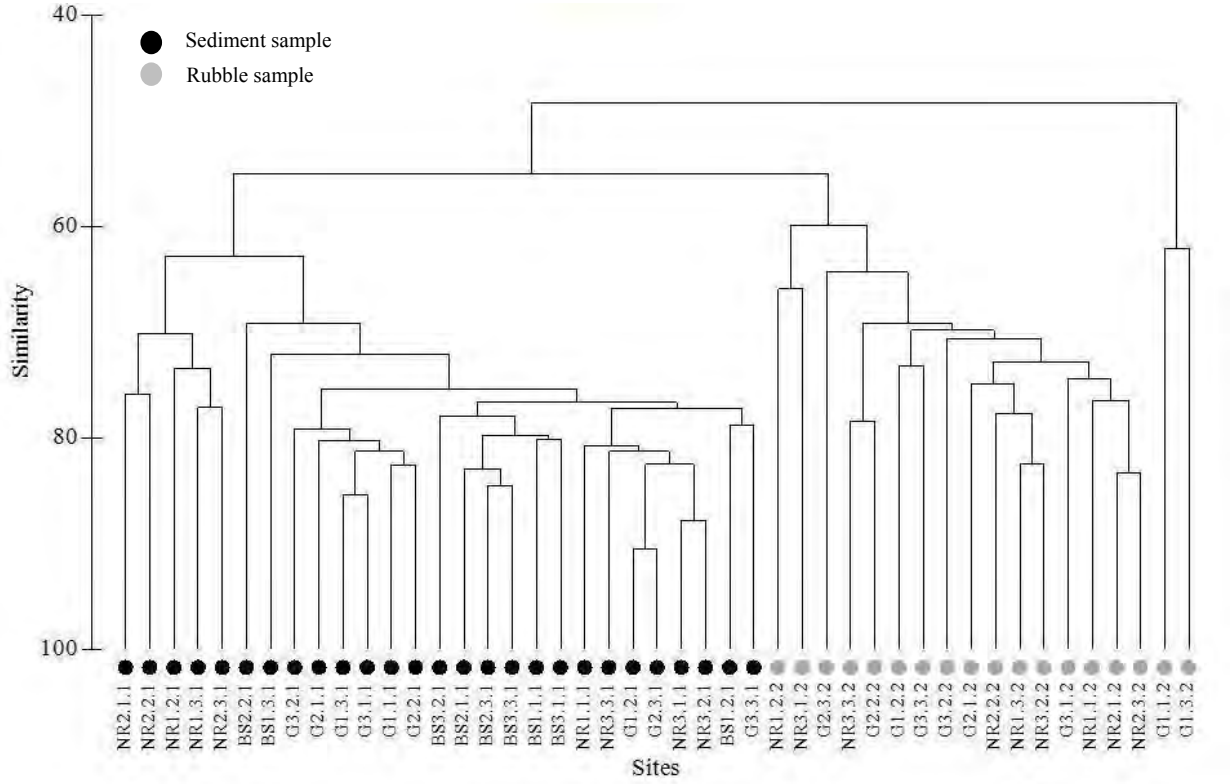

Figure 3.11. A Q mode cluster analysis using the Bray-Curtis similarities on fourth-root transformed total foraminiferal abundance data across all sampling sites (BS= bioclastic sediment, NR= near-reef, G= gully). Sites with #.1 as a third subcategory number (e.g.: NR 1.1.1) denote sediment samples whereas sites with #.2 as their third subcategory (e.g. NR 1.1.2) denote coral rubble samples.

A SIMPER analysis revealed the average dissimilarity between the sediment and rubble samples was 46.0%, with three distinguishing taxa (Table 3.8). *Amphistegina* spp. contributed the most to the dissimilarity between the substrata and was also the most distinguishing taxon having the highest Diss/SD ratio. The other distinguishing taxa were *Heterostegina depressa* and *Textularia* sp.1.

Table 3.8. SIMPER results of rubble versus sediment total foraminiferal assemblages. Only the taxa contributing >2% to the between-group average dissimilarity are shown. Shading denotes the taxon with the highest Diss/SD ratio.

Taxa	Sediment average abundance	Rubble average abundance	Average dissimilarity	Diss/SD
Amphistegina spp.	27.22	13.96	7.11	3.05
Heterostegina depressa	11.09	5.82	2.86	2.94
Textularia sp.1	11.12	7.09	2.27	1.37

Figure 3.12A depicts a non-metric multidimensional scaling (nMDS) ordination of the total foraminiferal abundances in the sediment samples; with Figure 3.12B showing the results for the rubble samples. Some separation was evident according to location for each substratum. Both nMDS plots had low stress values.

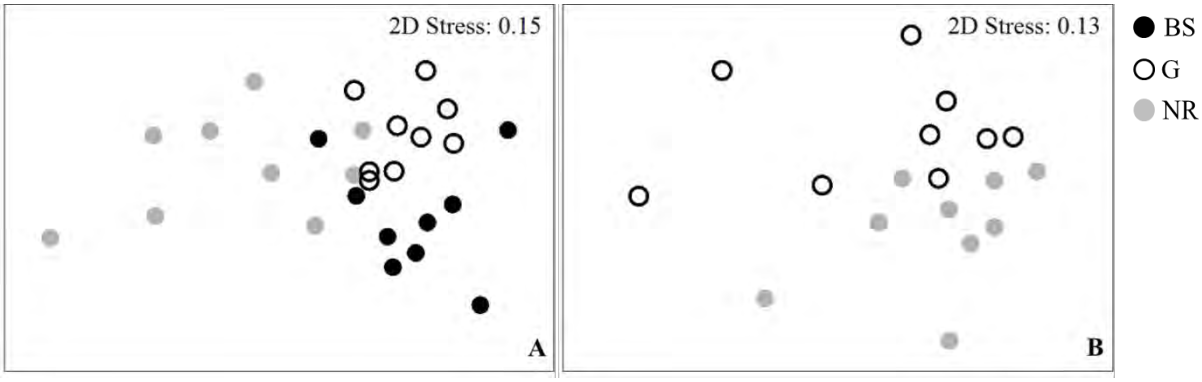

Figure 3.12. nMDS ordination of fourth-root transformed, total foraminiferal assemblage abundance data from **A** sediment and **B** rubble sites (BS= bioclastic sediment, NR= near-reef and G= gully).

A PERMANOVA using 9938 permutations was performed on fourth-root transformed total foraminiferal abundance data and revealed a significant difference (Pseudo-F= 23.103, *p*= 0.0001) between the two substratum assemblages. A significant difference was found in the total sediment assemblages across locations. A pair-wise PERMANOVA using permutations revealed significant differences between the total foraminiferal sediment assemblages across all locations, BS and NR (t= 2.684, *p*= 0.0002), BS and G (t= 2.0333, *p*= 0.0002), NR and G (t= 2.7754, *p*= 0.0001). A PERMANOVA with 8139 permutations revealed a significant difference (Pseudo-F= 2.3106, *p*= 0.0297) between the rubble total foraminiferal assemblages at the two locations.

Total sediment foraminiferal assemblages

In total, 59 taxa were identified within the suborders Rotaliina, Miliolina and Textulariina. The BS samples contained the highest number of genera (23) and the NR and G samples each had 20 and 18 genera respectively. *Amphistegina* was the dominant genus in the BS and G samples, followed by *Textularia* and *Heterostegina* (Figure 3.13). The NR samples were also dominated by *Amphistegina,* however, *Heterostegina* was the second most common genus, followed by *Textularia* (Figure 3.13). The most common taxa in the sediment samples were *Amphistegina* spp., *Textularia* sp.1, *Heterostegina depressa, Homotrema rubra* and *Planorbulinella larvata*. Fifteen species were found in low numbers and only in the sediment samples. A PERMANOVA using 99999 permutations revealed there was no significant difference ($p > 0.05$) between the total foraminiferal assemblages at the three sites within each location.

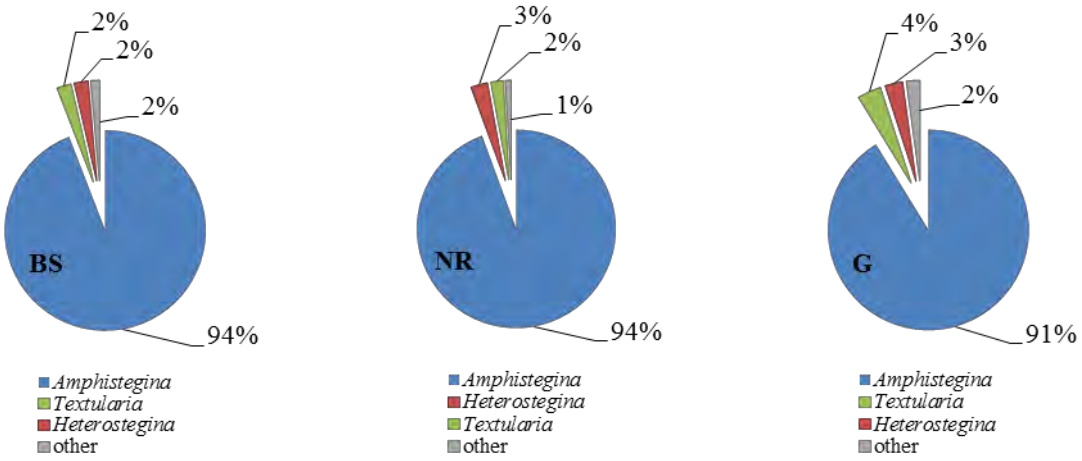

Figure 3.13. Graphs showing the top three genera contributions in sediment samples at the three locations on Two-mile Reef (BS= bioclastic sediment, NR= near-reef and G= gully).

A SIMPER analysis revealed a similarity between the three BS, NR and G sediment sites of 75.9%, 77.6% and 79.2% respectively. *Amphistegina* spp. was the most distinguishing taxon with the highest Sim/SD ratio as well as the highest contributor to the similarity at the BS and NR locations (Table 3.9). A SIMPER analysis revealed *Textularia* sp.1 had the highest Sim/SD ratio and was the most distinguishing species within the G sediment location (Table 3.9).

Table 3.9. SIMPER analysis results between sediment sites within the bioclastic sediment (BS), near-reef (NR) and gully (G) locations. Only the taxa contributing >2% to the within-group average similarity are shown. Shading denotes the taxa with the highest Sim/SD ratio.

Location	Taxa	Average abundance	Average similarity	Sim/SD
BS	*Amphistegina* spp.	28.51	21.41	13.56
	Textularia sp.1	11.21	8.50	11.19
	Planorbulinella larvata	6.34	4.53	10.12
	Homotrema rubra	7.21	5.32	6.92
	Heterostegina depressa	10.91	7.73	5.80
NR	*Amphistegina* spp.	25.53	29.11	7.20
	Textularia sp.1	9.66	11.08	6.86
	Heterostegina depressa	10.76	12.36	5.48
	Homotrema rubra	7.03	8.12	5.27
G	*Textularia* sp.1	12.48	9.59	16.71
	Heterostegina depressa	11.58	8.80	12.96
	Asterigerina sp.1	7.38	5.68	11.85
	Amphistegina spp	27.63	21.07	10.51
	Homotrema rubra	7.85	5.83	9.17

Total rubble foraminiferal assemblages

In the 18 samples analysed, 48 taxa were identified within three suborders: Rotaliina, Miliolina and Textulariina. The G samples contained the highest number of genera (23) and the NR samples had 20 genera. *Amphistegina* was the dominant genus at both locations, followed by *Textularia* and *Heterostegina* (Figure 3.14). The most common taxa in the rubble samples were *Amphistegina* spp.*, Textularia* sp.1*, Heterostegina depressa, Homotrema rubra* and *Sorites* sp.1 (Figure 3.14), with four species only in the rubble samples: *Triloculina* sp.8 and sp.11, *Acervulina* sp.1 and *Cyclocibicides* sp.1. A PERMANOVA test using 99999 permutations revealed there were no significant differences (p>0.05%) between the total foraminiferal assemblages at the three NR and three G rubble sites.

SIMPER analyses revealed an average similarity of 69.1% and 63.0% between the three NR and three G sites respectively. *Amphistegina* spp. had the highest Sim/SD ratio and was subsequently the most distinguishing taxon within the NR rubble samples (Table 3.10) and *Planorbulinella larvata* had the highest Sim/SD ratio and was the most distinguishing taxon within the G samples (Table 3.10).

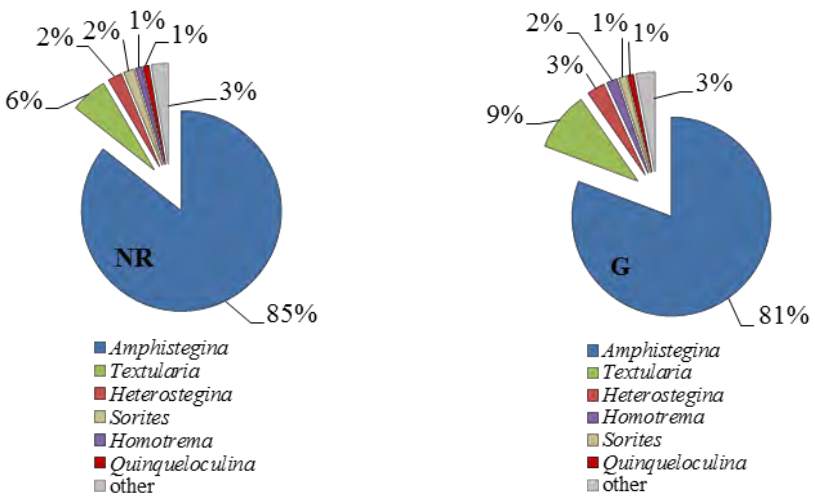

Figure 3.14. Graphs showing the top six mean generic contributions to the total rubble foraminiferal assemblages from the NR and G locations (NR= near-reef, G= gully).

Table 3.10. SIMPER analysis results for total foraminiferal assemblages in the rubble samples within the near-reef (NR) and gully (G) locations. Only the top five taxa contributing >2% to the within-group average similarity are shown together with the taxon with the highest Sim/SD ratio (shaded).

Location	Taxa	Average abundance	Average similarity	Sim/SD
NR	*Amphistegina* spp.	14.57	16.73	11.47
	Textularia sp.1	7.25	8.05	10.93
	Heterostegina depressa	5.84	6.71	9.39
	Sorites sp.1	4.90	5.82	7.07
	Homotrema rubra	4.75	5.50	4.62
G	*Planorbulinella larvata*	3.81	4.49	6.01
	Heterostegina depressa	5.80	7.43	5.54
	Amphistegina spp.	13.36	17.16	5.47
	Homotrema rubra	4.99	6.21	5.06
	Asterigerina sp.1	4.16	5.02	4.47
	Textularia sp.1	6.93	6.76	1.79

Concentration index

Following the methods outlined by Stephenson et al. (2015), a relative abundance index was calculated by dividing the mean abundances (%) of the 20 most common genera in the sediment (S) and rubble (R) samples (S/R_R) (Table 3.11). A second index (S/R_{Tot}) was also calculated using the absolute abundances (ind/m^2). The ind/m^2 of eight genera was 5–21 times higher in the sediment compared to the rubble samples. This included four symbiont-bearing Foraminifera, *Amphistegina, Asterigerina, Elphidium* and *Heterostegina*. The genera *Cibicides, Pyrgo, Sorites* and *Spiroloculina* were present in higher numbers in the rubble assemblages. The S/R_R index revealed that only *Amphistegina* and *Heterostegina* were proportionally more abundant in the sediment samples.

Table 3.11. Mean absolute and relative abundances of the 20 most common genera in the sediment and rubble samples, used to calculate the relative abundance index (S/R_R) and absolute abundance index (S/R_{Tot}). Shading denotes taxa which were proportionally more abundant in the sediment samples.

	Mean Absolute abundance (ind/m^2)			Mean Relative abundance (%)		
Genera	Sediment	Rubble	S/R_{Tot}	Sediment	Rubble	S/R_R
Ammonia	1.33×10^2	6.30	21.16	0.02	0.03	0.56
Amphistegina	5.98×10^5	4.12×10^4	14.52	92.78	83.63	1.11
Asterigerina	1.66×10^3	2.80×10^2	5.94	0.26	0.64	0.41
Borelis	5.90 x 10	4.50 x 10	1.31	0.01	0.11	0.09
Cibicides	7.41	1.90 x 10	0.38	0.00	0.03	0.03
Elphidium	6.85×10^2	1.15×10^2	5.95	0.10	0.24	0.43
Heterostegina	1.64×10^4	1.23×10^3	13.26	2.82	2.61	1.08
Homotrema	3.18×10^3	6.34×10^2	5.03	0.59	1.49	0.40
Lachlanella	7.00 x 10	3.30 x 10	2.08	0.01	0.06	0.24
Lenticulina	2.50 x 10	3.03	8.56	0.01	0.01	0.96
Marginopora	1.18×10^2	4.00 x 10	2.92	0.02	0.08	0.20
Planorbulinella	1.92×10^3	2.26×10^2	8.51	0.30	0.45	0.67
Pseudotriloculina	4.40 x 10	1.30 x 10	3.38	0.01	0.02	0.51
Pyrgo	1.40 x 10	2.02×10^2	0.07	0.01	0.34	0.02
Quinqueloculina	1.38×10^3	4.53×10^2	3.05	0.22	0.82	0.26
Septotextularia	9.20 x 10	1.90 x 10	4.66	0.01	0.08	0.19
Sorites	1.00×10^2	7.16×10^2	0.14	0.02	1.53	0.01
Spiroloculina	7.40 x 10	8.90 x 10	0.83	0.01	0.15	0.09
Textularia	1.73×10^4	3.68×10^3	4.72	2.78	7.12	0.39
Triloculina	1.00×10^2	8.80 x 10	1.13	0.01	0.18	0.08

Comparison of abundance and density of total sediment assemblage

An nMDS ordination was performed on the standardised Foraminifera density data (Figure 3.15B). As noted, significant differences were detected in the sediment foraminiferal communities at the different locations. Similar nMDS ordinations were depicted for the density and abundance data (Figure 3.15A and B). It also had a low stress value.

Results from the RELATE procedure showed that there was a highly significant correlation between the matrices constructed from total sediment abundance data compared to the density data ($\rho = 0.941$, $p = 0.001$). This highlights that either metric (ind/m^2 or ind/g) is suitable when assessing sediment foraminiferal assemblages.

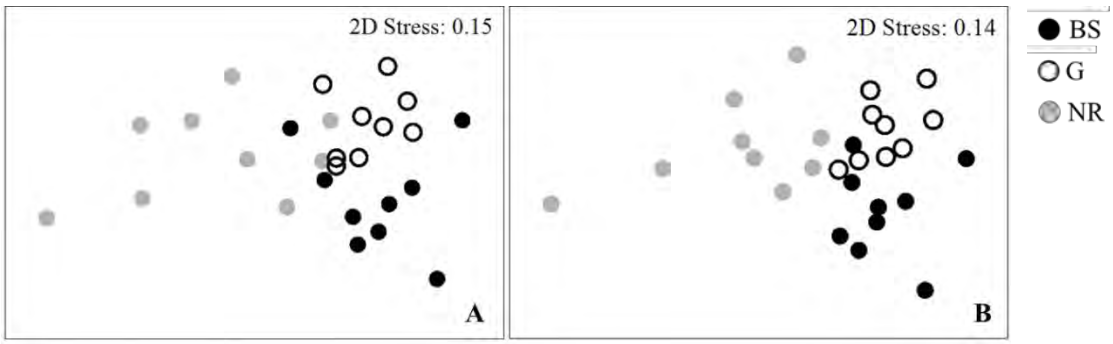

Figure 3.15. nMDS ordination of total fourth-root transformed, **A** abundance data and **B** density data from sediment sites (BS= bioclastic sediment, NR= near-reef and G= gully).

3.4.8 Statistical analysis of environmental and biological data

As significant differences were found between the live and total assemblages in the two substratum types, separate BVSTEP and CAP analyses were conducted. These were used to investigate if there were relationships between the sediment characteristics and water chemistry and the live and total foraminiferal assemblages. The 11 abiotic variables used in the analysis were percentages of gravel, ms and fs, sorting, skewness, carbonate (%), salinity, pH, temperature, T_A and Chl-*a* (Section 3.4.3).

A BVSTEP algorithm was run to determine which abiotic variables best accounted for the observed live and total foraminiferal abundance data across both substratum types. The combinations having the highest correlation values for one, two, three, four and five variables are displayed in Tables 3.12 and Table 3.13. Fine sand (fs) was the single variable that was correlated most highly with the live sediment foraminiferal assemblage ($\rho_s = 0.620$), whereas a combination of three variables - gravel, fs and T_A - were most highly correlated ($\rho_s= 0.787$) (Table 3.12). Temperature was the single variable that was correlated most highly with the total sediment foraminiferal assemblage data ($\rho_s= 0.585$). A combination of five variables - gravel, ms, skewness, salinity and temperature - had the highest correlation with the total sediment foraminiferal assemblages ($\rho_s= 0.752$) (Table 3.12). All these correlations were found to be significant ($p<0.01$) using the global BEST test. These variables were therefore used together with the foraminiferal assemblage data in a canonical analysis of principal coordinates (CAP). The Spearman rank correlation vectors of the three and five abiotic variables identified through BEST analysis for the live and total sediment assemblages were respectively overlain on the CAP ordinations to assess their interrelationship with the foraminiferal assemblages. Spearman rank correlation vectors of the distinguishing foraminiferal taxa (Appendix C, Plate C1), identified through the respective SIMPER analyses, for each sediment assemblage type were also plotted on the CAP ordination.

The first CAP analysis (Figure 3.16) was performed on the mean, fourth-root transformed live sediment abundance data and confirmed the foraminiferal communities present at the BS location were different from the NR and G samples. The first squared canonical correlation was large (δ_1^2 = 0.9427) and therefore adequately separated the samples. The second axis (CAP2) had a δ_2^2 = 0.2247. The first axis was positively correlated to the percentage of fs and T_A (ρ_s= 0.692 and 0.707) and the percentage of gravel was negatively correlated with the second axis (ρ_s= -0.934). Projection of the positions of the distinguishing taxa vectors on the axes showed that the abundances of the taxa, *Amphistegina* spp. and *Asterigerina* sp.1, appeared to be negatively correlated with T_A. CAP analysis of the total sediment foraminiferal assemblage abundance data confirmed a location effect for this substratum (Figure 3.17). The first squared canonical correlation was large (δ_1^2 = 0.8413) and was positively correlated with skewness and temperature (ρ_s= 0.536 and 0.647). CAP2 also had a large squared canonical correlation (δ_2^2 = 0.8254) and was positively correlated with salinity (ρ_s= 0.772). Temperature best described CAP1 and salinity best described CAP2 as they had the highest eigenvector values. *Textularia* sp.1 was the most distinguishing species within the G location and its abundance appeared to be negatively correlated with gravel.

Insignificant relationships were established through global BEST tests between the measured abiotic variables and the live and total rubble assemblage abundance data. A BVSTEP algorithm found lower correlation values, in comparison to the sediment assemblages, between the abiotic variables and the rubble, live foraminiferal communities (Best: ρ_s= 0.500) (Table 3.13). The CAP ordination on the mean, fourth-root transformed live rubble abundance data (Figure 3.18) showed the taxa, *Amphistegina* spp. appeared to be negatively correlated with pH and *Heterostegina depressa* with T_A. A combination of two abiotic variables – ms and T_A – had the highest correlation with the total rubble foraminiferal community (ρ_s= 0.711) (Table 3.13). The first axis (horizontal) of the CAP ordination using the total rubble assemblage (Figure 3.19) described all the variance in the foraminiferal communities (δ_1^2 = 1.000) and *Planorbulinella larvata* appeared to be positively correlated with T_A. The taxon, *Amphistegina* spp. best described CAP1.

Table 3.12. Correlation co-efficient (ρ_s in brackets) for various combinations of abiotic variables in relation to the live and total sediment foraminiferal assemblages obtained through a BVSTEP analysis. Bold text indicates best variable combination which was significant ($p < 0.01$) at 9999 permutations. Shading denotes highest correlations.

No. of variables	Sediment live assemblage	Sediment total assemblage
1	fs (0.620)	Temperature (0.585)
2	fs, T_A (0.741)	Gravel, temperature (0.710)
3	**Gravel, fs, T_A (0.787)**	Gravel, skewness, temperature (0.717)
4		Gravel, skewness, salinity, temperature (0.747)
5		**Gravel, ms, skewness, salinity, temperature (0.752)**

Table 3.13. Correlation co-efficient (ρ_s in brackets) for various combinations of abiotic variables in relation to the live and total rubble foraminiferal assemblages obtained through a BVSTEP analysis. The correlations were, however, not significant ($p > 0.05$). Shading denotes highest correlations.

No. of variables	Rubble live assemblage	Rubble total assemblage
1	pH (0.419)	ms (0.646)
2	pH, T_A (0.500)	ms, T_A (0.711)

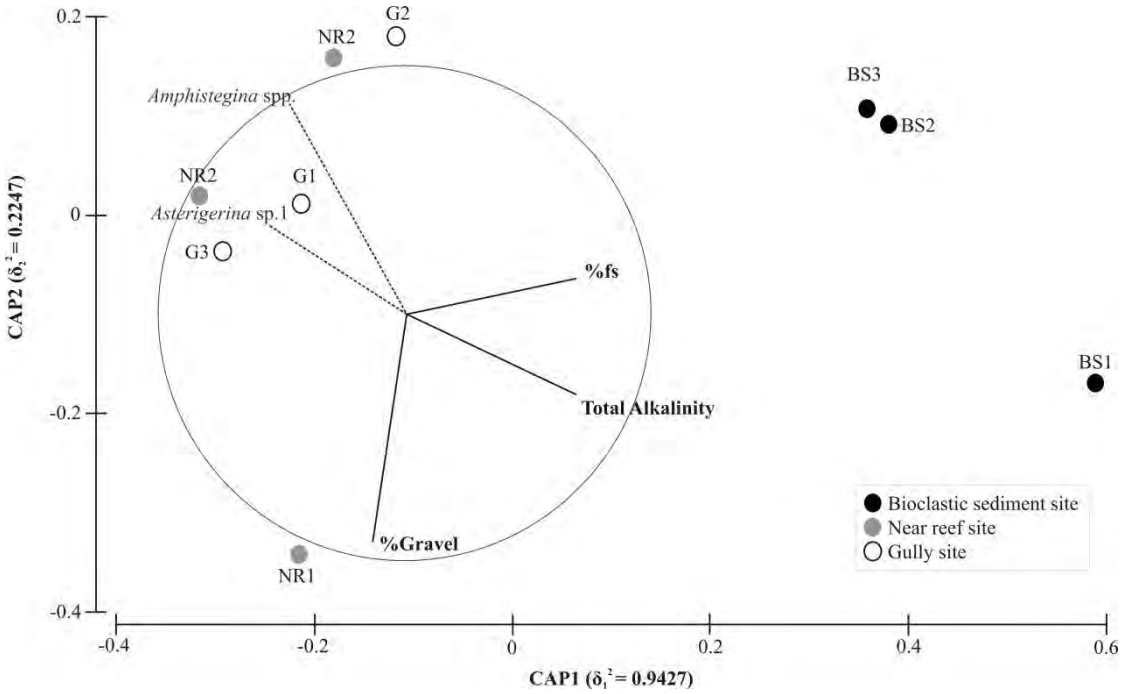

Figure 3.16. CAP analysis derived from the mean, fourth-root transformed, live sediment foraminiferal assemblage abundance data. The Spearman rank correlation vectors of the combination of abiotic variables identified through the BVSTEP analysis are plotted with the most distinguishing taxa (BS= bioclastic sediment, NR= near-reef and G = gully).

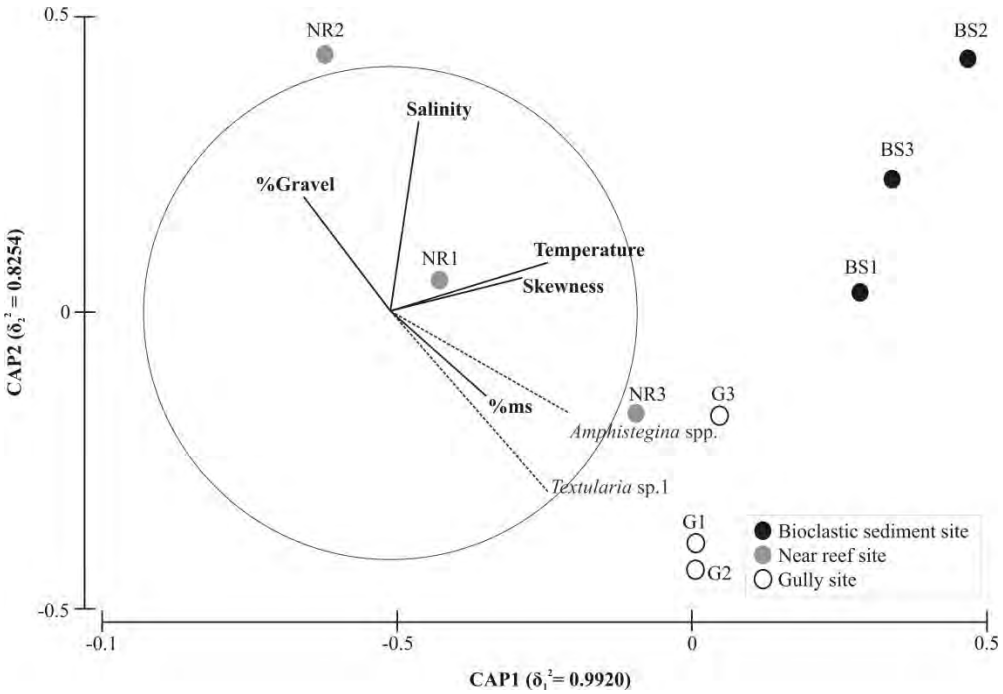

Figure 3.17. CAP analysis derived from the mean, fourth-root transformed total sediment foraminiferal assemblage abundance data. The Spearman rank correlation vectors of the combination of abiotic variables identified through the BVSTEP analysis are plotted with the vectors of the most distinguishing taxa (BS = bioclastic sediment, NR = near-reef and G = gully).

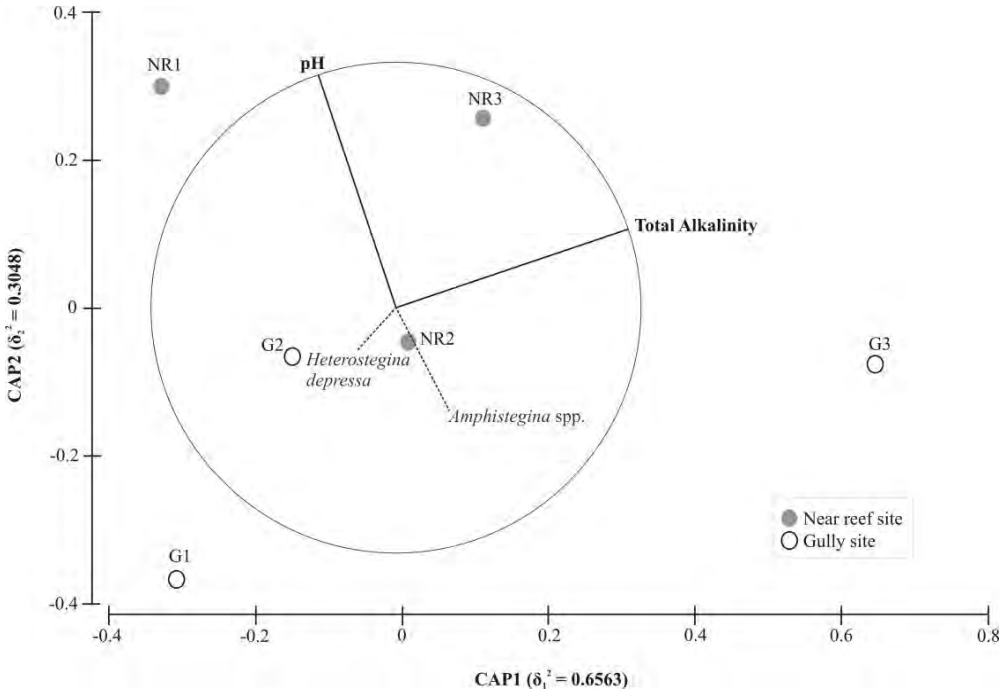

Figure 3.18. CAP analysis derived from the mean, fourth-root transformed live rubble foraminiferal assemblage abundance data. The Spearman rank correlation vectors of the combination of abiotic variables identified through the BVSTEP analysis are plotted with the vectors of the most distinguishing taxa (NR= near-reef and G = gully).

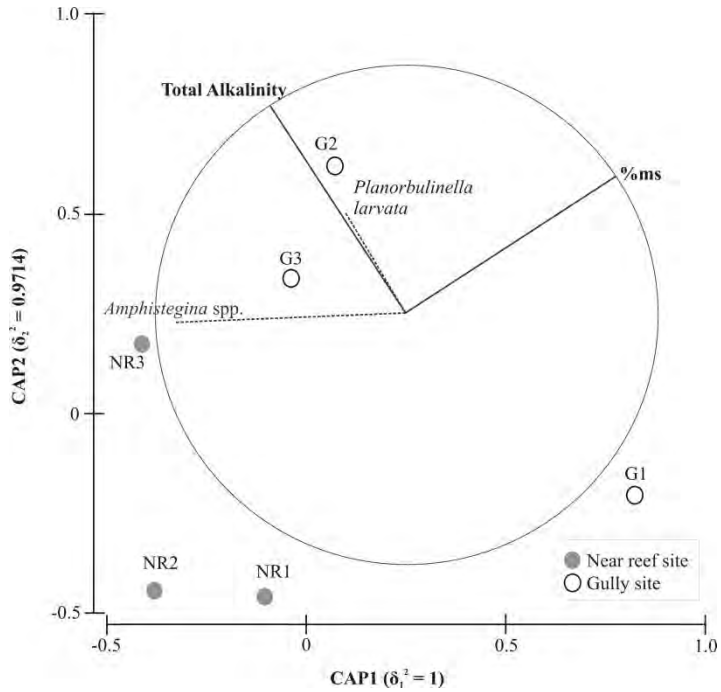

Figure 3.19. CAP analysis derived from the mean, fourth-root transformed total rubble foraminiferal assemblage abundance data. The Spearman rank correlation vectors of the combination of abiotic variables identified through the BVSTEP analysis are plotted with the vectors of the most distinguishing taxa (NR= near-reef and G = gully).

3.5. Discussion

3.5.1 Present-day seawater parameters on Two-mile Reef

Spatial separation was not evident for the majority of water chemistry parameters, however, temporal variation, showing a strong seasonal effect, was noted for temperature, salinity, T_A, Ω_{Ar} and Ω_{Ca}. No seasonal affect was found for pH. This insignificant result could have been confounded by the high degree of variation in the pH measurements obtained for December. Whether this variation was due to natural variation found in the environment is unclear. Nutrient parameters were all low, as anticipated for this oligotrophic environment. No significant difference between summer and winter Chl-*a* values were found, however, a location effect was evident in summer Chl-*a* values between the NR and G locations.

As expected, large differences were noted between summer and winter sea temperatures. The winter temperatures were relatively low and partially account for the marginal nature of Sodwana Bays reefs (Kleypas et al. 1999). Monthly salinity values varied, with the highest values recorded in January and the lowest in July. The differences noted in the monthly salinities could be attributed to differing contributions of TSW and STSW to the region. Higher salinities were noted in summer highlighting the dominance of STSW (>35.5). According to Duncan (1970), the greatest contribution of low salinity TSW (<35.3) occurs in winter. Lutjeharms (2006) reported the dominance of TSW along the east African coastline. Considering the vast quantities of fresh water bodies, in close proximity to the study site, submarine groundwater discharge is also a possibility. This phenomenon has been reported worldwide (e.g. Baltic coastal zone, Southeast and Gulf Coast regions, South Carolina, Sanggou Bay in China and the Western Mediterranean Sea among others) and can affect the salinity, temperature and nutrient regimes of the marine environment (Mejías et al. 2012; Kotwicki et al. 2014; Porubsky et al. 2014; Wang et al. 2014).

Another anomaly in the water chemistry data was seen in the T_A values for June. Differences across the sites were evident. Yet these differences were not mirrored in the June Ω_{Ar} and Ω_{Ca} values. Replicates were run for all T_A measurements, together with reference material to calibrate results, and were all similar. This indicates, similarly, differences could be due to natural variation found in the environment.

Sodwana Bay's reefs can be considered as non-reef coral communities, as the substratum the corals inhabit is a Pleistocene beachrock and aeolianite outcrop (Ramsay 1994). According to the Figure 3.20, a large portion of these non-reef communities are limited by Ω_{Ar} and extremely low sea

temperatures, however, unlike Sodwana Bay they are also limited by light penetration. Sodwana Bay has minimal sediment input and therefore the water remains clear for the majority of the year. This allows the reefs to be located deeper as there is increased light penetration. Silverman et al. (2007), reported mean global reef Ω_{Ar} to be 3.8. Kleypas et al. (1999), compiled Ω_{Ar} data from reefs worldwide and based on modelled projections, the Red Sea and Papua-New Guinea have the highest Ω_{Ar} values (4.1) with low aragonite (<3.5) occurring in Taiwan (3.50), Houtman Albatros Reef, Australia (3.36), Lord Howe Island (3.32) and New Zealand islands (3.06). In relation to worldwide studies, this study found TMR had extremely low Ω_{Ar} concentrations in winter (mean: 3.00 ±0.37 SD) and summer (mean: 3.54 ±0.36 SD). The reefs at Sodwana are classified as marginal (Celliers & Schleyer 2003) and Kleypas et al. (1999) anticipates the loss of accretion to commence in corals at an Ω_{Ar} of 3.4. This new data reinforces the marginal nature of Sodwana Bay's reefs.

Ω_{Ar} covaries with temperature, with maximum values found around the equator and the lowest around 20 - 30° latitude (Kleypas et al. 1999). Temperatures are limiting on these reefs and, in conjunction with the low Ω_{Ar} values, these factors appear to be contributing to these reefs being non-accretive in nature. Further annual water sampling, across various months and seasons, will need to be conducted to further constrain these observations and provide further insight into the water chemistry dynamics at Sodwana Bay.

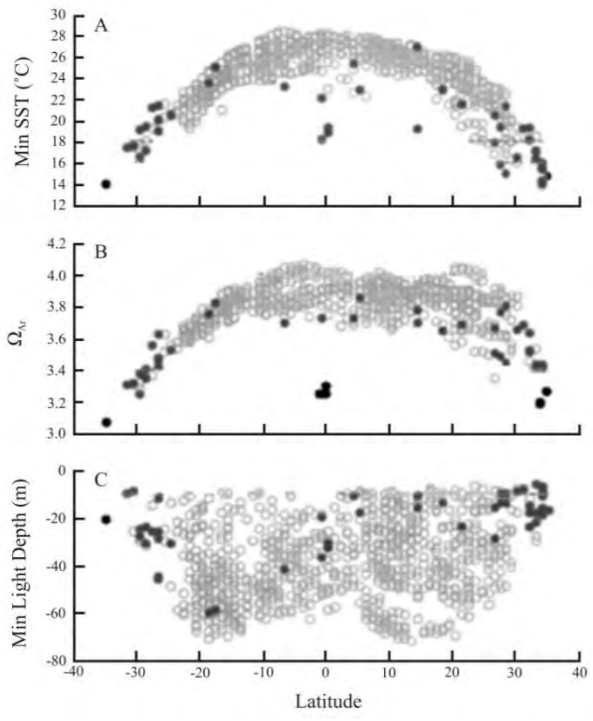

Figure 3.20. Compilation of reefs in accordance with latitude and **A** minimum sea surface temperature, **B** aragonite saturation state (Ω_{Ar}) and **C** minimum light penetration (m). Open circles designate reefs and filled circles denote non-reef coral communities. (after: Kleypas et al. 1999).

3.5.2 The living (coloured protoplasm) LBF population on Two-mile Reef

Similarly to previous reef studies, the majority of the living Foraminifera were present on the coral rubble. The living assemblages also differed according to location on TMR, for both substrata. This includes the univariate measure, abundance. The taxa present in the sediment samples were, however, more variable in comparison to the rubble samples. *Elphidium* was dominant in the live BS, sediment assemblages followed by *Ammonia* and *Heterostegina*. In comparison, *Asterigerina* was dominant in the NR and G sediment locations followed by *Amphistegina*. According to Riegl et al. (1995), gullies serve as conduits on reefs along which water is channelled, increasing the surge and resuspension of finer sediment.

According to Murray (1991), *Ammonia* and *Elphidium* are the most abundant benthic foraminiferal genera worldwide. *Elphidium* occurs from intertidal zones to the continental slope and from the tropics to polar regions (Murray 2006). *Ammonia* species are generally found from the subtidal zone to the outer continental shelves (Schweizer et al. 2011). Both are characterised as opportunistic and stress-tolerant genera. *Asterigerina* is a subtropical-tropical genus found on the inner shelf (Murray 2006) and is characteristic of high turbulence (Javaux & Scott 2003). Its dominance in the G and NR locations corroborates the high turbulence experienced. This genus also appears to be negatively correlated with T_A. However, no location affect was evident for T_A across the reef sites.

Amphistegina spp. was the highest contributor, and the most distinguishing taxon within the rubble, live assemblages. It was also most distinguishing taxon between the sediment and rubble live assemblages. *Amphistegina* is considered an invasive genus in the Mediterranean as it is tolerant of a wide range of environmental conditions (Langer et al. 2013b). It is also dominant in reef environments (Hallock 2000). It is a cosmopolitan genus and therefore not a good environmental indicator. Its distinguishing nature between the sediment and rubble assemblages can be attributed to it being present in higher numbers in the rubble samples in comparison to the sediment samples.

Heterostegina depressa was distinguishing in the rubble samples. The highest percentages of this symbiont-bearing species were found in the rubble assemblages. The species *H.depressa* is the only nummulitid which inhabits high energy environments (Beavington-Penney & Racey 2004). In Japan and Indonesia, it was found to prefer hard, solid substrata, however, in the Gulf of Aqaba, *H.depressa* was found on the base of corals as well as inhabiting coarse coral debris. This explains it's preference for hard substrata and hence its lack of significance and low abundance in the sediment samples.

3.5.3 Differences in total foraminiferal assemblages between substrata and locations

A high foraminiferal diversity (63 taxa) was identified from the >500 μm fraction from the 45 samples collected on TMR. Sediment and rubble foraminiferal assemblages appear to be affected by different environmental variables. The epiphytic Foraminifera present on rubble were not significantly related to the sediment variables and water parameters. Salinity, pH, temperature, T_A, Ω_{Ar}, Ω_{Ca} and nutrients showed no location affects, however, significant differences were found in the total assemblages, from rubble and sediment, according to location on the reef. Water depth differed across locations but was not the principal regulating factor of the foraminiferal assemblages. A significant difference in the foraminiferal assemblages between the two substrata was evident. *Amphistegina* spp. contributed the most to this dissimilarity and was also the most distinguishing taxon. The second highest contributor and distinguishing species was *H.depressa.*

Amphistegina spp. was the distinguishing and dominant taxon in the BS and NR sediment foraminiferal assemblages. *Amphistegina* spp. was also dominant in the G sediment samples; however, *Textularia* sp.1 was most distinguishing species in these samples. *Textularia* is a robust, sessile, infaunal genus which had the second highest abundances in both the sediment and rubble samples. Its robust agglutinated test, allows it to survive in turbulent, coarse surface sediments (Buosi et al. 2012). This could explain it being the distinguishing taxon in the G sediment samples. The G sediment samples had high percentages of cs, however, the NR sediment samples had the highest vcs and gravel percentages. Both the BS and NR sediment sites did, however, have higher mean and median grain sizes in comparison to the G sites. *Textularia* sp.1 was the second most distinguishing taxon at the other two locations. The CAP analysis revealed a positive correlation between *Amphistegina* spp. and *Textularia* sp.1 with ms and a negative correlation with gravel.

It is evident from the CAP analysis that *Textularia* sp.1 was dominant in the more turbulent environment (gullies); however, has preference to medium sand in comparison to larger size fractions. The third most distinguishing taxon in the G sediment samples was *Asterigerina* sp.1. As previously stated this genus is also characteristic of high turbulent areas (Javaux & Scott 2003).

The NR and G rubble samples each had different distinguishing taxa. *Amphistegina* spp. contributed the most to the similarity and was also the most distinguishing taxon in the NR rubble samples whereas *Planorbulinella larvata* was the most distinguishing taxon in the G location. This species has also been reported in neighbouring Mozambique (Hayward 2014). According to Langer (1993), the genus *Planorbulina* (synonymised name for *Planorbulinella*) represents Foraminifera which

permanently attach themselves by secreting a "glyco-glue". They can thus withstand more turbulent conditions. A study conducted by Buchan (2006) in San Salvador, Bahamas, found *Planorbulina* was dominant at study sites which experienced higher energy. The increased turbulence in the gullies is supported by the presence of the distinguishing *Planorbulinella*, as due to its permanent attachment, it can survive this higher energy environment.

Sorites was only distinguishing in the NR rubble samples. The *Sorites* genus has preference for calmer conditions (Buchan 2006). This again corroborates the higher turbulence at the G locations on the reef, making it a discriminant within the foraminiferal community structure. *Sorties* does not have an attachment surface and does not produce a "glycol-glue" (Langer 1993) and therefore can be easily removed from the substratum. It would thus need to inhabit calmer environments; hence its apparent lack of significance in the G rubble samples. The opposite correlation in *Amphistegina* spp. with percentage of ms was seen in the CAP analysis with the rubble total assemblages in comparison to the apparent positive correlation noted with the total sediment assemblage.

The ratio (S/R_{Tot}) revealed the main differences between the 20 most common genera were accounted for by genera which were present in high numbers in the sediment samples*, Amphistegina, Heterostegina, Planorbulinella* and *Asterigerina*. More delicate taxa, *Pyrgo*, *Sorites* and *Spiroloculina*, were present in higher numbers on the rubble samples. The genus *Cibicides* was also present in higher abundances on the rubble as this genus temporarily attaches to the substratum. Based on the S/R_R index, however, only two genera were present in higher proportions in the sediment in comparison to the rubble, *Amphistegina* and *Heterostegina*. These indices were performed on the relative abundance data. Both *Amphistegina* and *Heterostegina* were present in higher abundances in the rubble living assemblages, yet had the highest indices. *Ammonia* had the highest S/R_{Tot} index and was only found alive in the sediment samples. This index, together with those of *Amphistegina* and *Heterostegina*, reinforces the fact that the sediment assemblages provide a good reflection of the taxa in both the sediment and rubble substrata. The ind/m^2 of *Amphistegina* was extremely high in the sediment and this genus therefore dominates the sediment samples. Proportionally, *Amphistegina* were less abundant amongst the rubble Foraminifera and, therefore, other smaller, delicate taxa made up more of this assemblage. *Amphistegina* was, however, still present amongst the rubble Foraminifera.

Due to this study comparing rubble and sediment assemblages, the abundance metric (ind/m^2) was used for all analyses. It is important to note, however, it is customary to use densities (ind/g) of

foraminiferal species. The RELATE procedure showed a highly significant correlation between matrices constructed from abundance of total sediment Foraminifera compared with density. This demonstrates either metric is suitable when assessing sediment foraminiferal assemblages.

3.5.4 Comparison with previous reef studies

In studies conducted on the Florida reef sediments, Lidz and Rose (1989), found 50 foraminiferal species belonging to 32 genera with Wright and Hay (1971) reporting 117 species representing 60 genera. A more recent study conducted on Conch Reef in the Florida reef tract on both sediment and rubble samples reported 117 foraminiferal species representing 72 genera (Stephenson 2011; Stephenson et al. 2015). A study conducted by Natsir and Subkhan (2011) on the coral reef communities from Belitung Island in Indonesia reported 29 species in 18 genera in sediment samples with a study on sediment samples from the Great Barrier Reef by Nobes and Uthicke (2008) reporting 64 species representing 43 genera. This study only focused on the >500 μm fraction, yet 63 species belonging to 27 genera were identified. It is noted the aforementioned studies were on the >63 μm fraction which would account for this difference, yet even though only the >500 μm fraction was assessed for this study in comparison to other reef studies, Sodwana Bay's reefs also have a high foraminiferal diversity. In comparison with the study by Stephenson (2011), who found the highest number of taxa in the rubble samples, the rubble samples at Sodwana Bay had a lower number of taxa compared with the sediment samples. It is, however, noted, the study by Stephenson (2011) was on the >63 μm fraction which could account for the observed discrepancy.

3.6. Conclusions

With climate change, it is anticipated that more environments will become marginal for reef growth and accretion, therefore it is important to study these marginal reefs to gain a more comprehensive understanding of what to expect for other reefs in the future. Little is known about the foraminiferal assemblages on TMR and therefore this research serves as a baseline for future foraminiferal studies in this region.

Sea temperatures are limiting for Sodwana Bay's reefs, yet limited bleaching has been reported for these reefs (Celliers & Schleyer 2003). Cold-water upwelling from the adjacent shelf and potentially submarine canyons has been reported by Morris (2009) as a factor protecting these reefs from extreme temperature fluctuations. The Ω_{Ar} values recorded on TMR are considerably low in this study. It would appear both temperature and Ω_{Ar} are limiting coral growth and subsequent accretion of the reefs. The latter would appear to be more limiting to these reefs as, as stated by Kleypas et al. (1999),

loss of accretion is anticipated to commence at an Ω_{Ar} of 3.4. The water chemistry data revealed winter values to be below this threshold with borderline summer values.

The LBF communities studied on TMR showed distinct differences across the sample locations. Significant differences were evident between the sediment and rubble foraminiferal assemblages with both being influenced by different environmental parameters. As reported in previous studies, the majority of the living assemblage was present on the rubble. The sediment texture was insignificant in the distribution of the live and total rubble assemblages; however, percentages of gravel and ms were discriminants in the sediment assemblages. Rubble assemblages were not strongly correlated with sediment characteristics or the measured water chemistry parameters. Hence another, unaccounted for factor is affecting them. It is surmised that turbulence plays a role, overall, in the distribution in the rubble foraminiferal assemblages. A location affect was evident in the live (coloured protoplasm) rubble LBF. Therefore it would appear the increased resuspension of finer material within the gullies is potentially enough to discriminate among these assemblages.

According to Riegl et al (1995), the coral communities in shallow areas (6-25 m), along the east coast of South Africa, can be divided into a reef-top and gully subcommunity. They found the dominant factors influencing the coral community structure were location (flat reef top or gully) and depth. With this in mind, the foraminiferal assemblages appear to follow a similar trend with regards to location affects. The CAP analysis revealed depth was not a contributing factor for either sediment or rubble foraminiferal assemblages. No location affect in water chemistry parameters was evident across the reef, lending to the assumption that other environmental factors (e.g. turbulence) are also influencing foraminiferal distribution on the reef. No site differences were evident for the foraminiferal assemblages, showing the samples collected were very homogenous within each location. The species not found within both samples were uncommon and therefore the sediment foraminiferal assemblages were a good reflection of the taxa found on the rubble. The sediment total assemblages also had higher percentages of *Heterostegina depressa* in comparison to the rubble total assemblages, signifying once the Foraminifera dies, the tests are being washed off the rubble and deposited in the sand. The same is seen in *Amphistegina* spp. These taxa were found predominantly alive on the rubble samples yet the sediment total assemblage abundance far exceeds that seen in the rubble samples. This supports the theory that, once the Foraminifera die, their tests are being washed off the rubble and deposited within the sediment.

CHAPTER 4
SHALLOW, INSHORE SEDIMENT CORES AT TWO-MILE REEF

4.1. Overview

Coral growth at Sodwana Bay is surmised to have started ±5000 years BP, on top of a submerged dune and beach rock sequence (Ramsay 1994). A palaeoclimatic record, spanning the whole or a portion of this record would thus be beneficial in determining the effects of climate change in this environment. Numerous organisms (e.g. trees, Foraminifera, corals) change their growth and/or population dynamics in response to changes in the environment and these variations are then recorded in dead specimens or in fossil assemblages (Jansen et al. 2007). Pollen, plankton and Foraminifera extracted from sediment cores can be used in conjunction with their present-day distribution and current climate, to interpret past climatic variations (e.g. temperatures, salinity and pH) (Jansen et al. 2007). Isotopic signatures, incorporated within the calcium carbonate skeletons and tests, of these organism serve as proxies for a variety of ocean properties (e.g. temperature, pH, productivity) (Katz et al. 2010). Proxy measurements still, however, carry uncertainties. Some of the best-developed and understood proxy sources are from tree rings, ocean and lake plankton and pollen which can date millennia (Jansen et al. 2007).

Understanding long time-series in environmental parameters as well as the response of calcifying organisms is crucial due to the increasing threat climate change is posing to reef systems. As coral bommies, of adequate size, are not always available for collection and isotopic analysis, sediment records provide a useful alternative, as they contain other calcifiers. Foraminifera, within the reef sediment, are a valuable micropalaeonotological taxon due to their small size, abundance, preferences for specific ecological environments, resistance to breakage and preservation in the environment (Murray 2006). The Large Benthic Foraminifera (LBF) are particularly useful, as they are symbiont-bearing and require similar water conditions to corals. They are also abundant in coral reef environments and serve as alternatives to studying coral cores, with little disturbance caused on reef and unconsolidated sediments through their sampling. Their calcium carbonate tests serve as proxies for a variety of past ocean conditions and due to their high preservation capacity, they serve as ideal target organisms for reef palaeoclimatic studies. Studies worldwide have used these protists for palaeoenvironmental interpretations including sea-level reconstructions (e.g. Strachan et al. 2013), hurricane incidents (e.g. Das et al. 2013) and eutrophication (e.g. Osterman et al. 2008; Tsujimoto et al. 2008). Climatic reconstructions are increasingly becoming a tool in climate change research as

they provide a means to extract information beyond modern records and provide information regarding how organisms have responded to environmental changes in the past.

This study is based upon the guiding principle of Uniformitarianism (Bowden et al. 2014) that "the present is the key to the past" and that foraminiferal assemblages are a proxy of the past climatic regime of Two-mile Reef (TMR). The premise is that present-day abiotic controls on the distribution of foraminiferal morphogroups and species/genera provide a mechanism to interpreting the palaeoclimatic record.

4.2. Objectives and hypotheses

This chapter outlines the Late Holocene record of TMR using Foraminifera as indicator organisms. The main aim was to try and ascertain how the reef environment has changed during the Late Holocene and thereafter provide some comment on what to expect in the future.

4.2.1 Objectives

1. Identify the foraminiferal assemblages along a sediment core, to the lowest possible taxonomic level.
2. Establish whether the inshore sampling site incorporates a record of the past climate on TMR.

4.2.2 Hypotheses

H_{a1}: There is a difference in foraminiferal assemblages across sediment size fractions deposited with time.

H_{a2}: Distinct foraminiferal down-core trends are evident in the core.

H_{a3}: The inshore sampling site is suitable for recording the palaeoclimate of TMR.

4.3. Materials and methods

The shallow, dynamic reef environment, at Sodwana Bay, makes it difficult to collect sediment cores in the conventional manner and therefore a diver-operated hammer corer was used in this study. Down-core $\delta^{18}O$, $\delta^{13}C$ and ^{14}C isotope analyses were performed to try elucidate the sea temperature change over the study period and to provide age control points in the cores. Based on the recommendation by Katz et al. (2010), in order to avoid any potential bias in the results, through

interspecies isotopic offsets, a single foraminiferal species, *Amphistegina lobifera*, was selected for all isotopic analysis. Similar sized specimens were also selected, to avoid any isotopic effects due to ontogenetic variation.

4.3.1 Selection of core locations

Coring sites were selected based on geographic information systems (GIS) data of TMR, in conjunction with groundtruthing in field surveys. Trial cores, adjacent to the reef, were unsuccessful due to an abundance of coral rubble. Four intact cores were therefore collected at the outer fringe of a bioclastic sediment field, on the inshore side of TMR (Figure 4.1). The cores (X, Y, Z and A) were collected during field sampling trips in August, October and November 2012 from water depths ranging from 15.2 – 16.3 m. Only cores X, Y and Z were further analysed as upon splitting, core A displayed a high degree of disturbance.

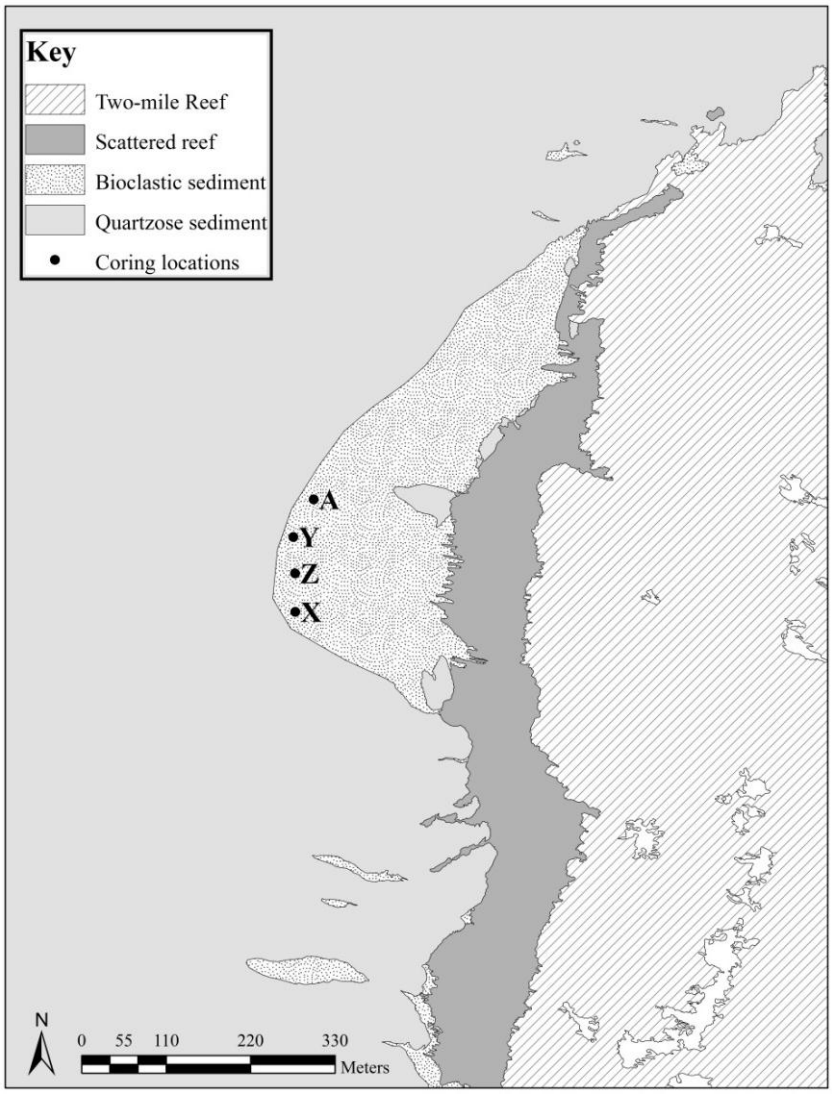

Figure 4.1. Map showing coring locations adjacent to Two-mile Reef.

4.3.2 Coring method

Cores were collected on SCUBA using a diver-operated hammer corer designed and manufactured in-house (Figure 4.2). It comprised a 35 kg stainless steel device with a slide hammer on a fixed sleeve to drive the 75 mm diameter stainless steel core cylinders. A handmade, brass shim-stock core-catcher was riveted to the bottom of the stainless steel core cylinder to minimize sediment loss from the cores (Figure 4.3). Upon reaching maximum penetration, the core cylinders were marked at the sediment surface, extracted, capped on both ends, and lifted to the surface using air-lift bags. All cores were transported back to the laboratory upright and stored in a vertical position until analysis.

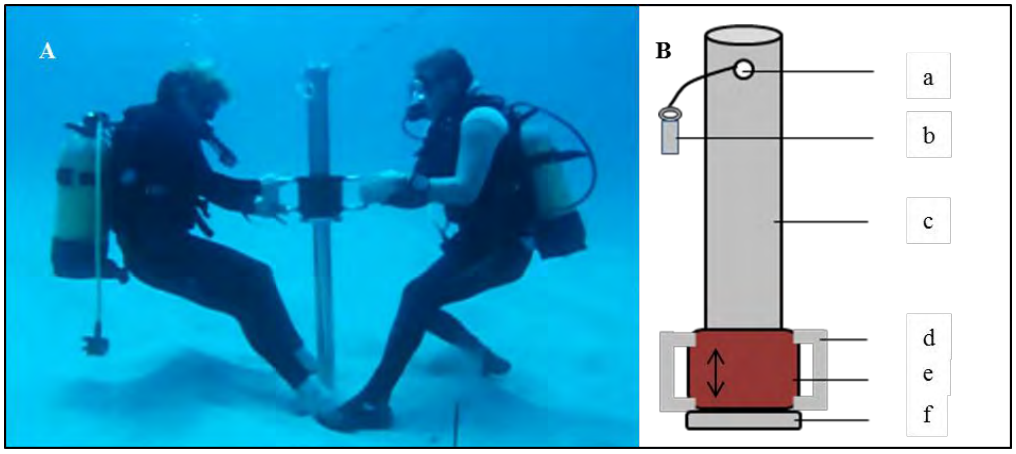

Figure 4.2. **A** Divers operating the hammer corer, **B** Diagrammatic representation of the hammer corer: (a) hole in sleeve through which core pipe is secured to corer, (b) pin to secure core pipe, (c) stainless steel sleeve, (d) handle, (e) weighted hammer, (f) impact flange for slide hammer.

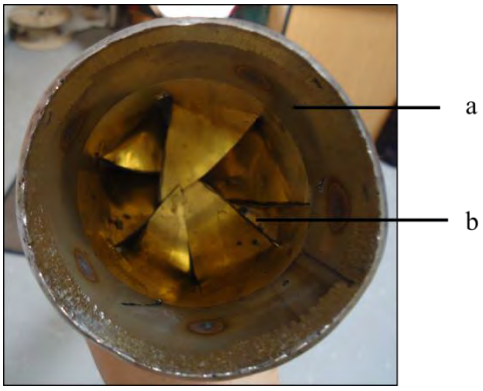

Figure 4.3. A scampered stainless steel collar (a) used to secure core-catcher (b).

Once back at the Oceanographic Research Institute (ORI) laboratories, all cores were split, visually logged and the lithology described. One half of each core was wrapped in plastic cling wrap and stored for archival purposes. The remaining half was sampled for sediment characterisation, foraminiferal assemblages, grain size distribution, carbonate content and Foraminifera isotopic signatures (Methods described in Chapter 2). The longest core, X, was subsampled in centimetre slices along its entire length. In total, 32 samples were then used for subsequent analysis, with approximately every second centimetre used. This ensured samples were analysed from each identified horizon. The samples were split into three subsamples for grain size analysis, carbonate content and foraminiferal assemblage determination (Chapter 2). The top 25 centimetres of cores Y and Z were also subsampled in centimetre slices. In total, 16 and 18 samples were used for subsequent analysis for cores Y and Z respectively. This again ensured a sample from each horizon was analysed. Core Y and Z samples were then split for grain size and carbonate content analysis only (Chapter 2). Table 4.1 displays the metadata for each core collected.

Table 4.1. Details of bioclastic sediment cores collected inshore of Two-mile Reef. Shaded sample denotes core A, which was not analysed further in this study.

Core	Date Collected	Latitude (S)	Longitude (E)	Depth (m)	Maximum penetration (cm)	Recovered core length (cm)
X	26/09/12	27° 31.161	32° 40.928	16.3	115.5	61.0
Y	01/10/12	27° 31.106	32° 40.931	16.0	115.5	47.0
Z	27/11/12	27° 31.134	32° 40.931	15.2	115.5	49.1
A	27/11/12	27° 31.082	32° 40.944	16.2	115.5	51.9

4.3.3 Foraminiferal analysis

Foraminifera were identified only in Core X, from three size fractions: 125 µm, 250µm and 500µm (Chapter 2). A Foraminifera study was not included for the other two cores as this was the most time consuming component of the study and was not deemed vital for the verification process.

Oxygen and carbon isotope analyses were performed on all samples collected from the three cores (Chapter 2). Tests without any signs of chemical or physical alterations were selected for stable isotope analyses. Care was taken to select adult specimens of *A.lobifera* of comparable size from the >500 µm fraction. The *A.lobifera* tests were picked out from the base of the longest core, Core X, at 54 cm as well as from the bottom half of cores X, Y and Z at 37, 38 and 41 cm respectively and sent for radiocarbon dating (Chapter 2).

4.3.4 Statistical analysis

An explanation of the statistical methods used is given in Chapter two. The sediment characteristics and isotope analysis results were first assessed individually for each core. Descriptive statistics of grain size and carbonate content as well as contour maps to visually assess the down-core changes were used.

Foraminiferal counts were first standardised to ind/g and percent contributions were assessed for each individual size fraction (500 μm, 250 μm and 125 μm) as well as all fraction data combined (whole sample) within core X. Down-core univariate statistics for each fraction were assessed including the main suborder and genera contributions to each fraction as a whole, followed by assessing the relative down-core contributions. The average contributions of each taxon together with the taxa which consistently contribute to the similarity within each size fraction were determined using similarity percentage (SIMPER) analyses. These were performed at species level. Multivariate statistics employed were a similarity profile (SIMPROF) cluster analysis on total taxa densities (whole sample data) from core X. The cluster analysis was based on a Bray Curtis Similarity Resemblance matrix of standardised, square-root transformed data. A SIMPER test was also used to determine the taxa contributing to the identified clusters as well as those contributing the most to the dissimilarity between clusters. The Spearman's rank correlation coefficients (ρ) were calculated to ascertain how distinct the foraminiferal assemblages, from each size fraction were, using the RELATE test (Primer v6).

Spearman correlations using a step-wise search (BVSTEP analysis in Primer v6) were further utilised to determine which suite of abiotic variables best accounted for the observed foraminiferal assemblages within core X (Table 4.2). Two separate analyses were performed. The first was based solely on the sediment characteristics, followed by the sediment characteristics and isotope data. The significance of the relationships (global BEST test) was then determined. A canonical analysis of principal coordinates (CAP) was then used to find the axes through the multivariate biotic dataset which had the highest correlation with the abiotic variables. This was used to show the relationship between the abiotic and biotic data.

Table 4.2. Measured sediment characteristics and isotopes.

Environmental variable	
Sediment characteristics	Gravel (%gravel)
	Very coarse sand (%vcs)
	Coarse sand (%cs)
	Medium sand (%ms)
	Fine sand (%fs)
	Very fine sand (%vfs)
	Mud (%mud)
	Carbonate content (%)
	Mean (phi)
	Mean (mm)
	Median (phi)
	Median (mm)
	Sorting
	Skewness
Foraminifera isotopes	$\delta^{18}O$ (‰)
	$\delta^{13}C$ (‰)

4.4. Results

4.4.1 Sediment characterisation and Foraminifera isotope results

Core lithology

The boundaries (i.e. sharp, erosional or gradational contact) between each unit are displayed on the respective core stratigraphic logs. A sharp boundary denotes a clear contact whereas an erosional contact exhibits some form of disturbance and a gradational contact displays no clear boundary between two units but rather transitions from one to the other. Visual interpretation of core X revealed 18 lithological units (XA – XR) (Figure 4.4). The top centimetre represented a disturbed core surface (Unit XA). Unit XB was light yellow-brown and Foraminifera rich. It consisted of coarsening upward gravel sediments. Unit XC was very poorly sorted and light brown, coarse to very coarse-grained sand. This was preceded by a light brown, massive unit which was composed of very course-grained sand to gravel (XD) followed by three alternating dark olive-gray medium-grained sand (XE, XG and XI) units and light yellow-brown very course-grained sand to gravel units (XF and XH). The mid-core was dominated by a crudely planar-laminated, light brown gravel unit (XJ) preceded by a thin (16.5 – 16.9 cm depth) very light brown gravel layer (XK). Unit XL consisted of medium to very coarse-grained sand which was poorly sorted and light yellow-brown in colour. The biggest unit, XM, from 17.9 – 35 cm depth was bioturbated with poorly-sorted sand infilled burrows. It was very coarse-grained sand to gravel in consistency and light yellow-brown in colour. The bottom of the core was made up of five units (XN -XR) consisting of a yellow-brown gravel unit (XN), another dark olive-gray medium-grained sand unit (XO), poorly sorted light olive-gray bioturbated gravel (XP) and a very thin lamination of light brown, coarse-grained sand (XQ). The bottom-most unit (XR) consisted

of an olive-gray fining upward very coarse-grained sand sequence, with a coral rubble plug at the very base of the core.

Figure 4.4. **A** Photograph of core X taken immediately once the core was cut open, **B** Sediment log of core X showing the 18 logged stratigraphic units.

Visual interpretation of core Y revealed 14 lithological units (YA - YN) (Figure 4.5). The top three centimetres consisted of disturbed sediment (YA) which was light brown, medium to coarse-grained sand. The following three units were yellow brown in colour with unit YB being medium to coarse-grained sand with an infilled olive-gray burrow. Unit YC consisted of coarse-grained sand and YD was coarse to very coarse-grained sand. These units were preceded by three alternating dark olive-gray medium-grained sand units (YE, YG and YI) with unit YF being yellow-brown, very coarse-grained sand with a high degree of shell debris and YH, a light yellow-brown, very coarse-grained sand to gravel unit. The mid-core was represented by an olive-green, very coarse-grained sand to gravel unit (YJ) which consisted a lot of shell debris with a coral rubble fragment encompassed within unit YK, a coarse to very coarse-grained, light brown sand unit. The base of the core was composed of three units, YL which encompassed very coarse-grained, light brown sand, unit YM another dark olive-gray medium-grained sand band and the basal unit (YN) of coarse, very dark olive-gray sand

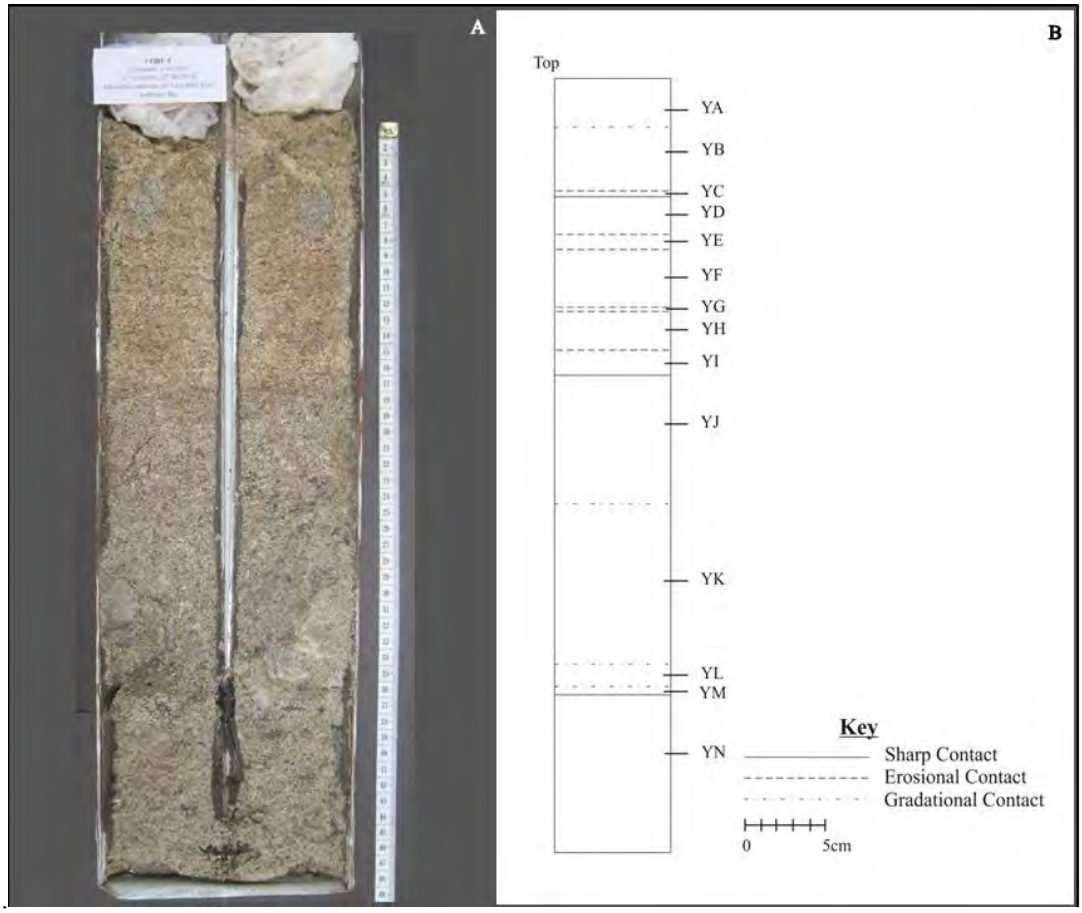

Figure 4.5. **A** Photograph of core Y taken immediately once the core was cut open, **B** Sediment log of core Y showing the 14 logged stratigraphic units.

Visual interpretation of core Z revealed 13 lithological units (ZA – ZM) (Figure 4.6). The top five centimetres, unit ZA, constituted of a Foraminifera rich, olive-brown layer. It was composed of very coarse-grained sand to grit. Unit ZB was composed of medium-grained, olive-gray sand which was followed by a coarse to very coarse-grained, Foraminifera-rich sand layer (ZC). Below was a very thin lens of dark olive-gray, medium-grained sand (ZD). A succession of three alternating dark olive-gray, medium-grained sand bands (ZF, ZH and ZJ) with brown sand-grained layers followed (ZE, ZG and ZK). Unit ZE being composed of medium-grained sand, ZG was composed of coarse-grained sand with a coral rubble cobble and ZK encompassed medium to coarse, light brown sand. The mid-core was dominated by a coral cobble found within a highly bioturbated, Foraminifera rich layer (ZL). This unit was composed of dark brown, coarse to very coarse-grained sand, with dark olive-gray, medium-grained bioturbations. The bottom-most unit fined upwards from a coral cobble at the base to very coarse-grained sand. It was Foraminifera rich and dark olive-gray to brown in colour.

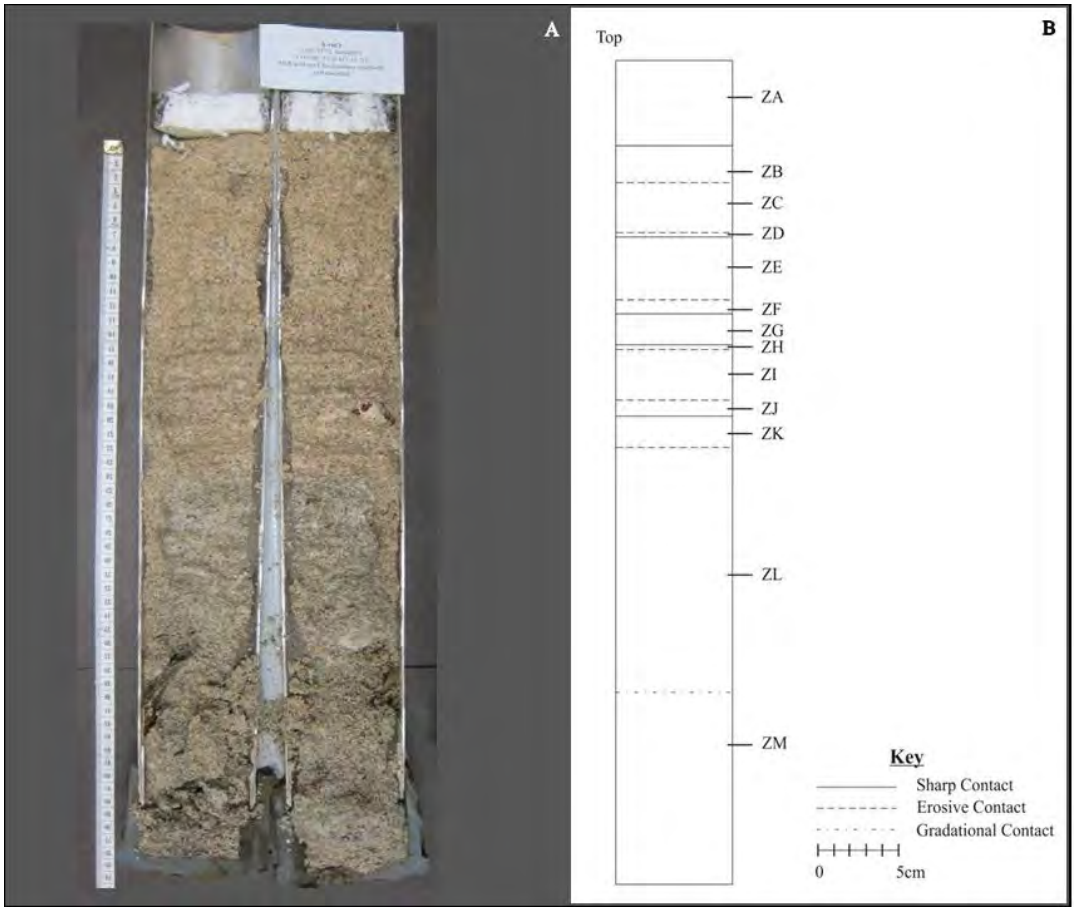

Figure 4.6. **A** Photograph of core Z taken immediately once the core was cut open, **B** Sediment log of core Z showing the 13 logged stratigraphic units.

Core logging revealed distinct horizons present within each core (Figure 4.7). On closer analysis of the stratigraphic logs, a visual agreement between various horizons (XE, YE, ZF and XG, YG, ZH and XI, YI, ZJ and XO, YM) across all three cores was evident and corresponded to an agreement between four dark olive-gray bands. The fourth dark olive-gray band was not present in core Z which can potentially be attributed to the high degree of bioturbations present in that portion of the core (unit ZL).

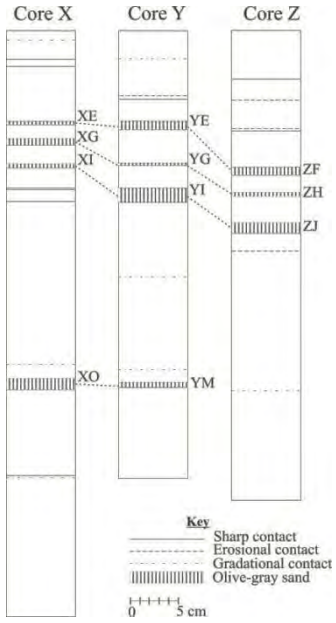

Figure 4.7. Comparison of the three core stratigraphic logs. Note the dotted lines connect units which are common to the cores.

Grain size and carbonate content results

Carbonate content and grain size analysis was conducted on all three cores and 32, 16 and 18 samples were analysed from core X, Y and Z respectively. Carbonate content (%) varied down-core across all three cores (Figure 4.8). Core X carbonate content ranged from 43.9 - 68.2% with an average of 54.6%. Core Y carbonate content ranged from 31.0 - 58.4% with an average of 48.0% and core Z carbonate content ranged from 44.6% - 75.4% with an average of 60.6%. Grain size varied down-core. The percentages of gravel (gravel), very coarse sand (vcs), coarse sand (cs), medium sand (ms), fine sand (fs), very fine sand (vfs), mean grain size, median grain size, sorting and skewness were determined, with all cores being dominated by coarse to medium sand (Figure 4.9). No mud was found and very little gravel (<7%) was present in the cores.

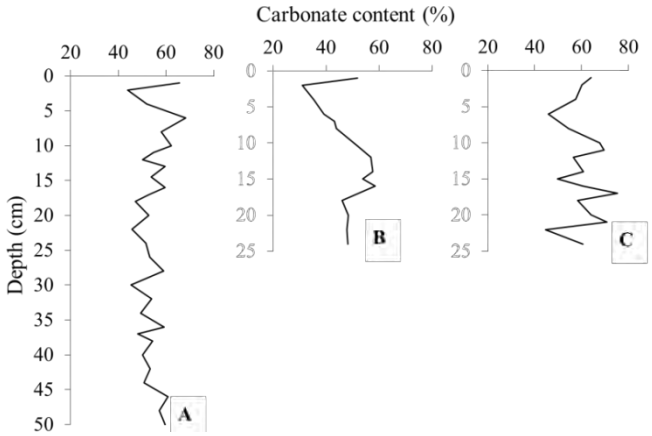

Figure 4.8. Down-core carbonate content (%): **A** Core X, **B** Core Y and **C** Core Z.

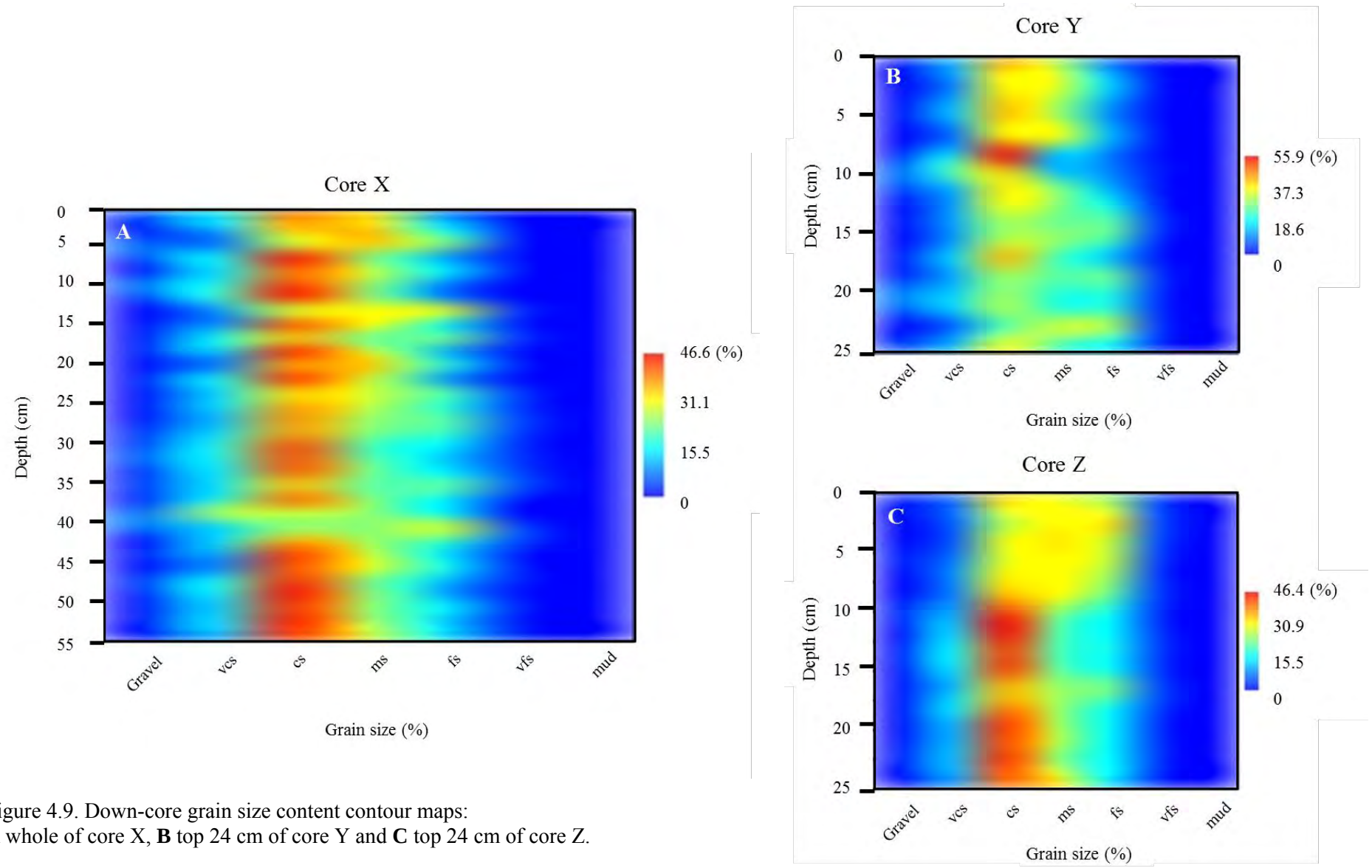

Figure 4.9. Down-core grain size content contour maps:
A whole of core X, **B** top 24 cm of core Y and **C** top 24 cm of core Z.

Radiocarbon dating

Four radiocarbon dates were obtained, two from core X and one each for cores Y and Z (Figure 4.10). A foraminiferal radiocarbon date obtained from the base of core X, gave a calendar-calibrated age of AD 680-920 (BP 1270 – 1030). This revealed that core X could be dated back 1212 ± 120 years. Units XO and YM were dated to have calendar-calibrated ages of AD 1390-1545 (BP 560-405) and AD 1455-1680 (BP 495-270) respectively. Due to the shape of the calendar calibration curve, three possible dates were obtained for unit ZM at 40 cm depth in Core Z. The dates were AD 1595–1605 (BP 355-345), AD 1615-1895 (BP 355-55) and AD 1940 – Post 1950 (BP 10 – Post 0).

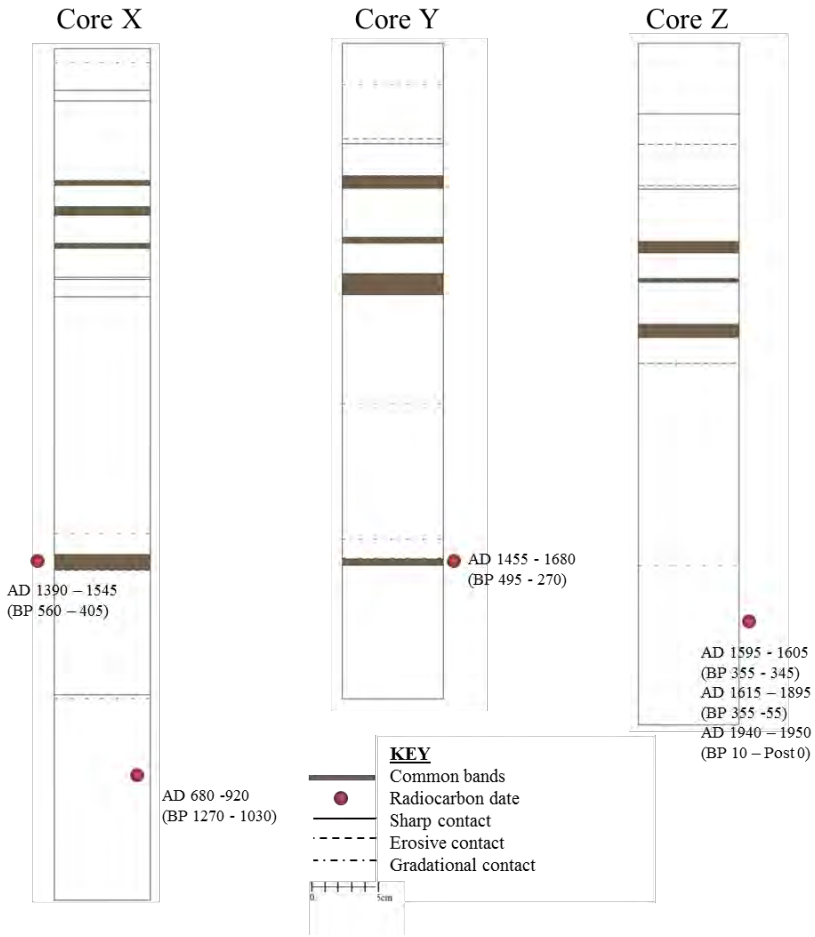

Figure 4.10. Sediment core logs showing common bands together with radiocarbon dates.

Stable isotope results

In total 32, 16 and 18 samples were analysed for $\delta^{18}O$ and $\delta^{13}C$ from cores X, Y and Z respectively. Two replicates of each sample were run, with the mean of the two values used in the analysis. All data are presented in the standard δ notation (‰) relative to VPDB (Figure 4.11).

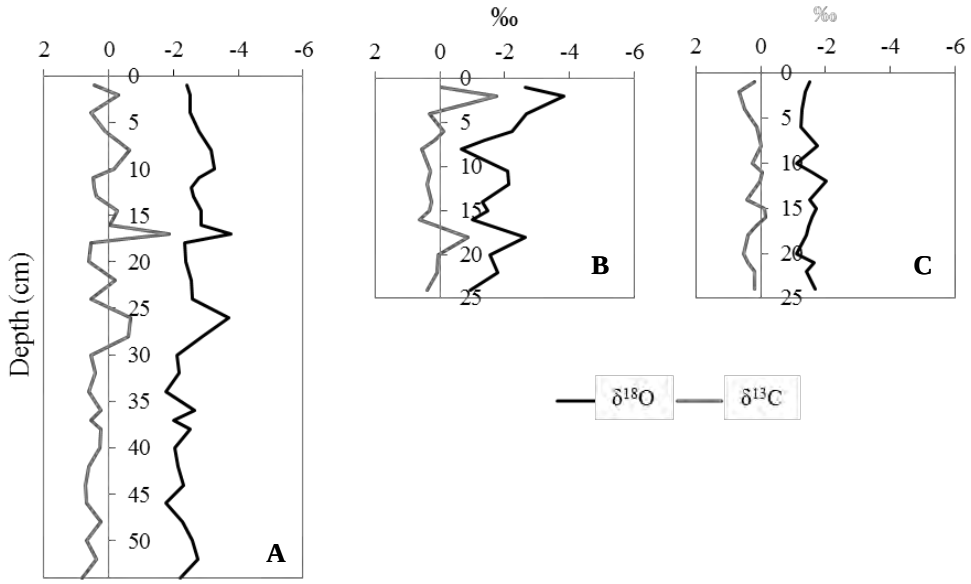

Figure 4.11. Down-core $\delta^{18}O$ and $\delta^{13}C$ foraminiferal signals: **A** Core X, **B** Core Y and **C** Core Z.

Calculated error based on repeat replicate measurements of the standards was 0.10‰ for $\delta^{18}O$ and 0.05‰ for $\delta^{13}C$. Core X $\delta^{18}O$ values ranged from -1.77 to -3.78‰ with a mean of -2.56‰. The mean standard deviation was 0.14 ‰. The $\delta^{13}C$ values ranged from -1.87 to 0.82‰ with a mean of 0.19‰ and a mean Standard deviation of 0.21‰. Core Y $\delta^{18}O$ values ranged from -3.82 to -0.68‰ with an average of -1.88‰. The mean standard deviation was 0.26‰. Core Y $\delta^{13}C$ values ranged from -1.74 to 0.63‰ with a mean of 0.23‰ and a mean standard deviation of 0.26‰. Core Z $\delta^{18}O$ values ranged from -2.00 to -1.09‰ with an average of -1.49‰. The mean standard deviation was 0.21‰. The $\delta^{13}C$ values ranged from -0.14 to 0.68‰ with a mean of 0.20‰ and a mean standard deviation of 0.18‰.

Statistical analysis of environmental variables

The full set of 14 sediment distribution datasets from core X (Table 4.2) were tested for collinearity using draftsman plots and a Spearman correlation matrix. The same analysis was repeated, including the stable oxygen and carbon datasets. Variables mean (phi) and mean (mm), and median (phi) and median (mm) were highly correlated ($\rho>0.9$), as expected, as they represented the same variable, however, on different scales. Subsequently mean (phi) and median (phi) were eliminated from the analyses including mud (%) as none of the latter was present. All other variables were retained in the test models. The mean (mm) grain size and vcs (%) data were log transformed as the data was right-skewed. Both datasets were then used for subsequent analysis in section 4.4.3.

4.4.2 Foraminiferal assemblage results

Cross verification was assessed using grain size, carbonate content, lithological descriptions and isotope analysis only. In total, 20 290 Foraminifera were picked from core X, with 12 630, 3228, and 4432 from the 500 µm, 250 µm and 125 µm fractions respectively. All Foraminifera counts were standardised to 1 g and the relative percentages used. Of the total number of Foraminifera picked, the 500 µm fraction constituted 62.3%, the smallest percentage (15.9%) was attributed to the 250 µm fraction and the 125 µm fraction contributed 21.8%. Percentage contribution fluctuated down-core for all the size fractions (Figure 4.12). The 500 µm down-core contribution ranged from 30.8 - 79.7% with an average contribution of 63.7%. The 250 µm down-core relative contributions ranged from 9.7 - 27.4% with an average contribution of 15.9% and the 125 µm fraction contribution ranged from 8.5 - 41.8% with an average contribution of 20.4%. Figure 4.13 displays the most abundant genera in each Foraminifera size fraction. Overall the samples were dominated by *Amphistegina*; however, *Pararotalia* was dominant in the 125 µm fraction.

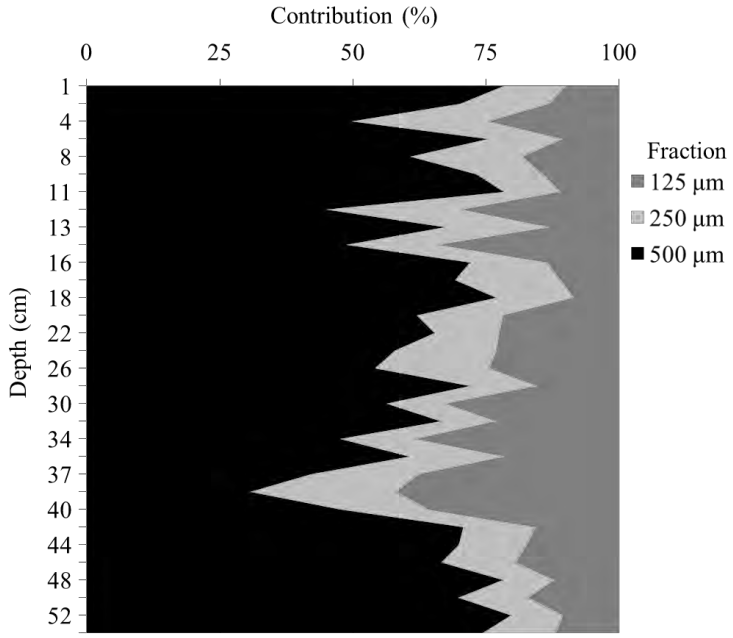

Figure 4.12. Down-core percentage contributions of the 500 µm, 250 µm and 125 µm fractions from core X. Data is expressed as percentages of the total Foraminifera picked.

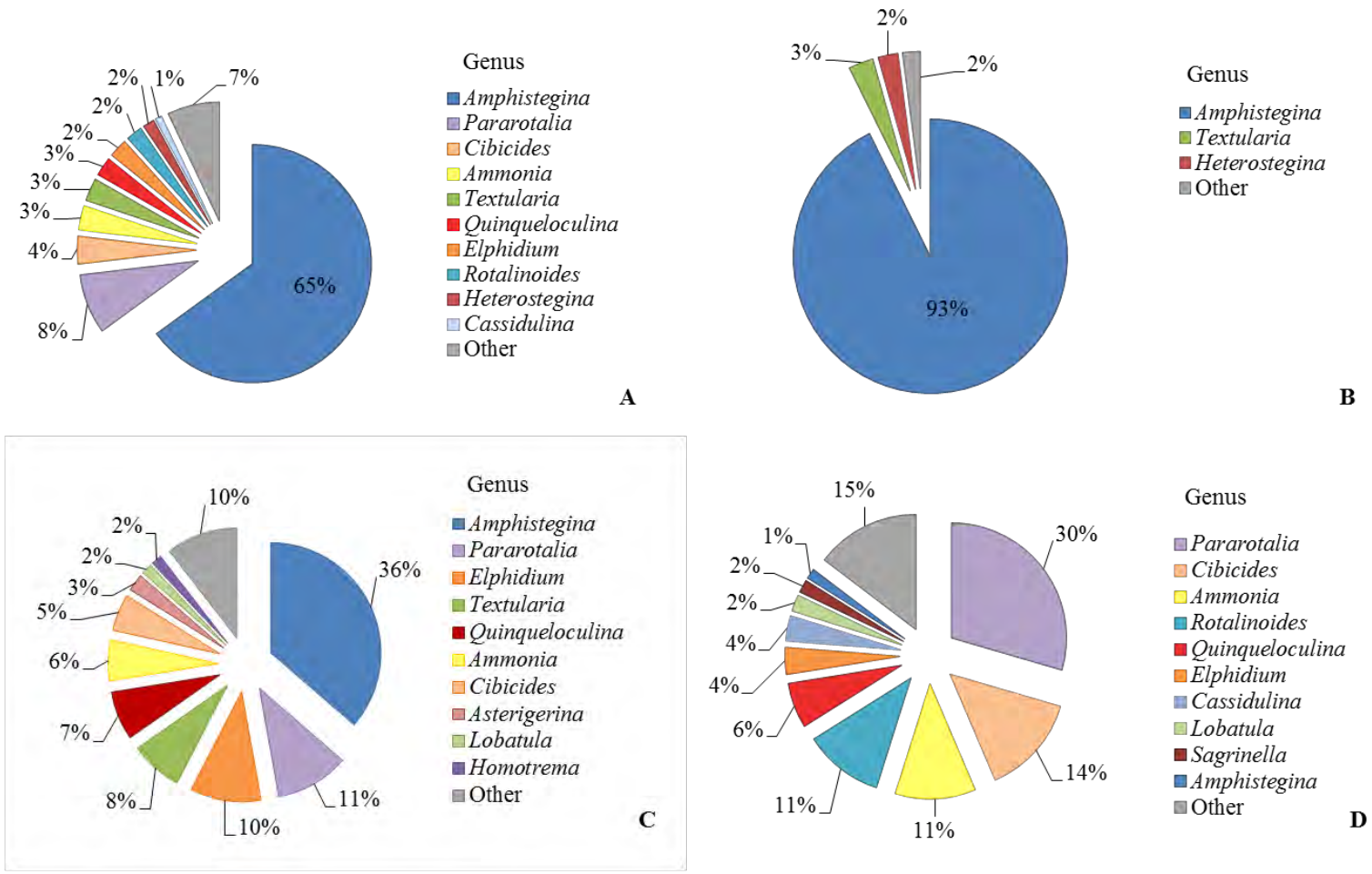

Figure 4.13. The main contributing genera to **A** the whole sample, **B** 500 µm, **C** 250 µm and **D** the 125 µm fraction.

Whole sample analysis

All taxa counts from all size fractions were combined and the data analysed. In total, 141 taxa were identified in all samples (Appendix B, Table B1). The ind/g ranged from 85 - 163 with a mean of 115 (Figure 4.14). The highest ind/g were found at 13, 12, 14.5 and 38 cm depths. Evenness (*J'*) ranged from 0.4 - 0.7 with an average of 0.5 and the Shannon Diversity Index (*H'*) ranged from 1.4 - 2.9 with an average of 1.9. Number of taxa (*S*) ranged from 29.0 – 89.0 with an average of 51.3. The highest Evenness values were noted at depths 12, 14.5 and 38 cm, highest Diversity at depths 12, 14.5, 34 and 38 cm and the highest number of taxa (*S*) were found at depths 12, 14.5, 30 and 38 cm.

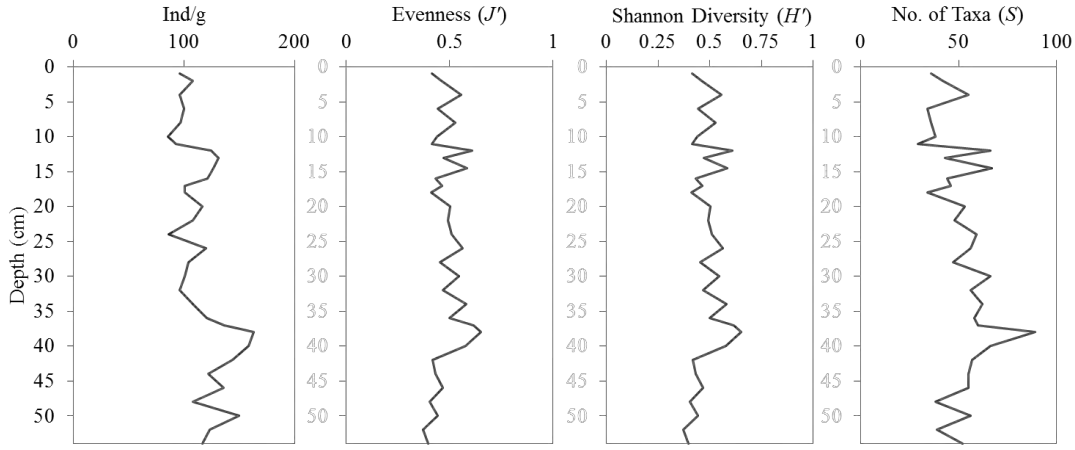

Figure 4.14. Down-core ind/g, evenness (*J'*), Shannon Diversity Index (*H'*) and number of taxa (*S*) for core X.

The dominant suborders, overall, were identified as Rotaliina; contributing 92.7% followed by Miliolina and then Textulariina each contributing 3.6% and 3.1% respectively. The down-core contribution of Rotaliina ranged from 88.8 - 95.8%. The down-core contribution of Miliolina ranged from 1.0 - 7.6% and Textulariina ranged from 1.5 - 6.1%. Within Rotaliina, *Amphistegina, Pararotalia* and *Cibicides* were the most prevalent genera with *Quinqueloculina* and *Textularia* being dominant in the Miliolina and Textulariina suborders respectively.

Down-core contributions fluctuated throughout all graphs in Figure 4.15**.** The genus *Amphistegina* remained the dominating genus at all the sampling points and fluctuated in its percent contribution down-core with distinct dips in the contribution at depths 12, 14.5 and 38 cm. The *Pararotalia* and *Cibicides* genera showed similar down-core fluctuations. A distinct peak in *Pararotalia* was seen at 38 cm depth with smaller peaks at 34 and 14.5 cm. Peaks in *Cibicides* and *Ammonia* were noted at 12, 14.5 and 37 cm and 12, 14.5, 34 and 37 cm respectively. After *Amphistegina, Pararotalia, Cibicides,*

and *Ammonia, Textularia, Quinqueloculina*, *Elphidium, Rotalinoides, Heterostegina* and *Cassidulina* were the most abundant genera. These ten genera contributed 92.9% to the total Foraminifera count with the remaining 47 genera making up the remaining 7.1%. There were concomitant increases in percentage contribution in the *Pararotalia, Cibicides* and *Ammonia* genera as well as diversity, evenness and number of taxa together with a concomitant dip in contribution within the *Amphistegina* genus at depths 12, 14.5, 37 and 38 cm. The most abundant taxa identified overall were *Amphistegina* spp., *Pararotalia* sp.2, *Pararotalia stellata*, *Cibicides refulgens*, *Textularia* sp.1, *Ammonia beccarii*, *Heterostegina depressa*, *Rotalinoides* sp.5, *Elphidium* sp.11 and *Elphidium macellum.*

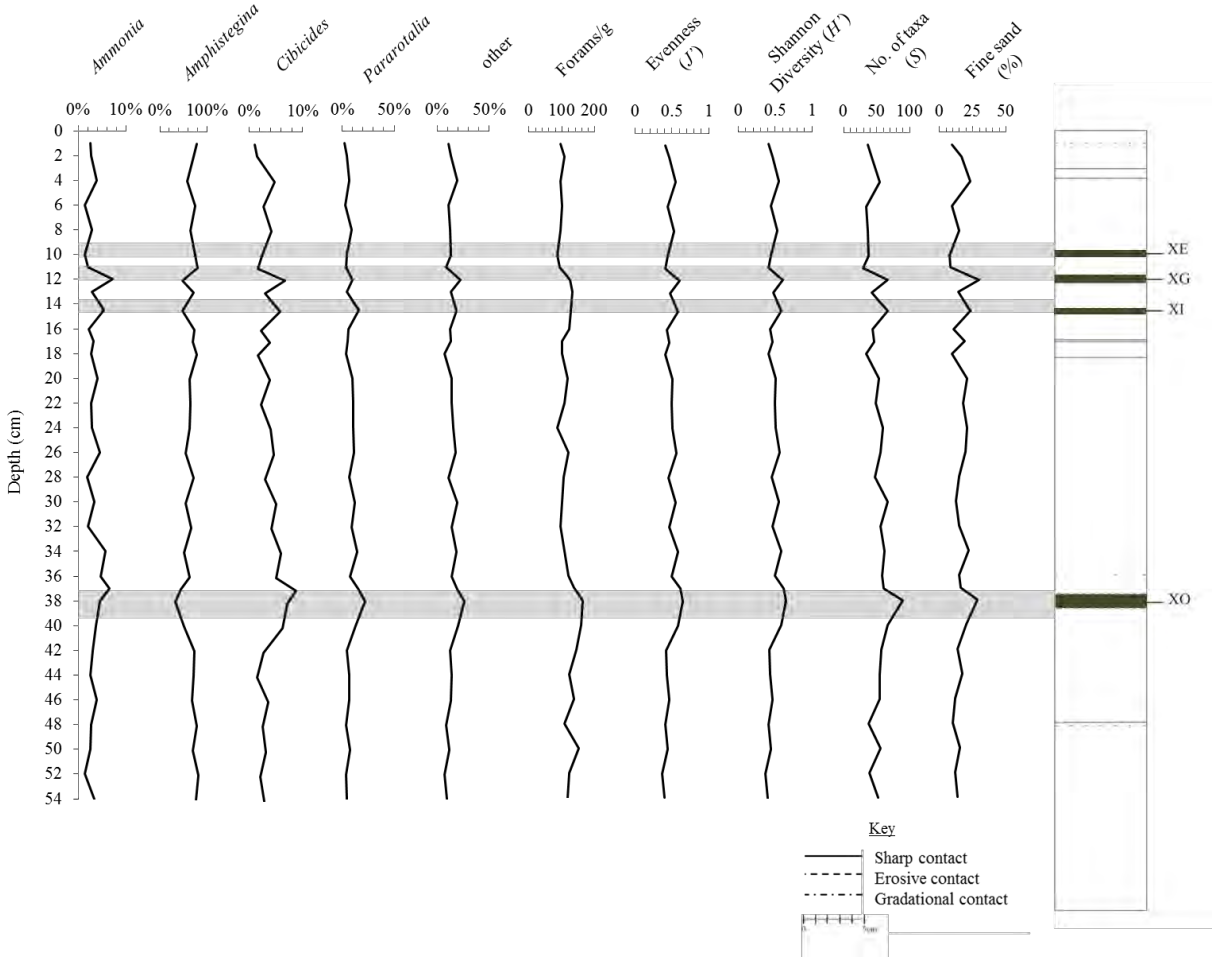

Figure 4.15. Core X sediment log with down-core relative contributions of symmetrical, rounded genera, univariate statistics and fs (%) for core X. Key defines the contact between each unit on core X. Note the scale changes between plots.

The 500 µm size fraction

In total, 34 taxa were identified in the 500 µm size fraction. The ind/g ranged from 48 – 104 with a mean of 72 (Figure 4.16). The highest ind/g were found at depths 42, 50, 13, 52 and 44 cm. Evenness ranged from 0.2 - 0.4 with an average of 0.2 (Figure 4.16). The Shannon Diversity Index ranged from 0.4 - 0.7 with an average of 0.5. The highest diversity index was noted at depths 38, 37, 12, 26 and 4

cm (Figure 4.16). Number of genera ranged from 6.0 – 12.0 with an average of 8.4 with the greatest numbers at depths of one, 32, 12, 40 and 17 cm (Figure 4.16).

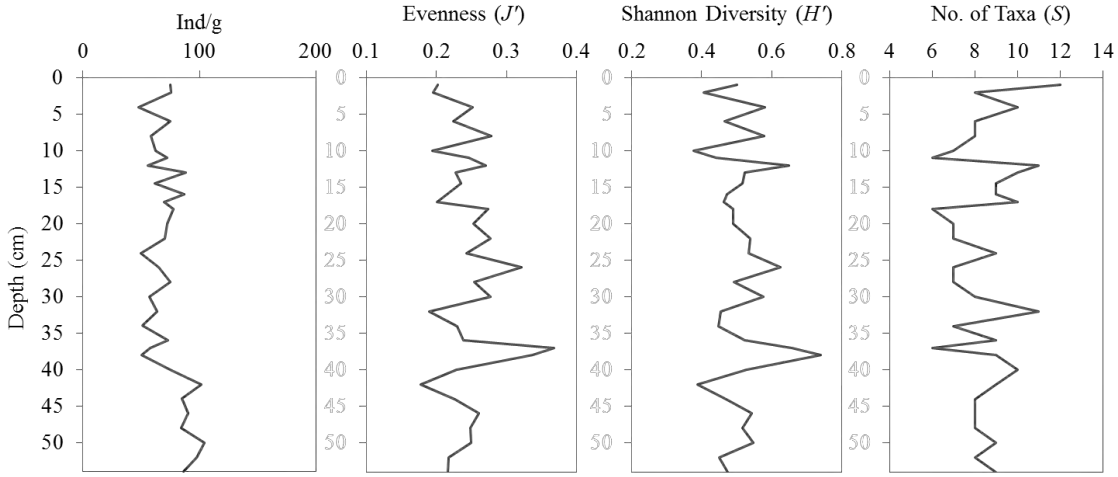

Figure 4.16. Down-core ind/g, evenness (*J'*), Shannon Diversity Index (*H'*) and number of taxa (*S*) for 500 μm size fraction.

Dominant suborders in the 500 μm fraction were identified as Rotaliina followed by Textulariina. The down-core contribution of Rotaliina ranged from 93.6 - 98.9% with an average of 96.7% (Figure 4.17). The down-core contribution of Textulariina ranged from 0.7 - 5.4% with an average contribution of 3.0%. A significant decrease up-core can be seen in the Rotaliina suborder (R^2= 0.4, *F*= 0.0001, *p*= 0.001) with a concomitant significant increase up-core in the Textulariina suborder (R^2= 0.4, *F*= 0.0002, *p* = 0.0002). No significant down-core trend was found in the Miliolina suborder, the third most abundant suborder present.

Within Rotaliina, *Amphistegina, Heterostegina* and *Homotrema* were the most prevalent genera with *Textularia* and *Quinqueloculina* being most prevalent in the Textulariina and Miliolina suborders, respectively. The most abundant genus overall was *Amphistegina* followed by *Textularia* and *Heterostegina.* The relative percentage contribution of *Amphistegina* ranged from 89.1 - 96.0% down-core with an average of 92.5%. *Textularia* percentage contribution ranged from 0.7 - 5.4% with an average of 2.9% and *Heterostegina* ranged from 0.9 - 4.7% with an average contribution of 2.3%. *Amphistegina* displayed the same significant decrease up-core as the Rotaliina suborder while *Textularia* contribution increased up-core showing the same trend as the Textulariina suborder (Figure 4.18). *Heterostegina* contribution fluctuated down-core (Figure 4.18). After *Amphistegina, Textularia* and *Heterostegina; Homotrema, Planorbulinella, Elphidium, Quinqueloculina, Asterigerina, Ammonia* and *Sorites* were the most abundant genera. These seven genera, however, only contributed

2.1% to the total Foraminifera count in the 500 µm fraction. The most abundant taxa in the 500 µm fraction were *Amphistegina* spp., *Textularia* sp.1, *Heterostegina depressa, Homotrema rubra* and *Planorbulinella larvata* each contributing 92.5%, 2.9%, 2.3, 1.0% and 0.4 % respectively to the 500 µm fraction.

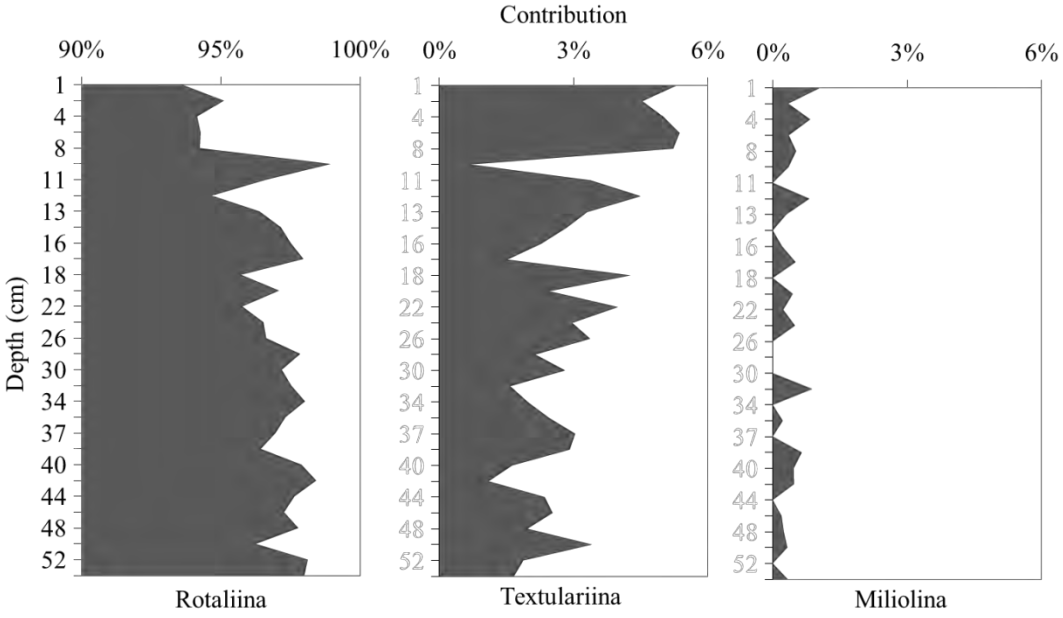

Figure 4.17. Down-core relative percentage contributions of the three suborders **A** Rotaliina, **B** Textulariina and **C** Miliolina within the 500 µm fraction. Note the scale changes between plots.

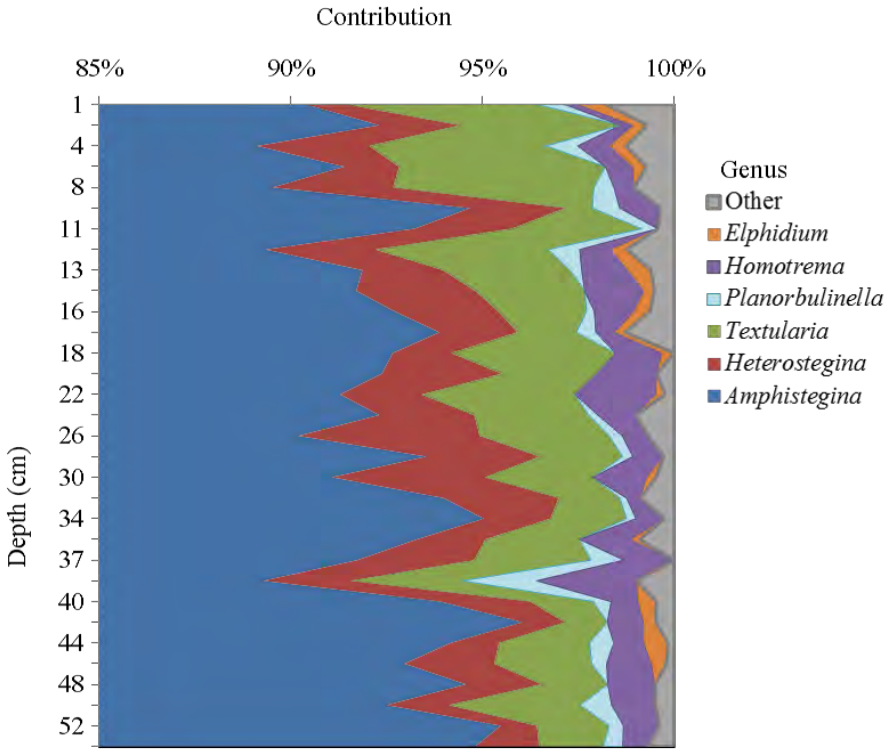

Figure 4.18. Down-core percent contributions of the six most abundant genera in the 500 µm fraction.

The 250 µm size fraction

In total, 90 taxa were identified in the 250 µm size fraction. The ind/g ranged from 10 – 45 with a mean of 19 and the highest values were noted at depths 38, 37, 40, 12 and 14.5 cm (Figure 4.19). Evenness ranged from 0.6 - 0.8 with an average of 0.7 and the Shannon Diversity Index ranged from 1.5 - 3.1 with an average of 2.2 (Figure 4.19). The highest diversity was found at depths of 38, 14.5, 12, 17 and 34 cm. Number of taxa ranged from 13.0 – 50.0 with an average of 25.6 with the highest values being noted at depths 38, 34, 14.5, 12 and 40 cm (Figure 4.19). The dominant suborders in the 250 µm fraction were identified as Rotaliina; contributing 80.7% followed by Miliolina and then Textulariina each contributing 10.4% and 7.8% respectively. The down-core percentage contribution of Rotaliina ranged from 67.6 - 88.7%. The down-core contribution of Miliolina ranged from 5.6 - 23.1% and Textulariina ranged from 1.5% - 17.6%. Within Rotaliina, *Amphistegina, Pararotalia* and *Elphidium* were the most prevalent genera with *Textularia* and *Quinqueloculina* being most prevalent in the Textulariina and Miliolina suborders.

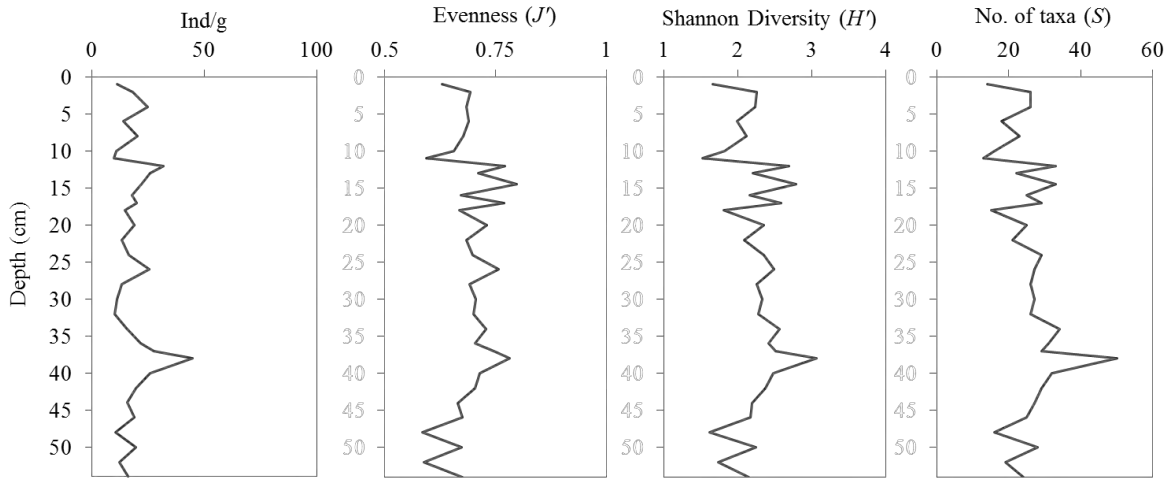

Figure 4.19. Down-core ind/g, evenness (*J'*), Shannon Diversity Index (*H'*) and number of taxa (*S*) for the 250 µm size fraction.

The percentage contribution of *Amphistegina* ranged from 17.4% - 54.8% down-core with an average of 36.3%. *Pararotalia* ranged from 0.0% - 18.8% with an average of 10.8% and *Elphidium* ranged from 4.8% - 7.3% with an average of 10.4%. Down-core percentage contributions fluctuated throughout all genera graphs (Figure 4.20), however, *Amphistegina* remained one of the dominating genera at all the sampling points. *Pararotalia* showed a noticeable decrease in the upper 15 cm, with *Elphidiums'* contribution constantly fluctuating down-core. A decrease was seen from 54 – 38 cm in the *Textularia* contribution where-by the percent contribution fluctuated considerably up-core. *Quinqueloculina* showed two distinct trends, in the upper 25 cm, contribution remained relatively

constant whereas from 54 – 28 cm a slight increase up-core was noted. After *Amphistegina*, *Pararotalia*, *Elphidium*, *Textularia* and *Quinqueloculina, Ammonia; Cibicides*, *Asterigerina, Lobatula* and *Homotrema* were the most abundant genera. These ten genera contributed 89.5% to the total Foraminifera count with the remaining 30 genera making up the remaining 10.5%. The most abundant taxa in the 250 µm fraction were *Amphistegina* spp., *Pararotalia* sp.2, *Textularia* sp.1, *Cibicides refulgens*, *Elphidium* sp.11, *Elphidium macellum*, *Ammonia* sp.1, *Pararotalia stellata*, *Ammonia beccarii* and *Lobatula Lobatula*.

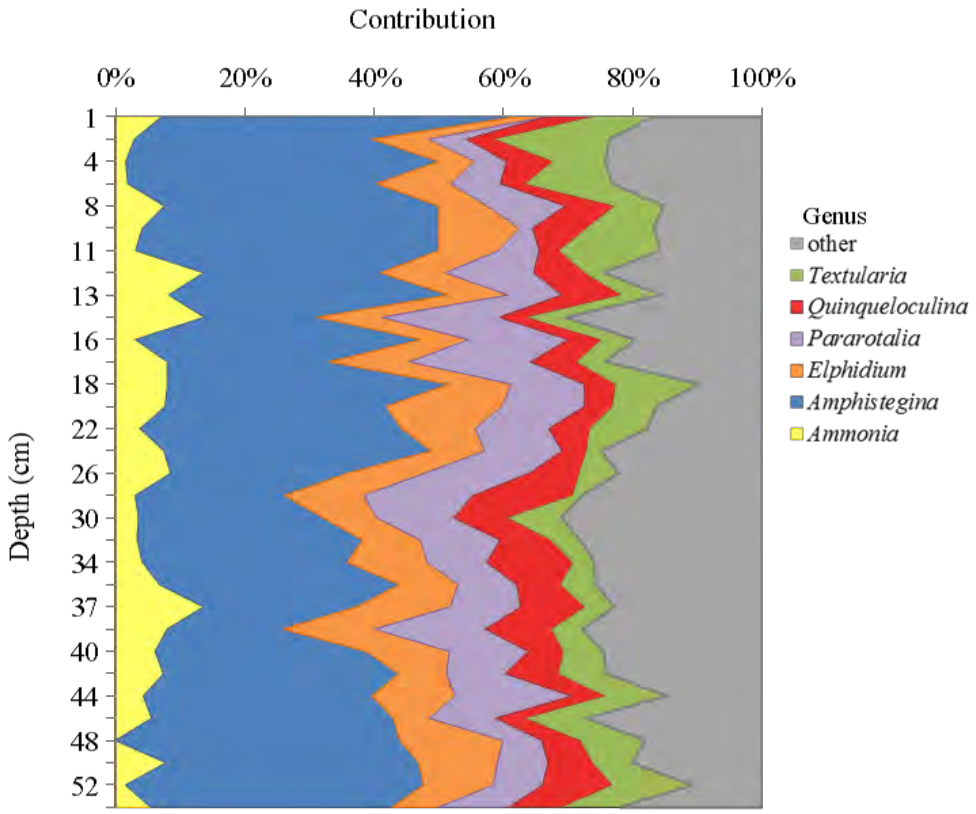

Figure 4.20. Down-core percentage contributions of the six most abundant genera for the 250 µm fraction.

The 125 µm size fraction

In total, 116 taxa were identified in the 125 µm size fraction. The ind/g ranged from 9 – 68 with a mean of 24 (Figure 4.21). The highest ind/g were noted at depths 14.5, 30 and 38 cm. Evenness ranged from 0.5 - 0.8 with an average of 0.7 and the Shannon Diversity Index ranged from 1.5- 2.9 with an average of 2.3 (Figure 4.21). The highest diversity was found at depths 12, 14.5, 30, 38 and 40 cm. Number of taxa ranged from 18.0 – 63.0 with an average of 35.3 (Figure 4.21). The highest number of taxa were found at a depth of 12, 14.5, 30, 38 and 40 cm.

The dominant suborders in the 125 µm fraction were identified as Rotaliina; contributing 89.3% followed by Miliolina and then Textulariina each contributing 8.4% and 0.3% respectively. The down-core contribution of Rotaliina ranged from 82.3 - 97.2%. The down-core contribution of Miliolina ranged from 0.0 - 16.7% and Textulariina ranged from 0.0 - 2.5%. Within Rotaliina, *Pararotalia*, *Cibicides* and *Ammonia* were the most prevalent genera with *Quinqueloculina* and *Textularia* being most prevalent in the Miliolina and Textulariina suborders.

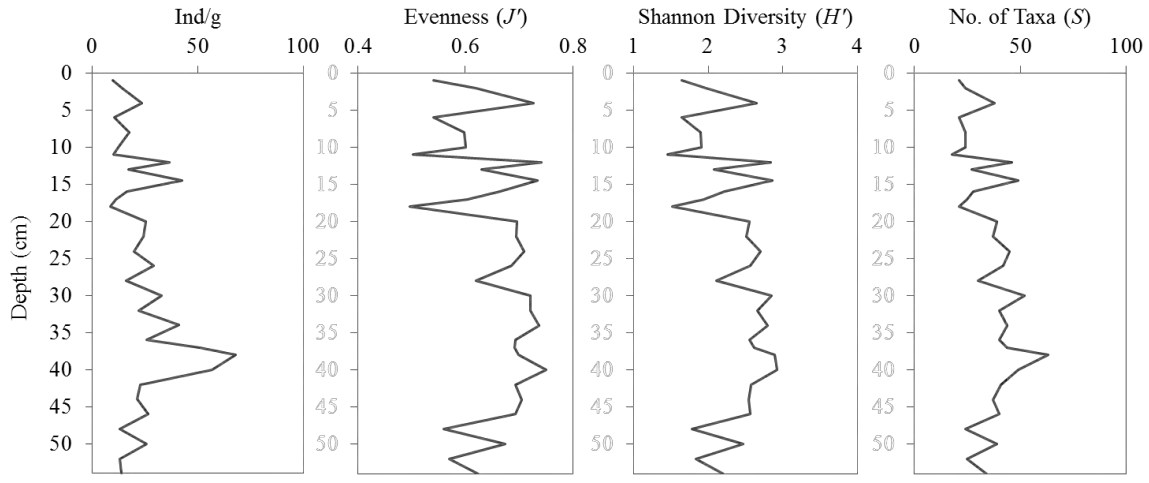

Figure 4.21. Down-core ind/g, evenness (*J'*), Shannon Diversity Index (*H'*) and number of taxa (*S*) for 125 µm size fraction.

The most abundant genus was *Pararotalia* followed by *Cibicides, Ammonia, Rotalinoides, Quinqueloculina* and *Elphidium* (Figure 4.22). The contribution of *Pararotalia* ranged from 17.7% - 41.4% down-core with an average of 29.5%. *Cibicides* ranged from 5.6 - 25.8% with an average of 14.0% and *Ammonia* ranged from 5.5 - 22.2% with an average contribution of 11.3%. *Pararotalia* remained the dominating genus at all the sampling points and fluctuated in its contribution down-core. The *Cibicides, Ammonia, Rotalinoides, Quinqueloculina* and *Elphidium* contributions all fluctuated down-core. A distinct peak in *Cibicides* was noted at 17 cm depth, with peaks in *Ammonia, Rotalinoides, Quinqueloculina* and *Elphidium* noted at 48, 44, 18 and ten centimetres respectively.

After *Pararotalia, Cibicides, Ammonia, Rotalinoides, Quinqueloculina* and *Elphidium; Cassidulina, Lobatula, Sagrinella* and *Amphistegina* were the most abundant genera. These ten genera contributed 85.3% to the total Foraminifera count with the remaining 40 genera making up the remaining 14.7%. The most abundant species in the 125 µm fraction were *Pararotalia* sp.2*, Pararotalia stellata,*

Cibicides refulgens, Ammonia beccarii, Rotalinoides sp.5*, Cibicides* sp.1*, Ammonia* sp.4*, Cassidulina* sp.2*, Rotalinoides* sp.2 and *Rotalinoides* sp.4.

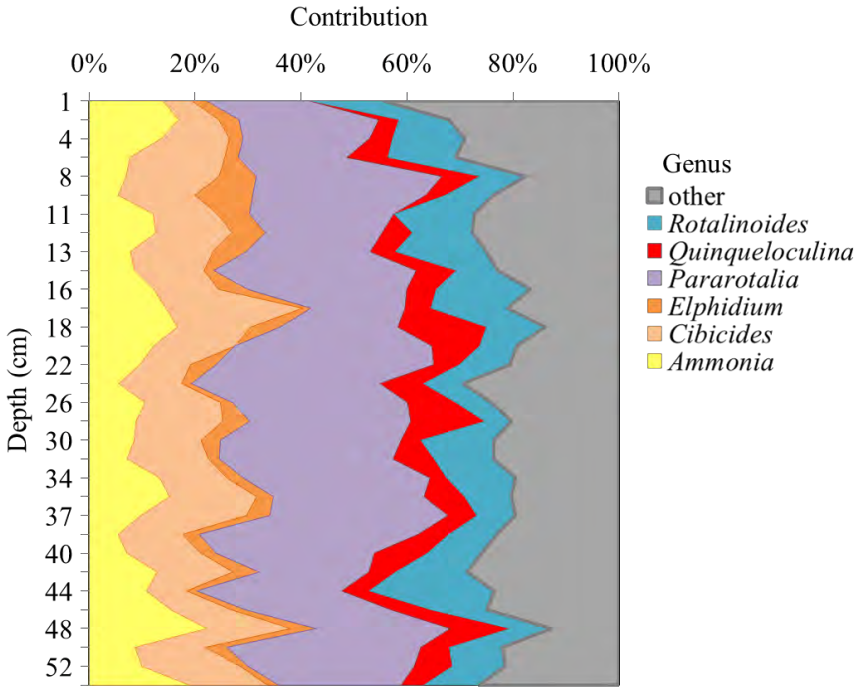

Figure 4.22. Down-core percentage contributions of the six most abundant genera within the 125 µm fraction.

Statistical analysis

A significant Spearman correlation was found to exist between the total foraminiferal assemblage and the 250 µm fraction, as well as between the total and 125 µm fraction using the RELATE function. The 125 µm fraction had the highest correlation (ρ= 0.794) with the total assemblage, however, the 250 µm had a Spearman correlation slightly lower at ρ= 0.635 (Table 4.3). The similarity profile analysis (SIMPROF) cluster groups (Figure 4.23), at 40% similarity, were overlain with the 2-D nMDS ordination (Figure 4.24) and showed the grouping of the total and 125 µm Foraminifera fractions. The samples from the 500 µm fraction were most similar with the most variability seen in the 250 µm and 125 µm fractions.

Table 4.3. Pairwise comparisons of the foraminiferal community structure using the RELATE function on the foraminiferal density data analysed to the lowest identifiable taxon. The Spearman rank correlations (ρ) are shown with the significance in brackets.

Fraction	Total
500 µm	0.339 (0.0020)
250 µm	0.635 (0.0001)
125 µm	0.794 (0.0001)

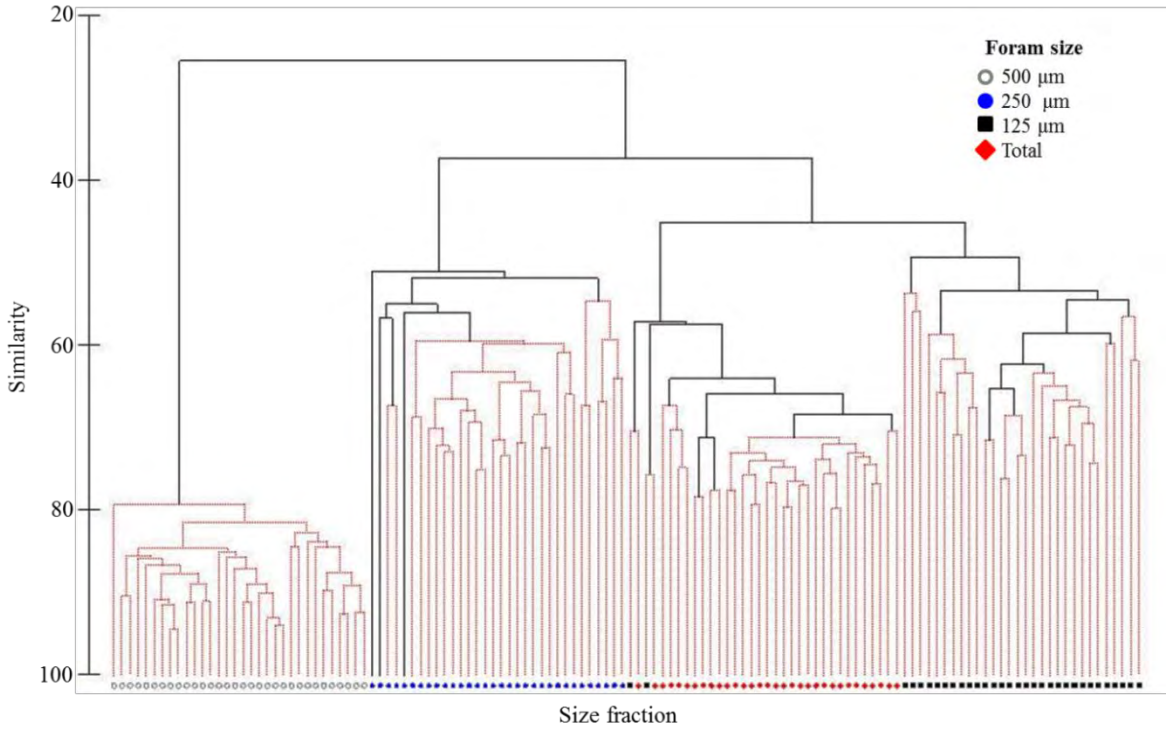

Figure 4.23. SIMPROF cluster analysis of foraminiferal assemblages, across all size fractions.

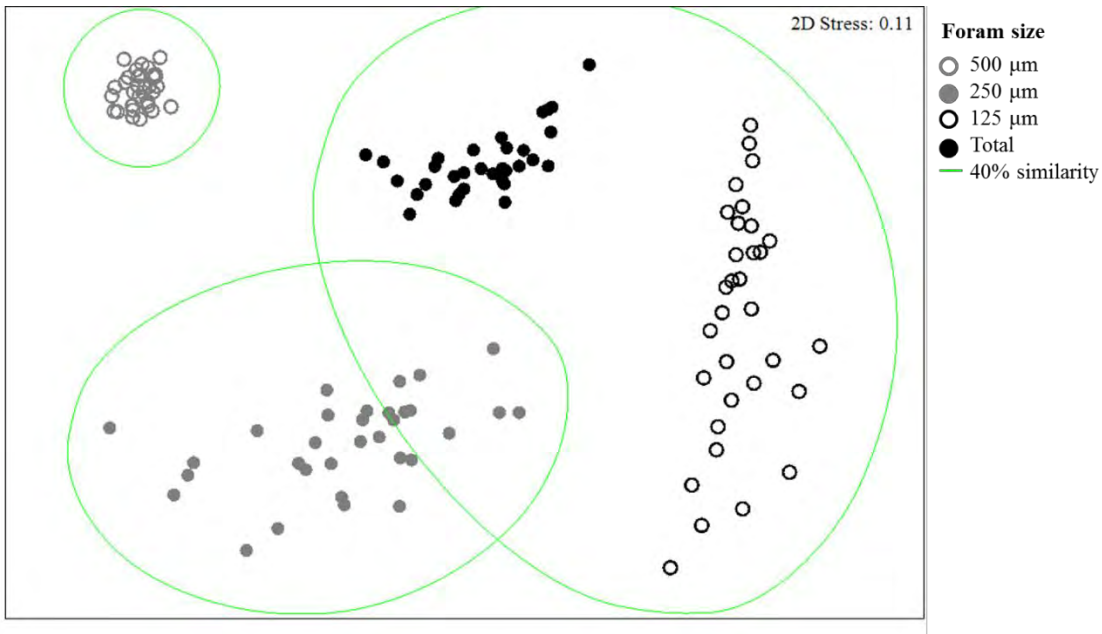

Figure 4.24. An nMDS ordination on foraminiferal density data across all size fractions for all samples.

A SIMPROF cluster analysis on the total density data from core X (Figure 4.25) revealed four different benthic foraminiferal assemblage zones (Clusters) (Table 4.4). Zone C had the highest number of occurrences (21) and contributed 65.6% to the total. Zone B and D each had 5 occurrences respectively contributing 15.6% each. Zone A had one occurrence and contributed 3.1% to the total.

Table 4.4. SIMPROF cluster analysis results, showing identified foraminiferal zones, number of occurrences and its representative percent out of the total samples.

Foraminiferal assemblages	Number of occurrences	Percentage of total
Cluster A	1	3.1%
Cluster B	5	15.6%
Cluster C	21	65.6%
Cluster D	5	15.6%
Total	32	100.0%

Cluster A comprised of sample one, representing the disturbed core top. It was logged as a distinct unit and had a distinct foraminiferal assemblage in comparison to the rest of the core (Unit XA, Figure 4.25). Cluster A had the lowest ind/g (96) and the second lowest number of taxa (*S*: 35) (Figure 4.26). It comprised of the lowest %vfs (0.27%) and had the second highest carbonate content (65.69%).Cluster B consisted of samples from depths 12, 14.5, 37, 38 and 40 cm. The samples 12, 14.5, 37 and 38 coincided with distinct horizons logged on core X (XG, XI and XO respectively). These bands were all visually logged as dark olive-gray, medium sand bands. Samples 12, 14.5, 38 and 40 cm had the highest percentages of vfs within core X (2.87%, 3.37%, 4.18 % and 4.34% respectively); however, sample 37 had a low percentage of vfs (0.22%) and the highest percentage of vcs (25.49%) within core X. These samples also had very high percentages of fs (12:29.51%, 14.5: 23.16%, 37: 15.77%, 38: 28.60% and 40: 20.03%). All samples from cluster B were dominated by ms and fs. Increased contributions were noted at these depths in the *Pararotalia, Cibicides* and *Ammonia* genera as well as distinct decreases in the *Amphistegina* genus contribution. This cluster represented enrichment zones as it had the highest mean ind/g (142 ± 16 SD) and mean number of taxa (*S*: 69 ±10 SD).

Cluster C comprised the highest number of samples, 21, denoting 65.6% of core X. This cluster had a mean number of taxa of 51 ± 8SD and mean ind/g of 113 ± 17 SD. Cluster C encompassed all of units XH, XJ, XK, XL, XN and XQ and partially units XM, XP and XR. Cluster D consisted of samples two, six, 11, 18 and 48. These samples had the lowest mean number of taxa (*S*= 34 ± 5 SD) and very low percentages of vfs (0.77%, 0.73%, 0.34%, 0.63% and 1.10% respectively).

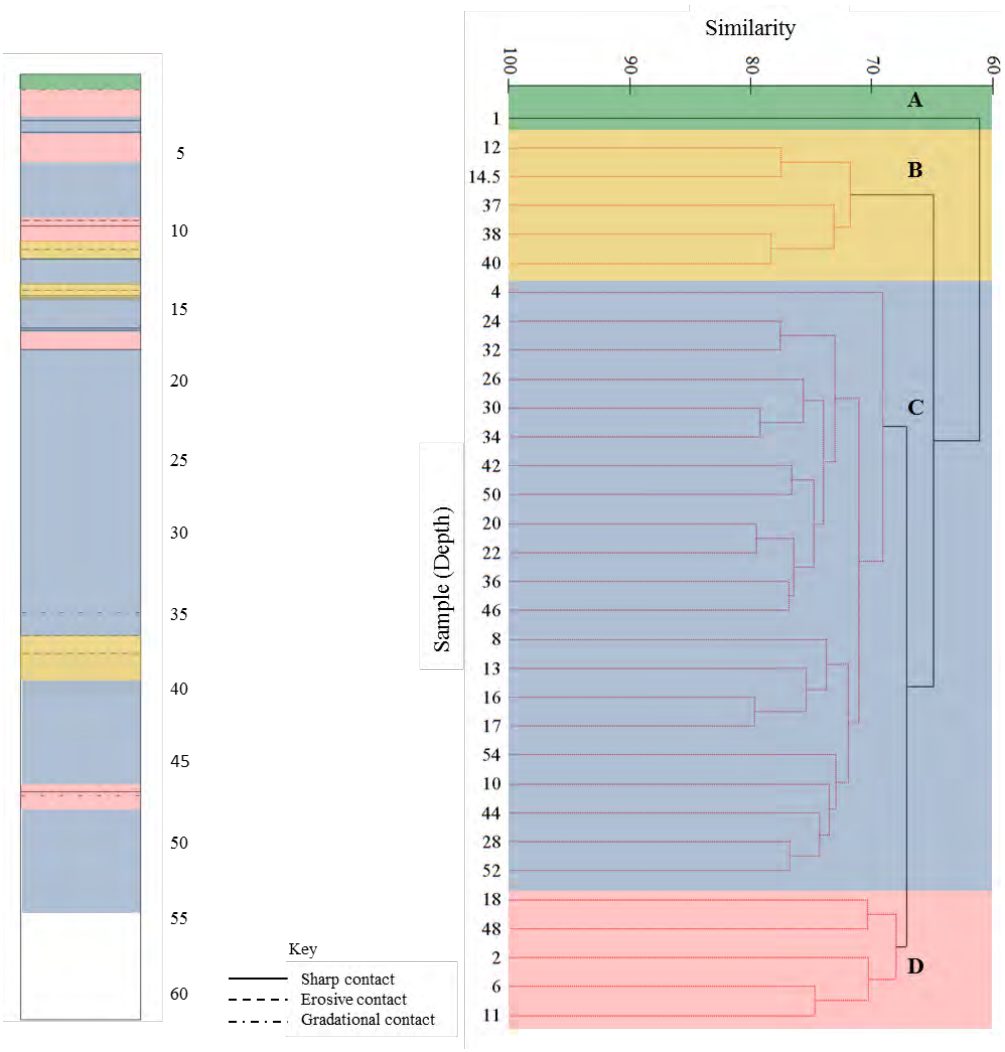

Figure 4.25. Dendrogram of SIMPROF cluster analysis of the total foraminiferal density data from core X (Sample numbers correspond to the respective depth on the core log) with position of the foraminiferal assemblage zones (Clusters A-D) on the log of core X. The sediment units are defined by their respective contacts (i.e. sharp, erosive or gradational contact).

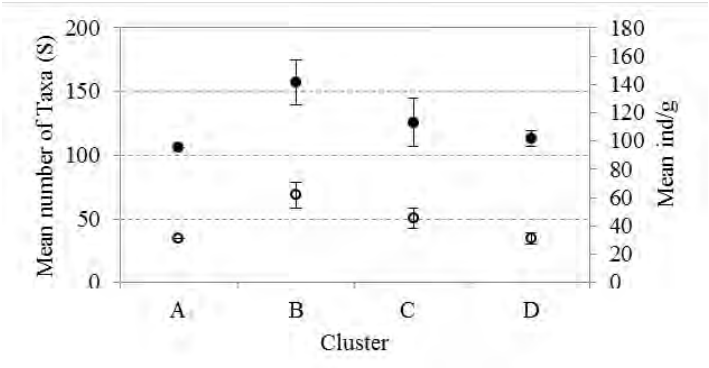

Figure 4.26. Mean ind/g (Black circles) and number of taxa (open circles) with standard deviations for each SIMPROF cluster group. Note a single sample represents cluster A.

The univariate indices, Shannon-wiener Diversity (*H'*), Margalef's Richness (*d*) and Pielou's Evenness (*J'*) were determined for each cluster (Table 4.5). The highest values throughout were noted within Cluster B whereas the lowest values were found within Cluster D.

Table 4.5. Univariate indices, (mean ± SD) Shannon-wiener Diversity (*H'*), Margalef's Richness (*d*) and Pielou's Evenness (*J'*) calculated from taxon density data for the various groups (A – D) identified through the SIMPROF cluster analysis.

Diversity Index	**Cluster**			
	A	B	C	D
Shannon-wiener Diversity (*H'*)	3.13 ± 0.00	3.89 ± 0.14	3.51 ± 0.18	3.09 ± 0.15
Margalef's Richness (*d*)	9.70 ± 0.00	16.08 ± 1.92	12.97 ± 1.76	9.44 ± 0.96
Pielou's Evenness (*J'*)	0.88 ± 0.00	0.92 ± 0.01	0.90 ± 0.01	0.87 ± 0.01

As a with-in cluster similarity percentage (SIMPER) analysis looks for similarities between samples grouping together, no analyses could be performed on cluster A. From the SIMPER analysis, all other clusters had a within-cluster similarity of >65%. Only the taxa contributing >2% to the with-in group average similarity are displayed in Table 4.6. *Amphistegina* spp. was dominant in all clusters. The top discriminating taxon in Cluster B was *Textularia* sp.1 and *Elphidium* sp.11 was identified as being unique for this cluster. *Pararotalia* sp.2 was most distinguishing for cluster C. All the SIM/SD ratios are similar, signifying normal conditions in the environment, with no changes having occurred. The top discriminating taxon in Cluster D was *Amphistegina* spp. with *Rotalinoides* sp.5 being unique for that cluster. *Heterostegina depressa* had the second highest SIM/SD ratio for cluster D. *Amphistegina* spp. was distinguishing because its contribution was extremely high, in comparison to cluster C, whereas the contribution from *H.depressa* was lower. A bloom in *Amphistegina* spp. has been recorded in the Cluster D samples. A between-cluster (A-D), SIMPER analysis revealed only one taxon, *Pararotalia* sp.2, contributed >2% to the average dissimilarity between clusters. It was distinguishing between clusters A and B; and B and D only.

Overall, three taxa, *Amphistegina* spp., *Pararotalia* sp.2 and *Textularia* sp.1 were distinguishing within the core, with *Rotalinoides* sp.5 and *Elphidium* sp.11 identified as unique for certain clusters (Figure 4.27, Appendix C, Plate C1).

Table 4.6. Distinguishing taxa, identified through a SIMPER analysis, contributing > 2% to the within-cluster average similarity, for each SIMPROF cluster group (B-D). Cluster A was represented by only one sample. Bold taxa had the highest SIM/SD ratios and are the main distinguishing taxa within each cluster. Shaded taxa were unique for that cluster.

Cluster	Taxa	Average Abundance	Average Similarity	Sim/SD
B	*Amphistegina* spp.	7.88	11.42	9.68
	***Textularia* sp.1**	**1.70**	**2.51**	**13.02**
	Elphidium sp.11	1.76	2.37	12.40
	Ammonia beccarii	2.17	2.99	11.91
	Pararotalia sp.2	3.75	5.04	9.71
	Cibicides refulgens	2.85	3.87	9.43
	Pararotalia stellata	2.65	3.41	6.50
C	***Pararotalia* sp.2**	**2.35**	**4.68**	**8.70**
	Amphistegina spp.	8.66	17.98	7.92
	Ammonia beccarii	1.26	2.43	7.69
	Cibicides refulgens	1.67	3.27	6.97
	Heterostegina depressa	1.33	2.67	6.87
	Textularia sp.1	1.70	3.35	5.98
	Elphidium macellum	1.03	2.06	5.75
	Pararotalia stellata	1.69	3.14	5.16
D	***Amphistegina* spp.**	**8.79**	**25.31**	**16.07**
	Heterostegina depressa	1.25	3.45	10.51
	Pararotalia sp.2	1.46	3.78	7.97
	Cibicides refulgens	1.28	3.23	6.87
	Rotalinoides sp.5	0.81	2.16	6.55
	Elphidium macellum	0.82	2.03	5.14
	Textularia sp.1	2.14	5.58	5.13
	Pararotalia stellata	1.25	3.21	5.05

.

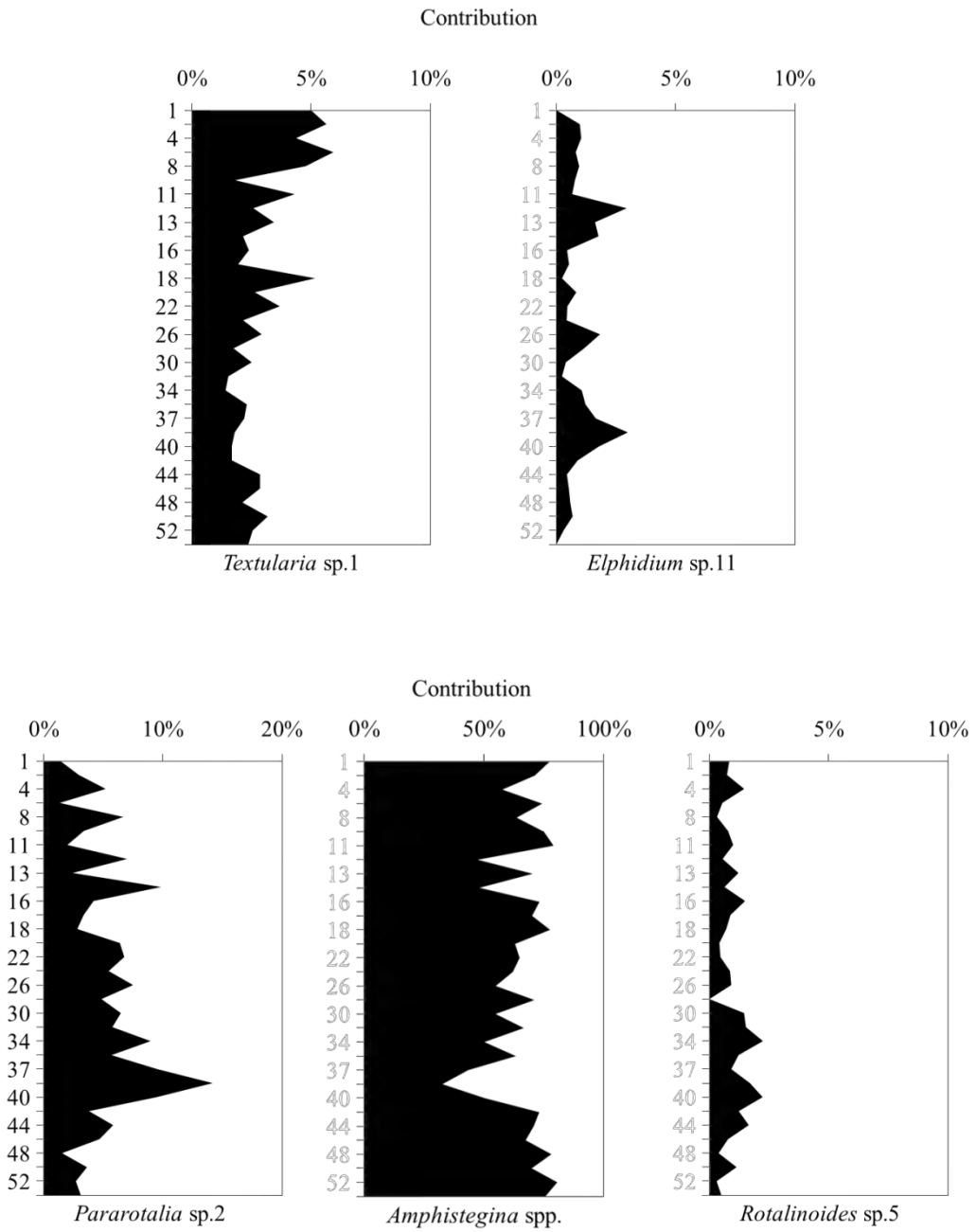

Figure 4.27. Overall, distinguishing and unique taxa within core X. Identified through the within-cluster SIMPER analyses. *Pararotalia* sp.2 was also distinguishing in the between-cluster SIMPER analysis. Note x-axis scale changes.

4.4.3 Possible drivers of foraminiferal distributions

The 11 abiotic variables (section 4.4.1) were used in a BVSTEP analysis. The respective Spearman correlation coefficients (ρ_s) are presented in Table 4.7. The sediment distribution skewness statistic was the single variable that was correlated most highly with the total down-core foraminiferal assemblages ($\rho_s = 0.436$). A combination of five variables -cs, ms, fs, vfs and carbonate content- had the highest correlation with the down-core foraminiferal assemblages ($\rho_s = 0.542$) and therefore, best explained the foraminiferal community structure. These five variables, still only explained 54.2% of the variation in the foraminiferal assemblages.

Table 4.7. Correlation co-efficient (ρ_s) for various combinations of sediment characteristics in relation to the total foraminiferal assemblages obtained through a BVSTEP analysis. Bold text indicates best variable combination which was significant ($\rho<0.0001$) at 9999 permutations.

No. of variables	ρ_s	Variables
1	0.436	Sediment skewness
2	0.514	cs, vfs (%)
3	0.517	cs, ms, vfs (%)
4	0.529	cs, ms, fs, vfs (%)
5	**0.542**	**cs, ms, fs, vfs, carbonate (%)**

The Spearman rank correlation vectors of the five distinguishing/unique taxa, as identified through the SIMPER analyses, together with the combination of abiotic variables identified through the BVSTEP analysis were overlain on the CAP ordination to assess the relationship between the clusters and these variables (Figure 4.28). The first canonical axis (horizontal) separated the clusters with minimal overlap, explained the majority of the variation ($\delta_1^2 = 0.9460$) and was positively correlated with ms (%) and negatively correlated with percentage of vfs. The second axis explained 84.73% of the variance and was negatively correlated with cs. The vfs and carbonate (%) are negatively correlated. Percentages of fs and cs similarly are negatively correlated. A strong correlation between cluster B and the species *Elphidium* sp.11, *Pararotalia* sp.2 and *Rotalinoides* sp.5, was noted and a negative correlation with *Amphistegina* spp. emerged.

Using the 11 abiotic variables, together with the isotope data, the BEST and CAP analysis were rerun to determine if any significant changes occurred. The oxygen and carbon stable isotopes made no difference to the BVSTEP analysis with the same combination of variables (percentage of cs, ms, fs, vfs and carbonate) having the highest correlation with the foraminiferal community structures.

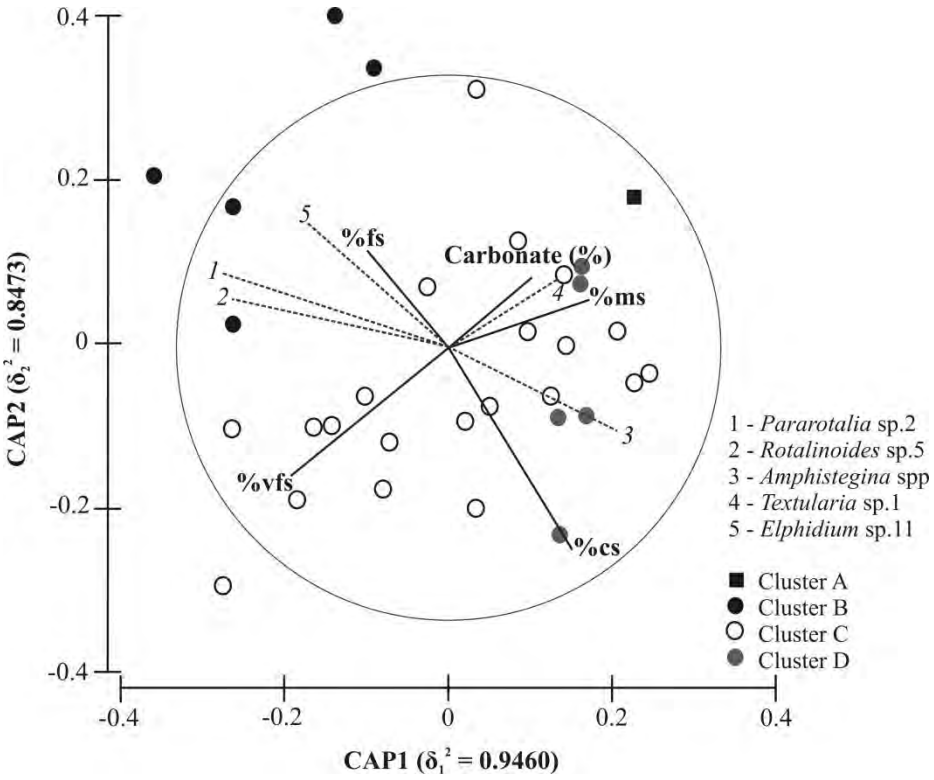

Figure 4.28. CAP analysis derived from the square-root transformed total foraminiferal assemblage density data. The Spearman rank correlation vectors of the distinguishing taxa, together with the combination of abiotic variables identified through the BVSTEP analysis are overlain to show the interrelationships present.

4.5. Discussion

4.5.1 Cross-validation of cores

Core logs were the first attempt at validating the integrity of the cores, in order to eliminate spatial variability as a confounding factor and to determine if the cores were true replicates. The common, dark olive-gray units, noted in all three cores, do not match up horizontally due to the varying degrees of compaction. This can be attributed to mechanical compaction and compaction experienced during core collection. Shallow, marine sediments experience mechanical compaction over time, as a result of the weight of subsequent sediment layers being deposited on top (Scholle & Halley, 1989). During coring, as a result of the hammering motion and impact from the weighted slide, further compaction is also plausible.

The grain size was variable in all three cores making it difficult to compare, however, the carbonate content graphs provided a more decisive means of comparison (Figure 4.29). By plotting all three carbonate content graphs on the same down-core axis, to account for the varying degrees of compaction, it was evident they all displayed the same set of peaks in carbonate content at similar

depths. Albeit these peaks are not exact matches, it is evidence enough that they have all recorded the same sedimentary record.

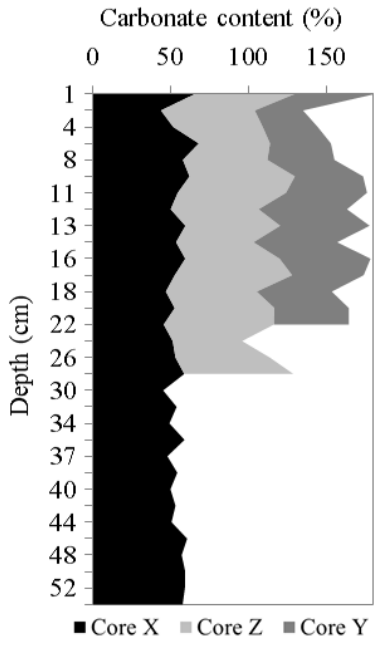

Figure 4.29. Area plot of core X, Y and Z carbonate content placed on the same depth axis to correct for varying compaction within each core.

The radiocarbon dates obtained for units XO and YM were similar; but the date from unit ZM did not correlate with the other cores. This was attributed to the presence of a coral rubble fragment in this unit. During the collection of the core, it is feasible the rubble fragment was pushed down from the surface, thereby introducing newer material towards the base of the core. This mixing of relic and new Foraminifera tests could have resulted in the distortion of the radiocarbon date. The oxygen isotope records, from the three cores, are questionable. A single species, from a restricted size range was used (Pearson 2012), eliminating interspecies-isotopic offsets as a possible explanation. As the isotopic measurement was performed on a sample, composed of up to 20 Foraminifera tests, sediment reworking can result in the mixing of relic and newer material (Renema at al. 2013). This could have distorted the foraminiferal isotopic signals. It is, therefore, apparent that down-core foraminiferal stable isotope records are not reliable in this highly turbulent environment.

The sediment stratigraphic logs, carbonate content results and radiocarbon dates demonstrate the limited spatial variation occurring across the bioclastic sediment patch. The inconsistencies in the grain size and stable isotope results cannot, however, be overlooked. The high degree of turbulence

experienced in this environment, could be discerning for these components. Sediment, of which dead Foraminifera tests form part of, are susceptible to reworking and as noted by Murray (2006), represent the time averaged dead assemblage.

4.5.2 Interpretation of the Late Holocene climate record of Two-mile Reef

Overall, a distinct difference in the foraminiferal assemblages across the size fractions was evident. The 500 µm fraction had the lowest richness and diversity values, yet revealed significant trends in the relative down-core contributions of *Amphistegina* and *Textularia*. Following the classification by Buchan (2006), in which LBF juveniles are >500 µm and adults >1000 µm, this data can be used to show the trends of the LBF populations within a core.

Amphistegina lobifera is the shallowest-dwelling, Indo-Pacific species in the *Amphistegina* genus and is dominant in reef-margin and back-reef settings (Benedetti et al. 2012). Classified as an invader species, it is the most common symbiont-bearing Foraminifera which has invaded the south eastern Mediterranean (Gruber et al, 2007). Modelling by Langer et al. (2013b) found that a range extension for *Amphistegina* spp. is expected, due to increasing sea surface temperatures (SST) associated with climate change. They predict a south-westward expansion along the south eastern coast of Africa, ranging from 8-2.7 km year-1 (Langer et al. 2013b). As an invader taxon, it is tolerant of a wide range of environmental conditions and potentially does not provide much palaeoenvironmental information on Sodwana Bay's coral reefs. According to Mazumder (2012), *Textularia* is an indicator of low salinity conditions in shallow water environments.

The main, symbiont-bearing, LBF present in the 500 µm fraction were *Amphistegina* spp. and *Heterostegina depressa*. *Amphistegina* spp. was dominant, with its contribution exceeding 85% for all depth levels. The *H. depressa* is a circum-tropical, cosmopolitan species (Murray 2006) and remained relatively consistent in its up-core contribution. Vogel and Uthicke (2012) and Schmidt et al. (2011; 2013; 2014) conducted laboratory experiments on *H.depressa*. Findings were that *H.depressa* was not affected by increased CO_2 levels at four pH levels (467, 784, 1169 and 1662 µatm) across one temperature (25°C) (Vogel and Uthicke 2012). The species, *H.depressa* did, however, bleach at higher temperatures in a temperature induced stress experiment across a temperature range of 23°C - 33°C (Schmidt et al. 2011). This species was also found to be negatively affected by a combination of increased temperature and reduced pH (Schmidt et al. 2013, 2014). *H.depressa* also appears to be more sensitive to increased temperatures in comparison to *Amphistegina* spp., which has the widest latitudinal range across the oceans (Langer et al. 2013b).

The common, dark olive-gray bands, present in all the cores, appear to represent extreme climatic events involving flooding and increased turbulence. This theory is supported by an increase in the finer sediments and the foraminiferal assemblages. The vast amounts of finer material are dark olive-gray in colour, signifying their high organic content. They potentially have terrestrial origins, resulting from flooding of a fresh water lake and estuarine system. The fine material would be suspended during these events, transported to the study site and subsequently settled afterwards. An increase in the rounded, symmetrical genera, *Cibicides*, *Ammonia* and *Pararotalia*, at those levels, is indicative of turbulent conditions (Nigam & Chaturvedi 2000; Lakhmapurkar & Bhatt 2010). Martins et al. (2006) also acknowledged *Cibicides* to be indicative of stronger bottom currents. Not only was an increase in certain genera seen in those units, but the foraminiferal assemblages were distinguishing from the rest of the core. These units also had the highest number of taxa (*S*) and diversity.

A plausible explanation at this time, to the cause of these bands, is a series of four major cyclonic events and/or cut-off lows resulting in subsequent flooding. Numerous tropical cyclones and cut-off lows have affected the east coast of South Africa in recent times. Both the Laingsburg floods of 1981 and the Natal flood disaster of 1987 were caused by cut-off lows (Rouault et al. 2002). The tropical cyclone Domoina in January 1984 caused a 100-year flood in South Africa and tropical cyclones Imboa and Eline caused flooding in February 1984 and 2000 respectively (Kovacs et al. 1985; Reason & Keibel 2004). Tropical cyclones only affect South Africa when they move into the Mozambique Channel. With global warming, the minimum sea surface temperature necessary for cyclone formation, 26.5°C (Dare & McBride 2011), is occurring south of Mozambique, resulting in the potential for cyclone formation further south. The formation of tropical cyclones requires low-level vorticity, a condition fulfilled by the Intertropical Convergence Zone (ITCZ), representing a zone of wind change and speed (Tory & Frank 2010).

The events causing the dark olive-gray bands were, therefore, large enough as to be preserved in the sedimentary record. Large cyclones could lead to flooding of coastal lakes, increased turbulence, and suspension of fines and could therefore have generated these concurrent bands present in the cores. St. Lucia Estuary, an estuarine lake system situated south of Sodwana Bay, is the largest in Africa (Cyrus & Blaber 1988). The only other freshwater system, close to Sodwana Bay, with some connection to the marine environment is Lake Mgobezeleni, with an area of 1.8km^2, and estuary, with an area of 1.3 ha (Bruton & Appleton 1975; Bruton 1980). This is a very small system in comparison to the St. Lucia complex, covering an area of 325 km^2 (Cyrus & Blaber 1988); however, flooding from this system is still plausible, yet unlikely. Prior to 1900, the Mfolozi River fed into the St Lucia estuary

and shared a common mouth (Whitfield & Taylor 2009). In addition, the estuary mouth was at times large enough to allow passage of small ships and initially part of this large system, the Mfolozi River sediment load was estimated at 0.68 x106 tonnes year^{-1} (Whitfield & Taylor 2009). Flooding of such a large system, due to a cyclone and/or cut-off lows, would result in vast quantities of sediment being deposited into the ocean. Turbulence would be greatly increased, due to increased wave heights and wind; and the prevailing winds could account for the sediment being transported northwards to Sodwana Bay. This is supported by findings by Morris (2009) who reported a northerly current flow for 27% of the time at Sodwana Bay over a 30 month study period. Cyclonic eddies and prevailing winds were found to cause these northerly reversals. Cyclonic eddies and tropical cyclones both rotate in a clockwise direction in the Southern Hemisphere and thus can cause a reversal in the currents.

A study conducted by Haug et al. (2001), on sediment cores collected off the northern shelf of Venezuela, captured southward pulses in the ITCZ during the Late Holocene. Extreme, southward pulses in the Venezuela core were recorded in the titanium (%) levels as a triplicate event 200–350 years BP with a fourth pulse ±680 years BP. These short-lived, southward pulses in the ITCZ could signify increases in precipitation (Oliver 2005) and as the rains are generally heavy and short in duration they are often characterized by frequent storms and can result in flash floods. A southward shift in the ITCZ results in increased rainfall south of the equator and signifies the potential for areas farther south, usually unaffected, to be hit by major cyclones. Within the Venezuela core; river runoff, during the northern hemisphere rainy season, when the ITCZ is farther north, has been recorded as dark-coloured laminations rich in terrigenous grains (Haug et al. 2001). This bears striking resemblance to the dark olive-gray units recorded in the cores collected in this study, supporting the speculation that these represent flooding events of the St Lucia Estuary. These southward pulses, recorded in the Venezuela core, fall within the timeframe constrained for core X, further supporting the hypothesis of flooding events.

The foraminiferal assemblage from the first dark olive-gray band in core X (XE) at ten centimetres depth did not, however, group with the other three bands in the SIMPROF analysis. The same peaks in *Cibicides*, *Ammonia* and *Pararotalia* were also not evident at this depth. This discrepancy could have been attributed to the horizon being very small, and due to the coarse sampling technique (one centimetre) the unique foraminiferal assemblages could have been distorted and lost. The top centimetre of the core also had a distinct assemblage; however, it was disturbed during sampling. Time-averaging results in the top 1 cm, incorporating a foraminiferal accumulation of the last decade to hundreds of years (Murray 2006). The significance of this grouping is, therefore, unclear and the results have been viewed with caution.

Turbulence was determined to be a major control in the structuring of the foraminiferal assemblages, through the determination of the symmetrical, rounded taxa, *Amphistegina* spp., *Elphidium* sp.11, *Pararotalia* sp.2 and *Rotalinoides* sp.2 together with the agglutinated species, *Textularia* sp.1, as being distinguishing and unique within the core. *Amphistegina* is epifaunal and is the most common reef-dwelling Foraminifera (Mazumder 2012). The genus *Elphidium* is part of the Elphidiidae foraminiferal family. This family has the highest diversity and abundance in shallow water environments worldwide (Pillet et al. 2013). They are common in both estuarine and coastal habitats and species are infaunal and epifaunal (Murray 2006). *Pararotalia* is an epifaunal genus, found in marine environments on the inner shelf (0-100 m depth) in warm water (Murray 2006). Species from the *Rotalinoides* genus have been reported in the Philippines, Japan, Mediterranean Sea, North Atlantic Ocean, off the east and west coast of India and Indonesia (Hayward & Gross 2015). It has also been reported from 0-100 m water depth in the Pacific Ocean (Jones 1994). In a monsoon-related foraminiferal study *Rotalinoides* was also found in an estuarine (River Sal estuary) and non-estuarine environment (Utorda) off the west coast of India (Devi Gadi & Rajashekhar 2009). *Textularia* is an agglutinated, epifaunal genus. It is found in both sediments and attached to hard substrates and inhabits depths from 0-500 m (Murray 2006). According to Mazumder (2012), *Textularia* is an indicator of low salinity conditions in shallow water environments. Considering *Textularia* sp.1 was the main distinguishing taxon for the dark olive-gray bands, this further supports the flooding theory from a fresh water source.

In future core studies at Sodwana Bay, if time is limited, only the 125 µm could potentially be analysed. This is due to the total and 125 µm fractions being most comparable. This would provide a quick means of determining overall trends and allow for initial analysis to be conducted. Significant results could, however, be overlooked and, therefore, using only a single fraction should be applied with caution.

4.6. Conclusion

In summary, benthic foraminiferal assemblages have limited application in palaeoenvironmental reconstructions within this reef-associated environment. This study revealed that extreme climatic events have been retained in the sedimentary record, yet finer scale changes in the environment have not been recorded. The four extreme climatic events were possibly as a result of flooding linked to large, tropical cyclone and/or cut-off low events affecting the south-east coast of South Africa. These could also potentially be attributed to episodic, extreme, southward shifts in the ITCZ. Additional carbon dating needs to be conducted to further constrain flooding events. A pitfall with the radiocarbon dating method may be the large standard deviation obtained in the results. This therefore,

might not be useful in constraining the exact dates for the triplicate of flooding events which occurred within a ±150 year period.

Significant up-core trends, noted in the 500 µm Foraminifera fraction, need to be viewed with caution. The effects of continuous sediment reworking on the deposition of the time-averaged assemblages, is unclear. The measured sediment characteristics also did not fully account for the variability in the down-core foraminiferal assemblages. Based on the distinguishing taxa within core X, turbulence could be discerning in the structuring of the foraminiferal assemblages. Oxygen isotope analysis was inconclusive and it appears this temperature proxy is not useful in turbulent, inshore reef environments.

According to Mazumder et al. (2012), the LBF *Amphistegina*, *Alveolinella* and *Operculina* are considered as characteristic coral reef Foraminifera. The coring sites represented a depositional environment for the transport of dead foraminiferal tests off TMR. Interesting to note, however, is the lack of distinguishing coral reef Foraminifera, aside from *Amphistegina*, within this marginal reef-associated environment. As previously noted, however, *Amphistegina* is a considered an invader taxon in the Mediterranean. *Operculina* is epifaunal and lives in low energy environments whereas *Alveolinella* inhabits marine environments with a temperature range of 18-26 °C (Murray 2006). It also prefers clinging to algal-covered; carbonate fragments (Murray 2006). High turbulence has been established as a major factor responsible for the structuring of the Foraminifera within the study site. This, together with TMR not being a true coral reef, with a dune and beach rock base, and higher than optimum sea temperatures recorded in Chapter 3 (maximum summer temperature: 27.23°C) could explain the absence of the latter two genera.

CHAPTER 5
FINAL SYNTHESIS AND CONCLUSIONS

5.1. Conclusions

The aims of the study were to gain insight on foraminiferal distribution in sediments associated with a marginal coral reef in South Africa, and whether they provide a record of past climate. This study on both the extant and past foraminiferal assemblages was the first to be implemented at Sodwana Bay and serves as a base-line for the use of Foraminifera in past climate interpretations in similar environments.

As noted by other authors, the living Large Benthic Foraminifera (LBF) were found primarily on the coral rubble. The present-day assemblages provided insight into potential abiotic factors influencing the foraminiferal distributions. Certain measured, sediment and water chemistry parameters affected the sediment assemblages yet did not account for the observed differences between locations, in the rubble assemblages. Turbulence was therefore noted as a potential factor influencing the rubble foraminiferal distributions. This was based on the distinguishing taxa present in the rubble samples.

In comparison to other reef studies, Sodwana Bay's reef-associated environment has a high foraminiferal diversity, with *Amphistegina* spp. being the dominant taxon. The species, *Heterostegina depressa* and *Asterigerina* sp.1*,* were distinguishing in the rubble and sediment samples respectively. Both appeared to be negatively correlated with total alkalinity. No trends were noted in the cores for these taxa, yet *H.depressa* was the dominant LBF in the core, after *Amphistegina* spp. Laboratory experiments have demonstrated the sensitivity of *H. depressa* to a combination of decreases in pH and increases in SST (Schmidt et al. 2011; Schmidt et al. 2013). As noted, the *H.depressa* down-core contributions fluctuated throughout yet showed no distinct trends. An insignificant change in the overall contribution from this species could represent a relatively stable reef environment over the last millennium with regards to total alkalinity, pH and/or temperature. This species also appears to be more sensitive to increased temperatures in comparison to *Amphistegina* spp., which has the widest latitudinal range across the oceans (Langer et al. 2013b). *Amphistegina* is an invader taxon, is tolerant of a wide range of environmental conditions and therefore, is not a good taxon to use in environmental and past environment interpretations in marine environments such as those at Sodwana Bay. *Amphistegina* is sensitive to anthropogenic influences and, due to the lack of rivers in the study area, terrestrial input and changes in nutrient levels are currently not a concern at Sodwana Bay. This supports the opinion that it is a poor indicator of changes in such marine environments.

Significant differences were found between total, sediment- and rubble-associated, foraminiferal assemblages. This was, however, mainly attributed to the relative abundances and not the taxa present. Foraminifera that live attached to firm substrata (e.g. seaweed, coral rubble), contribute to the sediment when they die. The sediment assemblage, therefore, is a combination of sediment-dwelling species and epifaunal species. It was suggested by Steinker and Rayner (1981) that in these circumstances, the sediment assemblages can be used to interpret the depositional environment of the sediment yet are not a good reflection of the living assemblages in that environment. Of the 63 identified taxa in Chapter 3, four species were found only in the rubble samples, yet they were present in very low numbers, and 15 species were found in low numbers and only in the sediment samples. The species composition was practically identical in both substrates; thus, demonstrating that sediment sufficiently represents the local assemblages in a reef-associated environment.

According to Murray (2006), dead assemblages in sediments have under gone a certain degree of time-averaging. Sediment reworking is anticipated due to post-mortem processes (e.g. faunal mixing, bioturbations, current transport) (Murray 2006). Core collection sites were at the interface between the bioclastic and quartzose sediment, signifying the farthest point for movement of debris off the reef and therefore provided a good depositional environment. The turbulent nature of this site, however, proved disadvantageous in recording the palaeoclimatic record, apart from major episodic flooding and extreme events. Representations of finer scale changes in the climate record were lost due to continuous sediment reworking. These flooding events could potentially be linked with tropical cyclones and/or cut-off lows, possibly as a result of periodic, south-ward pulses in the ITCZ. In a study by Green et al. (2012), a 6 m vibrocore was collected from 20 m water depth in July 2002 offshore of the Mgeni River mouth, north of Durban. This core represented 250–300 years of Late Holocene climate data and recorded three major storms with the storm wave base occurring at 30 m along this coastline. In comparison, the cores collected from TMR were collected from a turbulent, high-energy environment and represented ± 1200 years of palaeoenvironmental data. This signifies the potential of this site for the study of major/extreme climatic events in this area. The observed down-core foraminiferal trends potentially represent a time-averaged assemblage and, therefore, a longer core will better express any notable trends.

5.1.1 Main findings

Overall, no location affects were evident in the measured water chemistry parameters across TMR, for the sampling year. Significant differences, between one summer and one winter sampling period, in various parameters were noted. The live (coloured protoplasm) LBF assemblage was dominant on the rubble samples with a location affect evident. Significant differences were also noted in the total

foraminiferal assemblages between substratum types as well as locations. Location, therefore, played a major role in the extant foraminiferal assemblages, as the sediment texture varied and it is surmised the degree of turbulence is also variable and discriminating for the rubble foraminiferal assemblages. As reported by Murray (1991), the LBF, *Amphistegina*, *Heterostegina* and *Borelis*, have previously been reported for this region and were identified in the samples. The sediment cores proved Foraminifera are of limited use in climate interpretation for this reef-associated environment, recording only a limited portion of TMR's climate record. Only distinct flooding events, potentially related to south-ward pulses in the ITCZ, were recorded in the sediment cores. The time resolution of these sediment records was, however, not high enough for additional comparison with climatic events as recorded in the deep-sea sediment archives. Oxygen isotope analysis was, in addition, not useful in this highly turbulent environment.

5.1.2 Recommendations

Following analysis and interpretation of results, the following recommendations are presented for future studies: The full, extant foraminiferal assemblage, across the various size fractions (>63 μm) can be analysed at TMR in order to obtain a complete understanding of the foraminiferal diversity present. This can include consecutive time frames, to capture reproduction cycles and episodic blooms. If all the foraminiferal size classes are identified, Foraminifera indices (e.g. Foram index, SEDCON index) can be employed. Water sampling across seasons and years can also be implemented, to ascertain the true significance of the observed correlations with the foraminiferal assemblages. Laboratory experiments can be run to determine the effect climate change, increased temperature and decreased pH, will have on the dominant LBF in this reef-associated environment. With the continuous threat of climate change, the effects of Ocean Acidification on calcifying marine organisms are a concern. Controlled laboratory experiments will, therefore, provide possible responses of these symbiont-bearing LBF, to a changing environment. Further sediment cores can be collected on the offshore side of TMR. This region is deeper than the current study site and experiences less sediment reworking (Ramsay 1994). According to Ramsay (1994), reef-derived bioclastic debris is restricted to areas < 40 m depth. The collection of bioclastic sediment cores from areas > 40 m depth will incorporate a record of shelf-derived deposits (Ramsay 1994). This might provide useful information on long-term trends of extreme climatic events, within this marginal, reef habitat.

REFERENCES

Albani AD. 1965. The foraminifera in a sample dredged from the vicinity of Salisbury Island, Durban Bay, South Africa. Contributions from the Cushman Foundation for Foraminiferal Research 16 (2): 60 – 67.

Allégre CJ. 2005. Isotope Geology. Cambridge University Press, New York, pp 512.

Allen CD, Macalady AF, Chenchouni H, Bachelet D, McDowell N, Vennetier M, Kitzberger T, Rigling A, Breshears DD, Hogg EH, Gonzales P, Fensham R, Zhang Z, Castro J, Demidova N, J-H Lim, Allard G, Running SW Semerci A, Cobb N. 2010. A global overview of drought and heat-induced tree mortality reveals emerging climate change risks for forests. Forest Ecol. Manage. 259 (4): 660-684.

Anderson MJ, Walsh DCI. 2013. PERMANOVA, ANOSIM, and the Mantel test in the face of heterogeneous dispersions: What null hypothesis are you testing? Ecological Monographs 83 (4): 557-574.

de Andrade JC. 2005. Determination of Bicarbonate in Substrate Extracts Using Back-Titration and the Gran Plot Approach. Communications in Soil Science and Plant Analysis 36(17-18).

Armstrong HA, Brasier MD. 2005. Microfossils. Blackwell Publishing, Oxford, pp 306.

Armynot du Châtelet E, Bout-Roumazeilles V, Riboulleau A, Trentesaux A. 2009. Sediment (grain size and clay mineralogy) and organic matter quality control on living benthic foraminifera. Revue de micropaléontologie 52.

Arnaud F, Magand O, Chapron E, Bertrand S, Boës X, Charlet F, Mélières M-A. 2006. Radionuclide dating (210Pb, 137Cs, 241Am) of recent lake sediments in a highly active geodynamic setting (Lakes Puyehue and Icalma—Chilean Lake District). Science of the Total Environment 366: 837 – 850.

ASTM D4373-14. 2014. Standard Test Method for Rapid Determination of Carbonate Content of Soils. ASTM International, West Conshohocken, PA.

Bè AWH, McIntyre A, Breger DL. 1966. Shell microstructure of a planktonic foraminifer, Globorotalia menardii (d'Orbigny). Eclogae Geologicae Helvetiae 59: 885–896.

Beavington-Penney SJ, Racey A. 2004. Ecology of extant nummulitids and other larger benthic Foraminifera: applications in palaeonenvironmental analysis. Earth-Science Reviews 67: 219-265.

Begg GW. 1978. The estuaries of Natal. Natal Town and Regional Planning Report 41: 1-657.

Belanger PE, Curry WB, Matthews RK. 1981. Core- top evaluation of benthic foraminiferal isotopic ratios for paleo- oceanographic interpretations. Palaeogeography, Palaeoclimatology, Palaeoecology 33: 205–220.

Benedetti A, Pignatti J, Matteucci R. 2012. Depth distribution of Amphistegina from Lamu Archipelago (Kenya). Rend. Online Soc. Geol. It. 21: 1068-1070.

Bernhard JM. 2000. Distinguishing live from dead foraminifera: methods review and proper applications. Micropaleontology 46: 38–46.

Biesiot PG. 1957. Miocene foraminifera from the Uloa Sandstone, Zululand. Transactions and Proceedings of the Geological Society of South Africa 60: 61–80.

Birkeland CE. 1997. Life and death of coral reefs. Chapman & Hall, New York, pp 536.

Blott SJ, Pye K. 2001. Gradistat: A grain size distribution and statistics package for the analysis of unconsolidated sediments. Earth Surf. Process. Landforms 26: 1237–1248.

Boltovskoy E, Wright R. 1976. Recent Foraminifera. Junk, Amsterdam, pp 515.

Bowden AJ, Gregory FJ, Henderson AS. 2014. Landmarks in Foraminiferal Micropalaeontology: History and Development. Geological Society of London.

Boyett HV, Bourne DG, Willis BL. 2007. Elevated temperature and light enhance progression and spread of black band disease on staghorn corals of the Great Barrier Reef. Mar Biol 151: 1711-1720.

Broecker WS, Mix A, Andree M, Oescher H. 1984. Radiocarbon measurements on coexisting benthic and planktic foraminifera shells: potential for reconstructing ocean ventilation times over the past 20,000 years. Nuclear Instruments and Methods 5(33): 1-9.

Broecker WS, Klas M, Clark E, Trumbore S, Bonani G, Wolfli W, Ivy S. 1990. Accelerator mass spectrometric radiocarbon measurements on foraminifera shells from deep-sea cores. Radiocarbon 32: 119–133.

Brown L, Cook GT, MacKenzie AB, Thomson J. 2001. Radiocarbon age profiles and size dependency of mixing in northeast Atlantic sediments. Radiocarbon 43: 929-937.

Bruckner AW. 2012. Factors contributing to the regional decline of Montastraea annularis (complex). Proceedings of the 12th International Coral Reef Symposium, Cairns, Australia.

Bruton MN. 1980. An outline of the ecology of the Mgobezeleni lake system at Sodwana, with emphasis on the mangrove community. In: Bruton MN, Cooper KH (eds.), Studies on the ecology of Maputaland, Rhodes University Press, Grahamstown, pp 408-426.

Bruton MN, Appleton CC. 1975. Survey of Mgobezeleni lake-system in Zululand, with a note on the effect of a bridge on the Mangrove swamp. Trans. Roy. Soc. S. Afr. 41 Part 3.

Buchan OC. 2006. Relationships between Large Benthic Foraminifera and their seagrass habitats, San Salvador, Bahamas. MSc thesis, Auburn University.

Buosi C, Armynot Du Châtelet E, Cherchi A. 2012. Benthic foraminiferal assemblages in the current-dominated strait of Bonifacio (Mediterranean Sea). Journal of Foraminiferal Research 42(1): 39-55.

Cai W, Borlace S, Lengaigne M, van Rensch P, Collins M, Vecchi G, Timmermann A, Santoso A, McPhaden MJ, Wu L, England MH, Wang G, Guilyardi E, Jin F. 2014. Increasing frequency of extreme El Niño events due to greenhouse warming. Nature Climate Change 4: 111–116.

Cavalier-Smith T. 2003. Protist phylogeny and the high-level classification of Protozoa. Eur. J. Protistol. 39: 338-348.

Celliers L, Schleyer MH. 2003. Coral bleaching on high-latitude marginal reefs at Sodwana Bay, South Africa. Marine Pollution Bulletin 44: 1380-1387.

Chapman F. 1904. Foraminifera and Ostracoda from the Cretaceous of East Pondoland, South Africa. Annals of the South African Museum 4(5): 221–237.

Chapman F. 1907. Report on Pleistocene microzoa from a boring in the bed of the Buffalo River, East London. Albany Museum Records 2(1): 6–17.

Chapman F. 1916. Foraminifera and Ostracoda from the Upper Cretaceous of Needs Camp, Buffalo River, Cape Province. Annals of the South African Museum 12(4): 107–118.

Chapman F. 1923. On some Foraminifera and Ostracoda from the Cretaceous of Uzamba River, Pondoland. Transactions of the Geological Society of South Africa 26: 1–6.

Chapman F. 1924. A first report of foraminifera collected by the S. African Government Fisheries and Marine Biological Survey. Union of South Africa Fisheries and Marine Biological Survey Report 3, Special Report XI (for 1922): 1–19.

Chapman F. 1930. On a foraminiferal limestone of the Upper Eocene Age from the Alexandria formation, South Africa. Annals of the South African Museum 28(2): 291–296.

Chester RJ, Jickells T. 2012. Marine Geochemistry. John Wiley & Sons Inc, New York, pp 420.

Clarke KR, Ainsworth M. 1993. A method of linking multivariate community structure to environmental variables. Marine Ecology Progress Series 92: 205-219.

Clarke KR, Gorley RN. 2006. Primer v6: User Manual/Tutorial. PRIMER-E Ltd, Plymouth.

Clarke KR, Warwick RM. 1994. Change in marine communities: An approach to statistical analysis and interpretation. Natural Environment Research Council, Plymouth.

Clarke KR, Warwick RM. 2001. Change in marine communities: an approach to statistical analysis and interpretation, 2nd edition. PRIMER-E, Plymouth.

Clarke KR, Somerfield PJ, Gorley RN. 2008. Testing null hypotheses in exploratory community analyses: similarity profiles and biota-environmental linkage. J. Exp. Mar. Biol. Ecol. 366: 56-69.

Cockey E, Hallock P, Lidz BH. 1996. Decadal scale Changes in Benthic Foraminiferal Assemblages off Key Largo, Florida. Coral Reefs 15: 237-248.

Corliss BH. 1985. Microhabitats of benthic foraminifera within deep-sea sediments. Nature 314: 435–438.

Cyrus DP, Blaber SJM. 1988. The potential effects of dredging activities and increased silt load on the St. Lucia system, with special reference to turbidity and the estuarine fauna. Water SA 14(1).

Dare RA, McBride JL. 2011. The Threshold Sea Surface Temperature Condition for Tropical Cyclogenesis. J. Climate 24: 4570–4576.

Das O, Wang Y, Donoghue J, Xu X, Coor J, Elsner J, Xu Y. 2013. Reconstruction of paleostorms and paleoenvironment using geochemical proxies archived in the sediments of two coastal lakes in northwest Florida. Quaternary Science Reviews 68: 142-153.

Debenay J.-P, Tsakiridis E, Soulard R,Grossel H. 2001. Factors determining the distribution of foraminiferal assemblages in Port Joinville Harbor (Iled'Yeu, France): the influence of pollution. Marine Micropaleontology 43: 75–118.

Devi Gadi S, Rajashekhar KP. 2009. Monsoon-related periodicity in diversity and abundance of estuarine and non-estuarine foraminifera in the west coast of India.7th Asia Pacific Marine Biotechnology Conference, Nat. Inst. Oceanography. Goa, India: 101.

Dickson AG, Sabine CL, Christian JR (eds). 2007. Guide to best practices for ocean CO2 measurements. PICES Special Publication 3.

Diz P, Francés G, Costas S, Souto C, Alejo I. 2004. Distribution of benthic foraminifera in coarse sediment, Ría de Vigo, NW Iberian margin. Journal of Foraminiferal Research 34: 258–275.

Doney SC, Fabry VJ, Feely RA, Kleypas JA. 2009. Ocean Acidification: The Other CO2 Problem. Marine Science 1: 169-192.

Doo SS, Hamylton S, Byrne M. 2012. Reef-Scale Assessment of Intertidal Large Benthic Foraminifera Populations on One Tree Island, Great Barrier Reef and Their Future Carbonate Production Potential in a Warming Ocean. Zoological Studies 51(8): 1298-1307.

Duncan CP. 1970. The Agulhas Current. PhD thesis, University of Hawaii.

Duplessy JC, Lalou C, Vinot AC. 1970. Differential isotopic fractionation in benthic foraminifera and paleotemperatures reassessed. Science 168: 250–251.

Easterling DR, Evans JL, Ya Groisman P, Karl TR, Kunkel KE, Ambenje P. 2000. Observed Variability and Trends in Extreme Climate Events: A Brief Review. Bull. Amer. Meteor. Soc 81: 417-425.

Eichwald CE. 1830. Zoologia specialis. Vol 2, Villane, pp 323.

Falkowski PG, Barber RT, Smetacek V. 1998. Biogeochemical controls and feedbacks on ocean primary production. Science 281: 200-206.

Floros C, Samways MJ, Armstrong B. 2004. Taxonomic patterns of bleaching in a South African coral assemblage. Biodiversity and Conservation 13: 1175-1194.

Floros C, Schleyer MH, Maggs J, Celliers L. 2012. Ichthyological baseline assessment of high-latitude coral reef fish communities in southern Africa. African Journal of Marine Science 34(1): 55-69.

Folk RL. 1968. Petrology of Sedimentary Rocks. University of Texas Publication, Austin.

Fujita K, Fujimura H. 2008. Organic and inorganic carbon production by algal symbiont-bearing foraminifera on northwest Pacific coral-reef flats. J. Foraminifer. Res. 38: 117–126.

Fujita K, Osawa Y, Kayanne H, Ide Y, Yamano H. 2009. Distribution and sediment production of large benthic foraminifers on reef flats of the Majuro Atoll, Marshall Islands. Coral Reefs 28: 29-45.

Fujita K, Hikami M, Suzuki A, Kuroyanagi A, Sakai K, Kawahata H, Nojiri Y. 2011. Effects of ocean acidification on calcification of symbiont-bearing reef foraminifers. Biogeosciences 8: 2089-2098.

Gardner TA, Côté IM, Gill JA, Grant A, Watkinson AR. 2005. Hurricanes and Caribbean coral reefs: impacts, recovery patterns, and role in long-term decline. Ecology 86: 174–184. http://dx.doi.org/10.1890/04-0141.

Gazeau F, Quiblier C, Jansen JM, Gattuso J-P, Middelburg JJ, and Heip CHR. 2007. Impact of elevated CO2 on shellfish calcification. Geophysical Research Letters 34 (7).

Goldstein ST. 1999. Foraminifera: A biological overview. In: Sen Gupta BK (ed), Modern foraminifera. Kluwer Academic Publishers, Great Britain, pp 37-55.

Green A. 2009. Sediment dynamics on the narrow, canyon-incised and current-swept shelf of the northern KwaZulu-Natal continental shelf, South Africa. Geo-Mar Lett 29: 201-219.

Green A. 2011. Submarine canyons associated with alternating sediment starvation and shelf-edge wedge development: Northern KwaZulu-Natal continental margin, South Africa. Marine Geology 284(1-4): 114-126.

Green A, Uken R. 2008. Submarine landsliding and canyon on the northern KwaZulu-Natal continental shelf, South Africa, SW Indian Ocean. Marine Geology 254: 152-170.

Green AN, Ovechkina MN, Mostovski MB. 2012. Late Holocene shoreface evolution of the wave dominated Durban Bight, KwaZulu-Natal, South Africa: A mixed storm and current driven system. Continental Shelf Research 49: 56-64.

Grimmer A. 2011. Accretion versus bioerosion on the Maputaland reefs in South Africa - The major processes. MSc thesis, University of KwaZulu-Natal, South Africa.

Gruber L, Almogi-Labin A, Sivan D, Herut B. 2007, The life cycle of the symbiont-bearing larger foraminifera *Amphistegina lobifera*, A new arrival on the Israeli shelf. Rapp. Comm. Int. Mer Médit 38.

Hallock P. 1982. Evolution and extinction in larger foraminifera. Proceedings - Third North American Paleontological Convention 1: 221-225.

Hallock P. 1985. Why are larger foraminifera large? Paleobiology 11(2): 195- 208.

Hallock P. 2000. Larger Foraminifera as Indicators of Coral-Reef Vitality, In: Ronald ME (ed), Environmental Micropaleontology: The Application of Microfossils to Environmental Geology, Plenum publishers, New York.

Hallock P. 2012. The Foram Index revisited: uses, challenges, and limitations. Proceedings of the 12th International Coral Reef Symposium, Cairns, Australia.

Hallock P, Cottey TL, Forward LB, Halas J. 1986. Population Biology and Sediment Production of Archaias angulatus (Foraminiferida) in Largo Sound, Florida. Journal of Foraminiferal Research 16: 1-8.

Hallock P, Lidz BH, Cockey-Burkhard EM, Donnelly KB. 2003. Foraminifera as Bioindicators in Coral Reef Assessment and Monitoring: The FORAM Index. Environmental Monitoring and Assessment 81: 221-238.

Hallock P, Williams DE, Fisher EM, Toler SK. 2006. Bleaching in Foraminifera with Algal Symbionts: Implications for Reef Monitoring and Risk Assessment. Anuario de Instituto de Geociencias- UFRJ 29: 108-128.

Hansen HJ. 1999. Shell construction in modern calcareous Foraminifera. In: Sen Gupta BK (ed) Modern foraminifera. Kluwer Academic Publishers, Great Britain, pp 57-70.

Hart JR. 2011. Coral recruitment on a high-latitude reef at Sodwana Bay, South Africa: Research methods and dynamics, Master of Science thesis, University of KwaZulu-Natal, South Africa.

Hauck J, Gerdes D, Hillenbrand C-D, Hoppema M, Kuhn G, Nehrke G, Völker C, Wolf-Gladrow D. 2011. Distribution and mineralogy of carbonate sediments on Antarctic shelves. Preprint submitted to Journal of Marine Systems.

Haug GH, Hughen KA, Sigman DM, Peterson LC, Röhl U. 2001. Southward migration of the Intertropical Convergence Zone through the Holocene. Science 293: 1304.

Haynes JR. 1980. Foraminifera. John Wiley & Sons, New York.

Hayward B. 2014. Planorbulinella larvata (Parker & Jones, 1865). In: Hayward BW, Cedhagen T, Kaminski M, Gross O (eds). World Foraminifera Database. Accessed through: Hayward BW, Cedhagen T, Kaminski M, Gross O. World Foraminifera Database at http://www.marinespecies.org/foraminifera/aphia.php?p=taxdetails&id=418074 on 2015-03-02.

Hayward B, Gross O. 2015. Rotalinoides Saidova, 1975. In: Hayward BW, Cedhagen T, Kaminski M, Gross O (eds). World Foraminifera Database. Accessed through: Hayward BW, Cedhagen T, Kaminski M, Gross O. 2015. World Foraminifera Database at http://www.marinespecies.org/foraminifera/aphia.php?p=taxdetails&id=112268 on 2015-03-23.

Hemleben C, Spindler M, Anderson RO. 1989. Modern Planktonic Foraminifera. Springer, New York. pp 363.

Hoegh-Guldberg O. 1994. Mass bleaching of coral reefs in French Polynesia, April 1994. Report for Greenpeace International.

Hoegh-Guldberg O, Mumby PJ, Hooten AJ, Steneck RS, Greenfield P, Gomez E, Harvell CD, Sale PF, Edwards AJ, Caldeira K, Knowlton N, Eakin CM , Iglesias-Prieto R , Muthiga N, Bradbury RH, Dubi A, Hatziolos ME. 2007. Coral Reefs Under Rapid Climate Change and Ocean Acidification. Science 318 (5857): 1737-1742.

Hofmann GE, Barry JP, Edmunds PJ, Gates RD, Hutchins DA, Klinger T,Sewell MA. 2010. The Effect of Ocean Acidification on Calcifying Organisms in Marine Ecosystems: An Organism-to-Ecosystem Perspective. Annual Review of Ecology, Evolution, and Systematics 41: 127-147.

Hohenegger J. 2006. The importance of symbiont-bearing benthic foraminifera for west Pacific carbonate beach environments. Mar. Micropaleontol. 61: 4–39.

Jamshidi S, Bin Abu Baka N. 2011. A study on distribution of chlorophyll-a in the coastal waters of Anzali Port, south Caspian Sea. Ocean Sci. Discuss 8: 435–451.

Jansen E, Overpeck J, Briffa KR, Duplessy J-C, Joos F, Masson-Delmotte V, Olago DO, Otto-Bliesner B, Peltier WR, Rahmstorf S, Ramesh R, Raynaud D, Rind DH, Solomina O, Villalba R, Zhang D. 2007. Paleoclimate. Climate Change 2007: The Physical Science Basis. Contribution of Working Group I to the Fourth Assessment Report of the Intergovernmental Panel on Climate Change, Solomon S, Qin D, Manning M, Chen Z, Marquis M, Averyt KB, Tignor M, Miller HL (eds), Cambridge University Press, Cambridge, pp 433-498.

Javaux EJ, Scott DB. 2003. Illustration of modern benthic foraminifera from Bermuda and remarks on distribution in other subtropical/tropical areas. Palaeontologia Electronica 6(4).

Jones RW. 1994. The Challenger Foraminifera. Oxford University Press. pp 149.

Jones RJ, Bowyer J, Hoegh-Guldberg O, Blackall LL. 2004. Dynamics of a temperature-related coral disease outbreak. Marine Ecology Progress Series 281: 63-77.

Jordan IE, Samways MJ. 2001. Recent changes in coral assemblages of a South African coral reef, recommendations for long-term monitoring. Biodiversity and Conservation 10: 1027-1037.

Karl DM, Church MJ. 2014. Microbial oceanography and the Hawaii Ocean Time-series programme. Nat Rev Microbiol.(10): 699-713.

Karl DM, Winn CD, Hebel DVW, Letelier R. 1990. Hawaii ocean time-series program field and laboratory protocols.

Kasemann SA, Schmidt DN, Bijma J, Foster GL. 2009. In situ boron isotope analysis in marine carbonates and its application for foraminifera and palaeo-pH. Chemical Geology journal 260: 138–147.

Katz ME, Katz DR, Wright JD, Miller KG, Pak DK, Shackleton NJ, Thomas E. 2003. Early Cenozoic benthic foraminiferal isotopes: species reliability and interspecies correction factors. Paleoceanography 18. doi:10.1029/ 2002PA000798.

Katz ME, Cramer BS, Franzese A, Hönisch B, Miller KG, Rosenthal Y, Wright JD. 2010. Traditional and emerging geochemical proxies in Foraminifera. Journal of Foraminiferal Research 40(2): 165-192.

Keul N, Langer G, de Nooijer LJ, Bijma J. 2013. Effect of ocean acidification on the benthic foraminifera Ammonia sp. is caused by a decrease in carbonate ion concentration. Biogeosciences Discussions 10: 1147-1176.

Kleypas JA, McManus JW, Meñez LAB. 1999. Environmental Limits to Coral Reef Development: Where Do We Draw the Line? American Zoologist 39: 146-159.

Kotwicki L, Grzelak K, Czub M, Dellwig O, Gentz T, Szymczycha B, Böttcher ME. 2014. Submarine groundwater discharge to the Baltic coastal zone: Impacts on the meiofaunal community. Journal of Marine Systems 129: 118–126.

Koukousioura O, Dimiza MD, Triantaphyllou MV, Hallock P. 2011. Living benthic foraminifera as an environmental proxy in coastal ecosystems: A case study from the Aegean Sea (Greece, NE Mediterranean). J Mar Syst. 88: 489-501.

Kovacs ZP, Du Plessis DB, Bracher PR, Dunn P, Mallory GCL. 1985. Republic of South Africa Department of Water Affairs documentation of the 1984 Domoina floods. Technical report TR 122.

Kučera M. 2007. Planktonic Foraminifera as Tracers of Past Oceanic Environments. In: Hillaire-Marcel C, de Vernal A (eds), Proxies in Late Cenozoic Paleocenaography, Developments in Marine Geology vol. 1, Elsevier, Amsterdam, pp 213-62.

Lakhmapurkar J, Bhatt N. 2010. Geo-environmental Appraisal of the Meda Creek, Saurashtra, Gujarat. Journal Geological Society of India 75: 695-703.

Lambert G, Scheibnerová V. 1974. Albian foraminifer of Zululand (South Africa) and Great Artesian Basin (Australia). Micropaleontology 20(1): 76–96.

Langer MR. 1993. Epiphytic foraminifera. Marine Micropaleontology 20(3–4): 235–265.

Langer MR, Silk MT, Lipps JH. 1997. Global ocean carbonate and carbon dioxide production; the role of reef Foraminifera. J Foraminiferal Res. 27: 271–277.

Langer MR, Thissen JM, Makled WA, Weinmann AE. 2013a. The foraminifera from the Bazaruto Archipelago (Mozambique). N. lb. Geol. Paliiont. Abh. 267: 155-170.

Langer MR, Weinmann AE, Lötters S, Bernhard JM, Rödder D. 2013b. Climate-Driven Range Extension of *Amphistegina* (Protista, Foraminiferida): Models of Current and Predicted Future Ranges. PLoS ONE 8(2): e54443.

Lee JJ. 2006. Algal symbiosis in larger foraminifera. Symbiosis 42: 63-75.

Lee JJ, Hallock P. 1987. Algal symbiosis as the driving force in the evolution of larger Foraminifera. Ann N Y Acad Sci 503: 330–347.

Lidz BH, Rose PR. 1989. Diagnostic foraminiferal assemblages of Florida Bay and adjacent shallow waters: A comparison. Bulletin of Marine Science 44(1): 399-418.

Lipps JH. 1983. Biotic interactions in benthic foraminifera, In: Tevesz MJS, Mccall PL (eds), Biotic interactions in Recent and fossil benthic communities, Plenum Press, New York, pp 331-376.

Lirman D, Orlando B, Macia S, Manzello D, Kaufman L, Biber P, Jones T. 2003. Coral communities of Biscayne Bay, Florida and adjacent offshore areas: diversity, abundance, distribution, and environmental correlates. Aquatic Conserv: Mar. Freshw. Ecosyst. 13: 121–135.

Loeblich AR, Tappan H. 1987. Foraminiferal genera and their classification. Cushman foundation for foraminiferal research, Van Rostrand Reinhold Company, New York.

Loeblich AR, Tappan H. 1994. Foraminifera of the Sahul Shelf and Timor Sea. Cushman foundation for foraminiferal research, special publication 31.

Lutjeharms JRE. 2004. The coastal oceans of south-eastern Africa, volume 14B. Harvard University Press.

Lutjeharms JRE. 2006. The Agulhas Current. Springer, Germany, pp 329.

Lutjeharms JRE, Roberts HR. 1988. The Natal Pulse: an extreme transient on the Agulhas Current. Journal of Geophysical Research 93: 631-645.

Lutjeharms JRE, Cooper J, Roberts M. 2000. Upwelling at the inshore edge of the Agulhas Current. Contin Shelf Res. 20: 737–761.

Margalef R. 1958. Temporal succession and spatial heterogeneity in phytoplankton. In: Buzzati-Traverso (eds), Perspectives in Marine biology, Univ. Calif. Press, Berkeley, pp 323-347.

Martin RA. 1974. Benthonic foraminifera from the western coast of southern Africa. Joint Geological Survey South Africa/ UCT Marine Geoscience Unit Technical Report 6(14): 83–87.

Martin AK. 1978. Physical oceanography in the northernmost Natal Valley. Progress Reports for the year 1978. Technical report No. 11, Marine Geoscience Unit, University of Cape Town.

Martin RE. 1986. Habitat and Distribution of the Foraminifer Archaias Angulatus (Fitchel and Moll) (Miliolida, Soritidae) Northern Florida Keys. Journal of Foraminiferal Research 16: 201-206.

Martin JH, Fitzwater SE. 1988. Iron deficiency limits phytoplankton growth in the north-east Pacific subarctic. Nature 331: 341-343.

Martins V, Jouanneau J-M, Weber O, Rocha F. 2006. Tracing the late Holocene evolution of the NW Iberian upwelling system. Marine Micropaleontology 5: 35-55.

Mazumder A, Nigam R, Henriques PJ. 2012. Deterioration of Early Holocene coral reef due to sea level rise along west coast of India: Benthic foraminiferal testimony. Geosciences Frontiers 3(5): 697-705.

McIntosh F. 2010. Atlas of dive sites of South Africa and Mozambique, Map Studio, Cape Town.

McIntyre-Wressnig A, Bernhard JM, McCorkle DC, Hallock P. 2011. Non-lethal effects of ocean acidification on two symbiont-bearing benthic foraminiferal species. Biogeosciences Discussions 8: 9165-9200.

Mejías SM, Ballesteros BJ, Antón-Pacheco C, Domínguez JA, Garcia-Orellana J, Garcia-Solsona E, Masqué P. 2012. Methodological study of submarine groundwater discharge from a karstic aquifer in the Western Mediterranean. Journal of Hydrology 464–465: 27–40.

Morris T. 2009. Physical oceanography of Sodwana Bay and its effect on larval transport and coral bleaching. MSc thesis, Cape Peninsula University of Technology.

Murray JW. 1991. Ecology and palaeoecology of benthic foraminifera. Univ. Southampton, Southampton, pp 402.

Murray JW. 2006. Ecology and applications of Benthic Foraminifera, Cambridge University Press, New York, pp 426.

Murray JW, Bowser SS. 2000. Mortality, protoplasm decay rate, and reliability of staining techniques to recognize 'living' foraminifera: a review. Journal of Foraminiferal Research 30: 66–77.

Naser H. 2011. Human Impacts on Marine Biodiversity: Macrobenthos in Bahrain, Arabian Gulf, The Importance of Biological Interactions in the Study of Biodiversity, LÃ3 pez-Pujol J (Ed.), ISBN: 978-953- 307-751-2.

Natsir SM, Subkhan M. 2011. The Distribution of Benthic Foraminifera in Coral Reefs Community and Seagrass Bad of Belitung Islands based on Foram Index. J Coastal Dev doi: 10.4172/1410-5217.10000329.

Nigam R, Chaturvedi SK. 2000. Foraminiferal study from Kharo creek, Kachchh (Gujarat), north west coast of India. Indian Journal of Marine Science 29: 133-138.

Nobes K, Uthicke S. 2008. Benthic Foraminifera of the Great Barrier Reef: A guide to species potentially useful as Water Quality Indicators. Report to the Marine and Tropical Sciences Research Facility. Reef and Rainforest Research Centre Limited, Cairns.

Oliver JE. 2005. The Encyclopedia of World Climatology, Springer, The Netherlands.

Osterman LE, Poore RZ, Swarzenski PW. 2008. The last 1000 years of natural and anthropogenic low-oxygen bottom-water on the Louisiana shelf, Gulf of Mexico. Marine Micropaleontology 66: 291-303.

Parker WC, Arnold A. 1999. Quantitative methods of data analysis in foraminiferal ecology. In: Sen Gupta (ed), Modern Foraminifera, Kluwer Academic Publishers, Great Britain, pp 71-89.

Parker WK, Jones TR. 1865. On some foraminifera from the North Atlantic and Arctic Oceans, including Davis Straits and Baffin's Bay. Philosophical Transactions of the Royal Society 155: 325-441.

Parkinson MC. 2012. Contributions of inshore and offshore sources of primary production to the foodweb, and the trophic connectivity between various habitats along a depth-gradient, in Sodwana Bay, KwaZulu-Natal, South Africa, MSc thesis, Rhodes University.

Parr WJ. 1958. The foraminifera of the Bluff Beds, Durban and some other South African calcareous coastal rocks. Transactions and Proceedings of the Geological Society of South Africa 61: 103–109.

Pearson PN. 2012. Oxygen Isotopes in Foraminifera: Overview and historical review, In: Ivany LC, Huber BT (eds), Reconstructing Earth's Deep-Time Climate-The State of the Art in 2012, Paleontological Society Short Course, November 3, 2012. The Paleontological Society Papers 18: 1–38.

Pielou EC. 1966. The measurement of diversity in different types of biological collections. J. Theoret. Biol. 13: 131-144.

Pillet L, Voltski I, Korsun S, Pawlowski J. 2013. Molecular phylogeny of Elphidiidae (foraminifera). Marine Micropaleontology 103: 1–14.

Pollard JH. 1979. A Handbook of Numerical and Statistical Techniques with Examples Mainly from the Life Sciences, Cambridge University Press.

Poppe LJ, Eliason AH, Fredericks JJ, Rendigs RR, Blackwood D, Polloni CF. 2000. Grain size analysis of marine sediments: methodology and data processing. In: Poppe LJ, Polloni CF (eds), USGS East-coast sediment analysis: procedures, database, and georeferenced displays, US Geological Survey Open-File Report 00-358.

Porubsky WP, Weston NB, Moore WS, Ruppel C, Joye SB. 2014. Dynamics of submarine groundwater discharge and associated fluxes of dissolved nutrients, carbon, and trace gases to the coastal zone (Okatee River estuary, South Carolina). Geochimica et Cosmochimica Acta 131: 81–97.

Prothero DR. 2004. Bringing Fossils to Life; An Introduction to Paleobiology 2nd edition. McGraw-Hill, New York.

Ramsay PJ. 1991. Sedimentology, coral reef zonation and late Pleistocene coastline models of the Sodwana Bay continental shelf, northern Zululand. PhD thesis, Department of Geology and Applied Geology, University of Natal, South Africa.

Ramsay PJ. 1994. Marine geology of the Sodwana Bay shelf, southeast Africa. Marine Geology 120: 225-247.

Ramsay PJ. 1997. Quaternary marine geology and sea-level changes: Sodwana Bay shelf. Maputaland Workshop Field Guide and Abstracts.

Ramsay PJ, Cohen AL. 1997. Coral Palaeoclimatology Research on the Southeast African Shelf. Council for Geoscience, unpublished internal report.

Ramsay PJ, Mason TR. 1990. Development of a type zoning model for Zululand coral reefs, Sodwana Bay, South Africa. Journal of Coastal Research 6(4): 829-852.

Rapp GR, Hill CL. 2006. Geoarchaeology: The Earth-science Approach to Archaeological Interpretation (2nd ed). New Haven, Yale University Press.

Ravelo AC, Fairbanks RG. 1992. Oxygen isotopic composition of multiple species of planktonic foraminifera: Recorders of the modern photic zone temperature gradient. Paleoceanography 7: 815–831.

Reason CJC, Keibel A. 2004. Tropical Cyclone Eline and Its Unusual Penetration and Impacts over the Southern African Mainland. Weather and forecasting 19:789-805.

Rees GN, Baldwin DS, Watson GO, Perryman S, Nielsen DL. 2004. Ordination and significance testing of microbial community composition derived from terminal restriction fragment length polymorphisms: application of multivariate statistics. Antonie van Leeuwenhoek 86: 339–347.

Renema W, Beaman RJ, Webster JM. 2013. Mixing of relict and modern tests of larger benthic foraminifera on the Great Barrier Reef shelf margin. Marine Micropaleontology, http://dx.doi.org/10.1016/j.marmicro.2013.03.002.

Riegl B, Schleyer MH, Cook PJ, Branch GM. 1995. Structure of Africa's southernmost coral communities. Bulletin of Marine Science 56(2): 676-691.

Roberts MJ, Ribbink AJ, Morris T, van den Berg MA, Engelbrecht DC, Harding RT. 2006. Oceanographic environment of the Sodwana Bay coelacanths (Latimeria chalumnae), South Africa. South African Journal of Science 102: 435–443.

Rollion-Bard C, Erez J. 2010. Intra-shell boron isotope ratios in the symbiont-bearing benthic foraminiferan *Amphistegina lobifera*: Implications for δ11B vital effects and paleo-pH reconstructions. Geochimica et Cosmochimica Acta 74: 1530–1536.

Rosenzweig C, Iglesias A, Yang XB, Epstein PR, Chivian E. 2001. Climate change and extreme weather events: Implications for food production, plant diseases, and pests. Global change and human health 2(2): 90-104.

Ross CA. 1974. Evolutionary and ecological significance of large, calcareous Foraminiferida (Protozoa), Great Barrier Reef. Proceedings Second International Coral Reef Symposium 1: 327-333.

Rouault M, White SA, Reason CJC, Lutjeharms JRE, Jobard I. 2002. Ocean–Atmosphere Interaction in the Agulhas Current Region and a South African Extreme Weather Event. Weather Forecasting 17: 655–669.

Salmon DA. 1979a. Quaternary foraminifers in piston cores from the S. W. Indian Ocean. Joint Geological Survey South Africa/ UCT Marine Geoscience Unit Technical Report 11(8): 72–79.

Salmon DA. 1979b. Quaternary foraminifers in piston cores from the S. W. Indian Ocean. Joint Geological Survey South Africa/ UCT Marine Geoscience Unit Technical Report 11(9): 80-88.

Salmon DA. 1980. Tertiary planktic foraminiferida and biostratigraphy of cores from three deep sea areas in the SW Indian Ocean. Joint Geological Survey South Africa/ UCT Marine Geoscience Unit Technical Report 12(1): 1-17.

Santos IR, Glud RN, Maher D, Erler D, Eyre BD. 2011. Diel coral reef acidification driven by porewater advection in permeable carbonate sands, Heron Island, Great Barrier Reef. Geophys. Res. Lett. 38: L03604.

Saraswati PK, Seto K, Nomura R. 2004. Oxygen and carbon isotopic variation in co-existing larger foraminifera from a reef flat at Akajima, Okinawa, Japan. Marine Micropaleontology 50: 339-349.

Schmidt C, Heinz P, Kucera M, Uthicke S. 2011. Temperature-induced stress leads to bleaching in larger benthic foraminifera hosting endosymbiotic diatoms. Limnol Oceanogr. 56(5): 1587-1602.

Schmidt C, Kucera M, Uthicke S. 2013. Investigation of the simultaneous effects of ocean acidification and warming on coral reef foraminifera. Interdisciplinary Conference of Young Earth System Scientists.

Schmidt C, Heinz P, Kucera M, Uthicke S. 2014. Combined effects of warming and ocean acidification on coral reef Foraminifera Marginopora vertebralis and Heterostegina depressa. Coral Reefs 33: 805-818.

Scholle PA, Halley RB. 1989. Burial diagenesis: Out of sight, out of mind! In: Scholle PA, James NP, Read JF (eds.), Carbonate Sedimentology and Petrology, Part 3 Volume 4 of Short course in geology, Short Course in Geology.

Schweizer M, Polovodova I, Nikulina A, Schönfeld J. 2011. Molecular identification of Ammonia and Elphidium species (Foraminifera, Rotaliida) from the Kiel Fjord (SW Baltic Sea) with rDNA sequences. Helgol Mar Res. 65: 1–10.

Sen Gupta BK. 1999. Systematics of modern Foraminifera. In: Sen Gupta BK (ed.), Modern foraminifera, Kluwer Academic Publishers, Great Britain, pp 7-36.

Severin KP. 1983. Test morphology of benthic foraminifera as a discriminator of biofacies. Marine Micropaleontology 8:65-76.

Shackleton NJ. 1974. Attainment of isotopic equilibrium between ocean water and the benthonic foraminifera genus Uvigerina: isotopic changes in the ocean during the last glacial. Colloques Internationaux du Centre National de la Recherche Scientifique 219: 203–225.

Shannon C, Weaver W. 1963. The Mathematical Theory of Communication, University of Illinois Press, pp 144.

Sharp Z. 2007. Principles of Stable Isotope Geochemistry, Pearson Education Inc., Upper Saddle River, New Jersey.

Shongwe ME, van Oldenborgh GJ, van den Hurk BJJM, de Boer B, Coelho CAS, van Aalst MK. 2009. Projected Changes in Mean and Extreme Precipitation in Africa under Global Warming. Part I: Southern Africa. American Meteorological Society 22: 3819-3837.

Silverman J, Lazar B, Erez J. 2007. Effect of aragonite saturation, temperature, and nutrients on the community calcification rate of a coral reef. Journal Of Geophysical Research 112: C05004, doi:10.1029/2006JC003770.

Solomon S, Qun D, Manning M, Chen Z, Marquis M, Averyt KB, Tignor M, Miller HL. 2007. Climate change 2007: The physical science basis. Contribution of working group I to the fourth assessment report of the Intergovernmental Panel on Climate Change. Cambridge University Press, New York.

Southon J, Kashgarian M, Fontugne M, Metivier B, Yim WWS. 2002. Marine reservoir corrections for the Indian Ocean and Southeast Asia. Radiocarbon 44(1): 167–80.

Spero HJ, Lea DW. 1993. Intraspecific stable isotope variability in the planktic foraminifera Globigerinoides sacculifer: results from laboratory experiments. Marine Micropaleontology 22: 221–234.

Steinker DC, Rayner AL. 1981. Some habitats of nearshore foraminifera, St. Croix, U.S. Virgin Islands. Compass of Sigma Gamma Epsilon 59(11): 15-26.

Stephenson CM. 2011. Foraminiferal Assemblages on Sediment and Reef Rubble at Conch Reef, Florida, USA. MSc thesis, University of South Florida.

Stephenson CM, Hallock P, Kelmo F. 2015. Foraminiferal assemblage indices: A comparison of sediment and reef rubble samples from Conch Reef, Florida, USA. Ecological Indicators 48: 1-7.

Strachan KL, Finch JM, Hill T, Barnett RL. 2013. A late Holocene sea-level curve for the east coast of South Africa. S Afr J Sci.

Takahashi T, Sutherland SC, Chipman DW, Goddard JG, Newberger T, Sweeney C. 2014. Climatological Distributions of pH, pCO2, Total CO2, Alkalinity, and CaCO3 Saturation in the Global surface Ocean. Report no. ORNL/CDIAC-160, NDP-0XXXX.
doi: 10.1016/j.marchem.2014.06.004.

Talmage SC, Gobler CJ. 2010. Effects of past, present, and future ocean carbon dioxide concentrations on the growth and survival of larval shellfish. PNAS. 107 (40): 17246-17251.

Toefy R. 2010. Extant benthic Foraminifera from two bays along the SW coast of South Africa, with a comment about their use as indicators of pollution. Phd thesis, University of the Western Cape.

Toefy R, McMillan IK, Gibbons MJ. 2003. The effect of wave exposure on the foraminifera of Gelidium pristoides. Journal of the Marine Biological association, U.K. 83: 705–710.

Tory KJ, Frank WM. 2010. Tropical cyclone formation. In: Chan JCL (ed.), Global Perspectives on Tropical Cyclones: From Science to Mitigation, World Scientific Publishing, Singapore, pp 55-92.

Troelstra SR, Jonkers HM, de Rijk S. 1996. Larger Foraminifera from the Spermonde Archipelago (Sulawesi, Indonesia). Scripta Geol.113: 93-120.

Tsujimoto A, Yasuhara M, Nomura R, Yamazaki H, Sampei Y, Hirose K, Yoshikawa S. 2008. Development of modern benthic ecosystems in eutrophic coastal oceans: The foraminiferal record over the last 200 years, Osaka Bay, Japan. Marine Micropaleontology 69: 225-239.

Tudhope AW, Scoffin TP. 1988. The relative importance of benthic foraminiferans in the production of sediments on the central Queensland shelf. Proceedings of the Sixth International Coral Reef Symposium Australia, pp 583–588.

Uthicke S, Altenrath C. 2010. Water column nutrients control growth and C:N ratios of symbiont-bearing benthic foraminifera on the Great Barrier Reef, Australia. Limnol. Oceanogr. 55(4): 1681–1696.

Uthicke S, Momigliano P, Fabricius KE. 2013. High risk of extinction of benthic foraminifera in this century due to ocean acidification. Scientific Reports 3: DIO: 10.1038/srep01769.

Uwadia RE. 2009. Response of Benthic Macroinvertebrate Community to Salinity Gradient in a Sandwiched Coastal Lagoon. Report and Opinion 1(4).

Vogel N, Uthicke S. 2012. Calcification and photobiology in symbiont-bearing benthic foraminfiera and responses to a high CO2 environment. Journal of Experimental Marine Biology and Ecology 424-425: 15-24.

Wang X, Du J, Ji T, Wen T, Liu S, Zhang J. 2014. An estimation of nutrient fluxes via submarine groundwater discharge into the Sanggou Bay—A typical multi-species culture ecosystem in China. Marine Chemistry 167: 113–122.

Weiner S, Dove PM. 2003. An Overview of Biomineralization and the Problem of the Vital Effect. In: Dove PM, Weiner S, De Yoreo JJ (eds.), Biomineralization. Mineralogical Society of America, Washington, D.C. 54: pp 1-31.

Weinmann AE, Rödder D, Lötters S, Langer MR. 2013. Heading for New Shores: Projecting Marine Distribution Ranges of Selected Larger Foraminifera. PLoS ONE 8(4): e62182. doi:10.1371/journal.pone.0062182.

Wentworth CK. 1922. A scale of grade and class terms for clastic sediments. J. Geology 30: 377-392.

Whitfield AK, Taylor RH. 2009. Case studies and reviews: A review of the importance of freshwater inflow to the future conservation of Lake St Lucia. Aquatic Conserv: Mar. Freshw. Ecosyst. 19: 838-848.

Wilkinson C. 2002. Status of coral reefs of the world, Australian Institute of Marine Science.

Wright RC, Hay WW. 1971. The abundance and distribution of foraminifers in a back-reef environment, Molasses Reef, Florida. Memoir Miami Geological Society 1: 74-121.

Yassini I, Jones BG. 1995. Foraminiferida and ostracoda from estuarine and shelf environments on the southeastern coast of Australia: University of Wollongong Press, Wollongong.

Yoshioka PM. 2008. As I see it: Misidentification of the Bray-Curtis similarity index. Marine Ecology Progress Series 368:309-310.

APPENDIX A
WATER CHEMISTRY CONTOUR MAPS

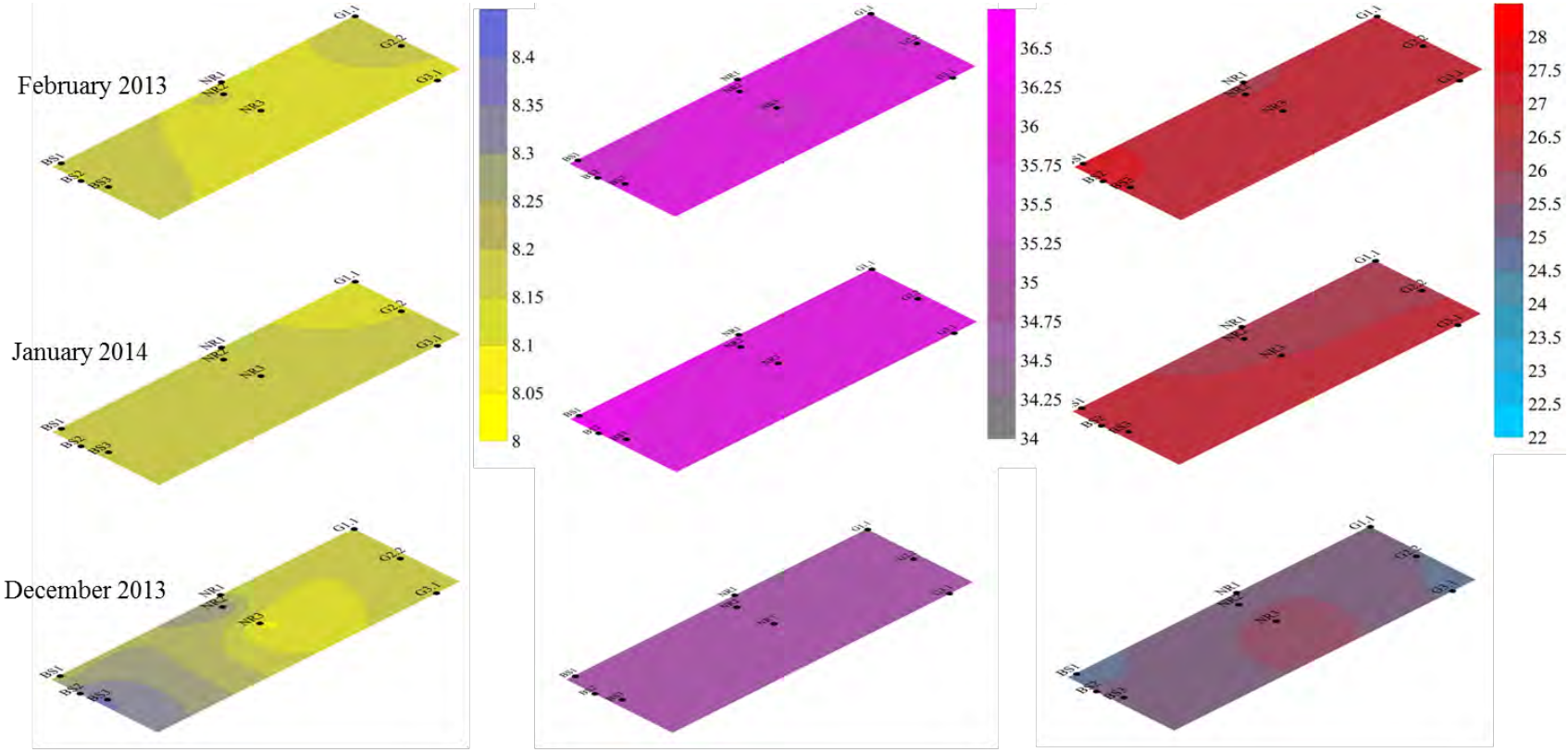

Figure A1. Summer contour maps showing pH, salinity and temperature variation across three locations on Two-mile Reef.

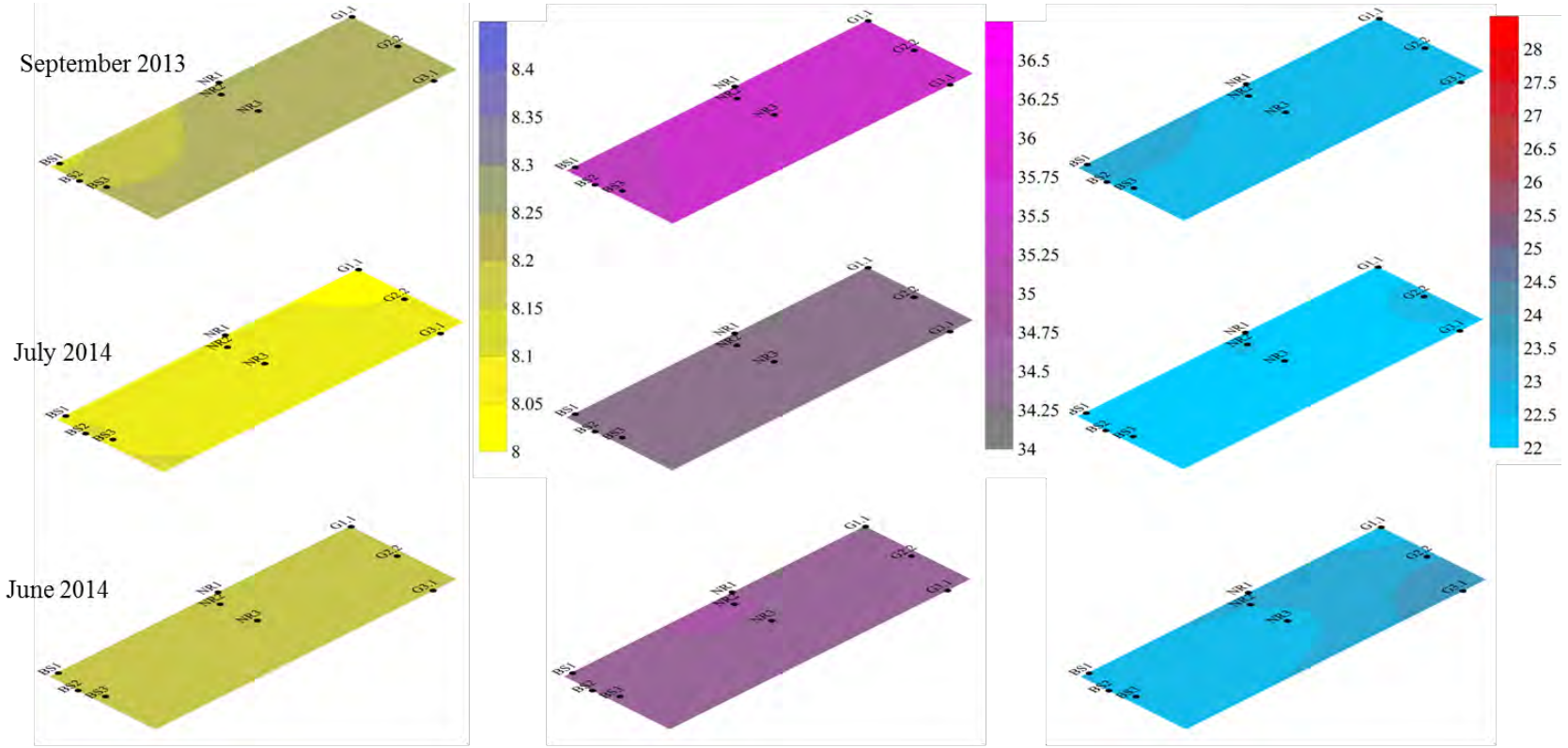

Figure A2. Winter contour maps showing pH, salinity and temperature variation across three locations on Two-mile Reef.

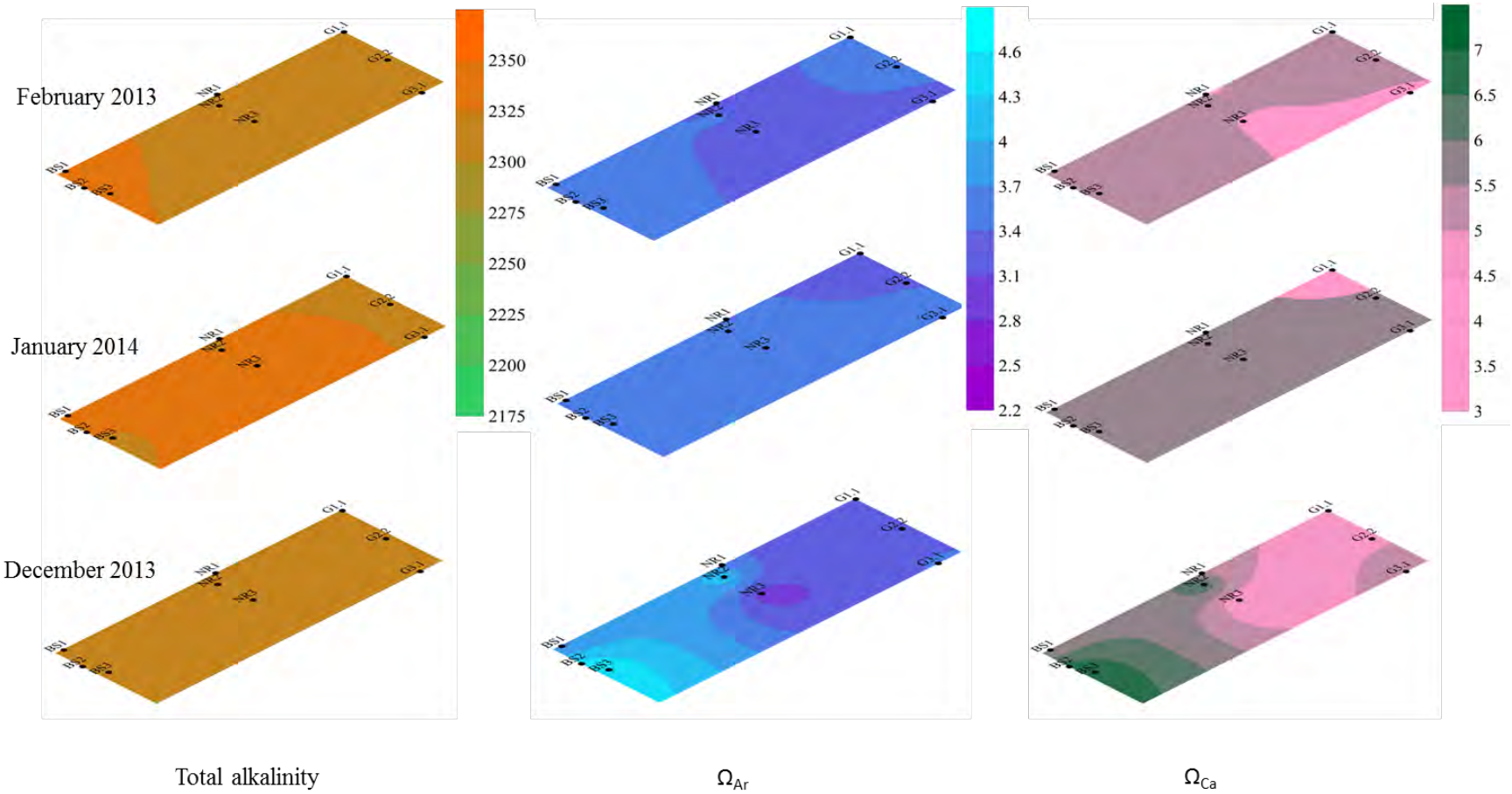

Figure A3. Summer contour maps showing total alkalinity, Ω_{Ar} and Ω_{Ca} variations across three locations on Two-mile Reef (BS = bioclastic sediment, NR = near reef and G = Gully location).

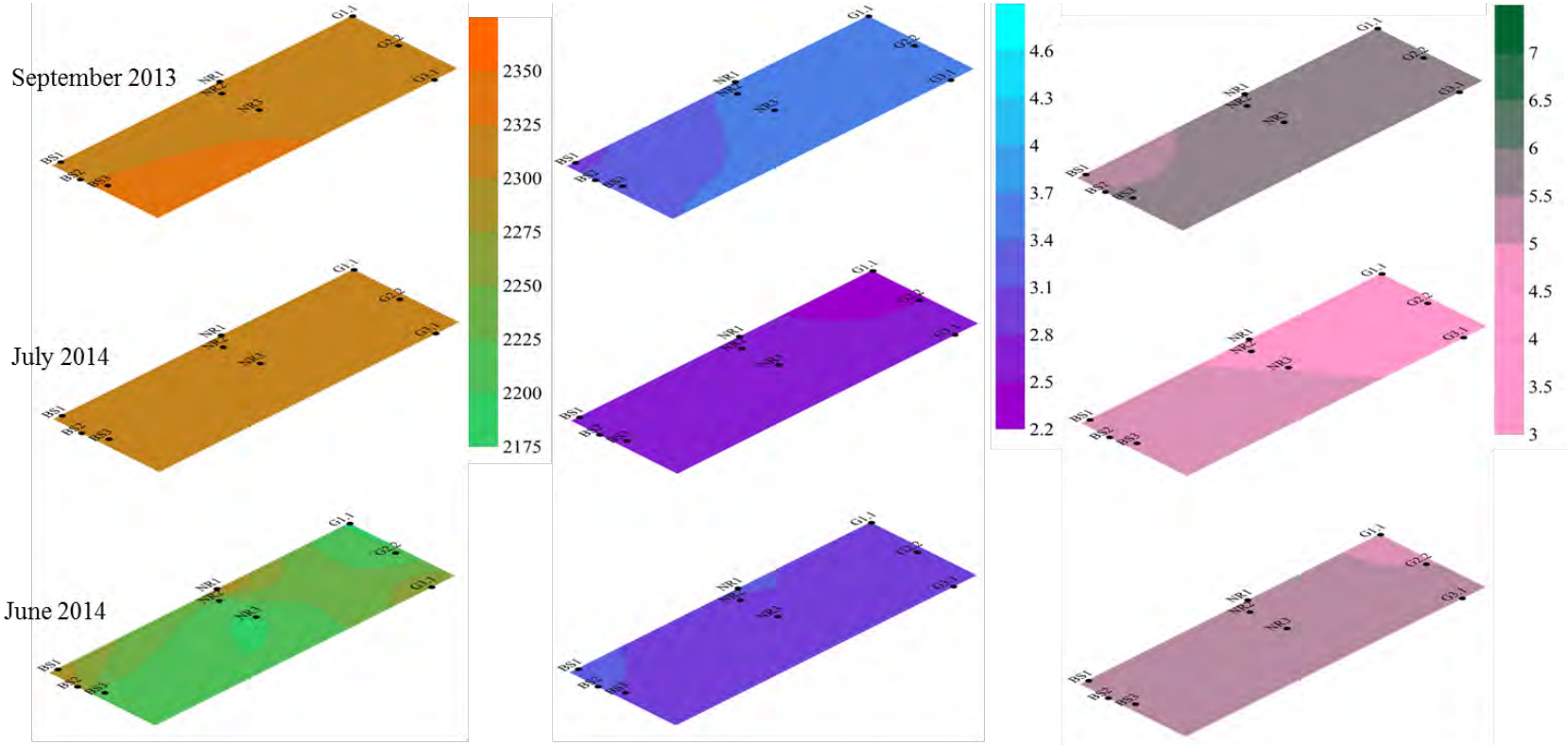

Figure A4. Winter contour maps showing total alkalinity, Ω_{Ar} and Ω_{Ca} variations across three locations on Two-mile Reef (BS = bioclastic sediment, NR = near reef and G = Gully location).

APPENDIX B
TAXON LIST

Table B1. Compiled taxon list for habitat comparison (Chapter 3) and core (Chapter 4) component. X denotes taxon was present in samples. (BS = bioclastic sediment, NR = near-reef and G = gully).

Taxon			Habitat comparison					Core X		
			Sediment samples			Rubble samples		Size (μm)		
			BS	NR	G	NR	G	125	250	500
Globigerinina	*Globorotalia*	sp.1						X		
	Globigerina	spp.						X	X	
Lagenina	*Glandulina*	sp.1						X		
Miliolina	*Adelosina*	sp.1	X							
		sp.2							X	
	Ammonia	sp.1	X		X		X	X	X	X
		sp.3	X				X			
		sp.4						X	X	
		beccarii						X	X	
	Articularia	sp.1						X		
	Articulina	sp.2						X		
	Borelis	sp.1							X	
		melo	X	X	X	X		X	X	
		schlumbergei	X	X	X	X	X		X	X
	Cycloforina	sp.1	X							
		sp.3						X		
		sp.4						X	X	
		sp.5						X		
		contorta						X	X	
	Hauerina	sp.1						X	X	
	Lachlanella	*barnardi*	X	X	X	X	X		X	
	Marginopora	*vertebralis*	X	X	X	X	X			
	Miliolinella	sp.2						X	X	
	Peneroplis	sp.1						X	X	
		sp.2						X	X	
	Pseudotriloculina	sp.3			X	X				
		sp.4						X		
		kerimbatica	X	X	X	X	X			
	Pyrgo	sp.3						X		
		denticulata		X		X	X			
		depressa	X			X	X			
	Quinqueloculina	sp.1	X	X	X	X	X			
		sp.3	X	X	X	X	X	X		X
		sp.4	X	X	X	X	X	X	X	X
		sp.5	X	X	X	X	X			
		sp.6	X			X		X	X	X
		sp.9	X	X	X	X	X	X	X	X
		sp.10	X							
		sp.18	X					X	X	X
		sp.20						X	X	X
		sp.23	X	X	X					
		sp.24	X							
		sp.25	X							
		sp.30							X	
		sp.31						X	X	X
		sp.32						X	X	
		sp.35						X	X	

		sp.37						X	X	
		sp.38						X	X	X
		sp.39						X	X	X
		sp.40						X	X	
		sp.42						X	X	
		sp.44						X	X	
		sp.45						X	X	
		sp.46						X	X	
		sp.47						X	X	
		sp.48						X		
		sp.49						X		
		sp.50							X	
		sp.51							X	
	Sorites	sp.1	X	X	X	X	X			
		sp.3	X	X	X	X	X			X
		orbiculus						X	X	X
	Spiroloculina	sp.1			X	X			X	X
		sp.2	X	X	X	X	X			
		sp.4	X	X	X		X			
		sp.5			X	X	X			
		sp.8								X
	Triloculina	sp.3	X		X			X	X	X
		sp.4		X	X	X	X	X	X	
		sp.5	X	X	X	X	X			
		sp.6	X		X	X	X			
		sp.7			X		X			
		sp.8				X				
		sp.10	X							
		sp.11				X				
		sp.12							X	
		sp.13							X	
		sp.14							X	
		sp.15						X		
		sp.16						X	X	
		sp.17						X		
		tricarinata							X	
		trigonula							X	X
Rotaliina	*Acervulina*	sp.1				X	X			
	Amphistegina	spp.	X	X	X	X	X	X	X	X
	Assilina	sp.1						X		
	Asterigerina	sp.1	X	X	X	X	X	X	X	X
		sp.2						X	X	X
	Asterigerinata	*mamilla*						X		
	Bolivina	sp.1						X		
		sp.2						X		
		sp.3						X		
		sp.4						X		
		nitida						X		
	Cassidulina	sp.1						X	X	
	Cassidulina	sp.2						X	X	
	Challengerella	*bradyi*						X		
	Cibicides	sp.1						X	X	
		refulgens	X	X		X	X	X	X	
	Cyclocibicides	sp.1					X			
	Dentalina	sp.1						X		

	Elphidium	sp.2	X				X	X	X	X
		sp.6						X	X	
		sp.9						X		
		sp.10							X	
		sp.11						X	X	X
		macellum	X	X	X	X	X	X	X	X
	Eupatellinella	*fastidiosa*	X					X	X	
	Fissurina	sp.1						X		
	Gavelinopsis	*praegeri*						X		
	Glabratella	*tabernacularis*						X	X	
	Haynesina	sp.1						X		
	Heterostegina	*depressa*	X	X	X	X	X		X	X
	Homotrema	*rubra*	X	X	X	X	X		X	X
	Hyalinea	sp.1						X		
		balthica						X	X	
	Lenticulina	sp.1	X		X			X	X	
		sp.2		X			X			
	Lobatula	*lobatula*						X	X	X
	Neoeponides	sp.1						X		
	Nodosaria	sp.1						X		
	Nonion	sp.1						X		
		sp.2						X		
		fabum						X	X	
	Nonionoides	sp.1						X	X	
		sp.2						X	X	
	Pararotalia	sp.2						X	X	
		stellata						X	X	
	Pavonina	*flabelliformis*		X		X	X		X	
	Pileolina	*patelliformis*						X		
	Planoglabratella	sp.3						X		
		opercularis						X	X	
	Planorbulina	sp.1							X	X
	Planorbulinella	sp.1						X	X	
		larvata	X	X	X	X	X		X	X
	Planorbulinoides	*retinaculatus*			X					
	Pseudobrizalina	*lobata*						X		
	Rosalina	sp.1						X	X	X
		sp.2						X	X	X
		sp.3						X		
		sp.4						X		
		sp.5						X		
	Rotalinoides	sp.1						X		
		sp.2						X		
		sp.3						X		
		sp.4						X		
		sp.5						X		
	Rotorbis	sp.1						X	X	
	Sagrinella	*jugosa*						X	X	
Spirillinina	*Spirillina*	sp.1						X	X	
Textulariina	*Septotextularia*	*rugosa*	X	X	X	X	X	X	X	X
	Textularia	sp.1	X	X	X	X	X		X	X
		sp.2		X	X	X	X			
		sp.4		X	X	X	X			
		sp.6	X	X	X	X	X			
		sp.7						X	X	X

		sp.8						X	X	
		sp.9						X		
		foliacea	X	X	X	X	X	X	X	X
Unknown	Unknown	Foraminifera sp.2	X							
		Foraminifera sp.4	X			X				
		Foraminifera sp.7							X	
		Foraminifera sp.8							X	
		Foraminifera sp.11						X	X	
		Foraminifera sp.13						X	X	
		Foraminifera sp.19						X	X	
		Foraminifera sp.26	X				X		X	
		Foraminifera sp.31	X							
		Foraminifera sp.36	X							
		Foraminifera sp.40						X		
		Foraminifera sp.44						X		
		Foraminifera sp.46						X		
		Foraminifera sp.52						X		
		Foraminifera sp.55						X		
		Foraminifera sp.68						X		

APPENDIX C

MAIN TAXA MENTIONED IN TEXT

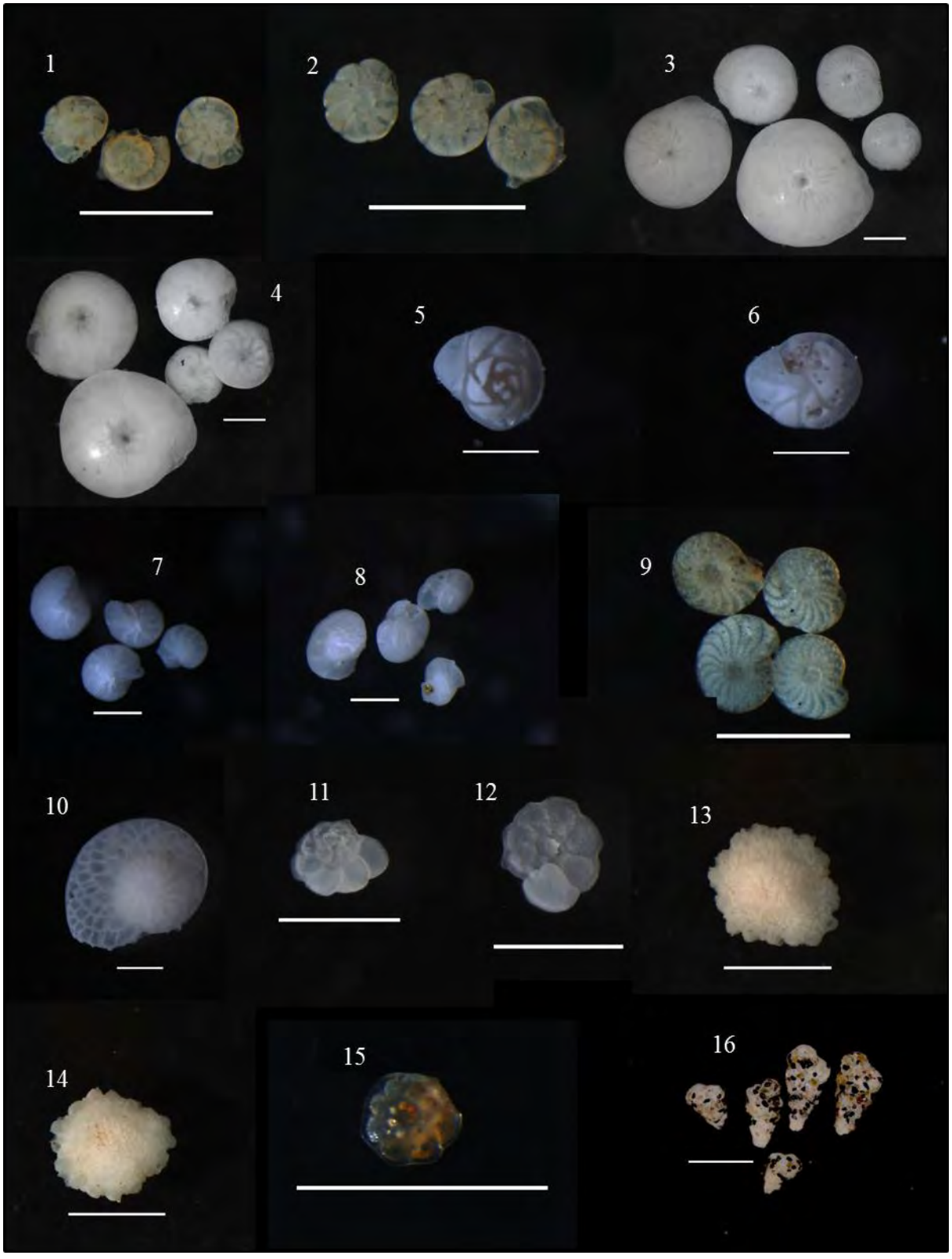

Plate C1. **1-2** *Ammonia* sp., **3-4** *Amphistegina* spp., **5-6** *Asterigerina* sp.1, **7-8** *Cibicides* sp, **9** *Elphidium* sp.11, **10** *Heterostegina depressa* (d'Orbigny), **11-12** *Pararotalia* sp.2, **13-14** *Planorbulinella larvata* (Parker & Jones), **15** *Rotalinoides* sp.5, **16** *Textularia***,** sp.1. Scale bars represent 500 µm.